Ferry free E39 –Fjord crossings Bjørnafjorden | 304624

0	15.08.19	Issued for use	TN/SGR/SAH	SAH	KH	
Rev.	Publish date	Description	Made by	Checked by	Project appro.	Client appro.

Client Statens vegvesen	
Contractor Norconsult DR. TECHN. OLAV OLSEN	Contract no.: 18/91094

Document name: K12 – Design of abutments		
Document no.: SBJ-33-C5-OON-22-RE-020	Rev.: 0	Pages: 65

K12 - DESIGN OF ABUTMENTS

Norconsult

DR. TECHN. OLAV OLSEN

Prodtex IFE Pure Logic HEYERDAHL ARKITEKTER AS H&BB MIKO MARINE AS BUKSÉR OG BERGING FORCE TECHNOLOGY SWERIM

REPORT

Project name:

CONCEPT DEVELOPMENT FLOATING BRIDGE E39 BJØRNAFJORDEN

Document name:

K12 - DESIGN OF ABUTMENTS

Project number:	12777
Document number:	SBJ-33-C5-OON-22-RE-020
Date:	15.08.2019
Revision:	0
Number of pages:	65
Prepared by:	Torbjörn Nilsson, Simon Grøterud, Stein Atle Haugerud
Controlled by:	Stein Atle Haugerud
Approved by:	Kolbjørn Høyland

Summary

General

Both abutments are founded on prepared bedrock base. The south location is on the island Reksteren and the north is located on the islet Gullholmane. The bridge box girder is monolithically connected to the abutments in both ends. The restraint of the superstructure is resolved by concrete gravity base structures with a box-shaped, cellular configuration. Solid ballast (olivine) and post-tensioned rock anchors are used to enhance the overturning and sliding resistance.

This report focuses on the design of the structural features deemed crucial for the feasibility and performance of the integral abutment concept:

- The direct, integral connection between bridge girder and abutment
- Abutment global stability

Bridge girder end section

The flexural response in the bridge girder increases substantially towards the abutments and is significantly higher than what can be resisted by the standard box girder cross section generally adopted for the Low Bridge. To strengthen the steel box girder at the ends, the trapezoidal section is transformed into a rectangular section by removing the chamfer and introducing longitudinal diaphragms as well as T-stiffeners for the arrangement of post-tensioning anchors at the joint. The rectangular box has a width of 28.0 m towards abutment north, and a width of 27.6 m towards abutment south. The deck height is 3.5 m as in rest of the bridge.

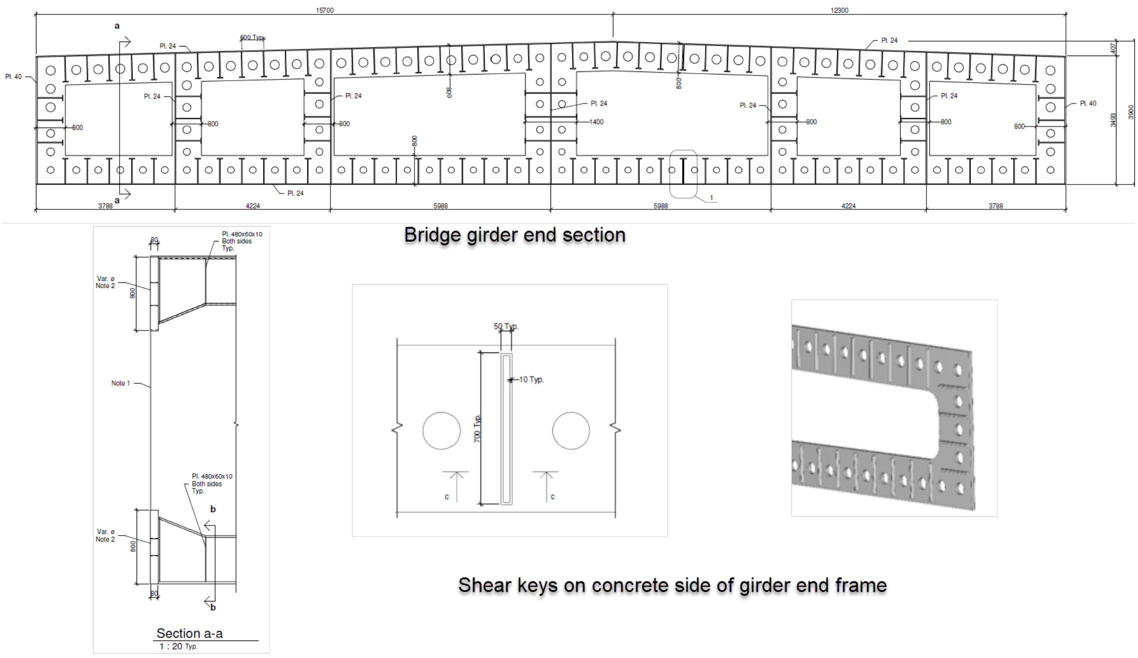

Figure S-1: Bridge girder end section towards abutment north. Front view and section.

The center distance between the trapeze stiffeners in the bridge girder end section matches the T-stiffeners in the general bridge girder section. Within the bridge end girder there is a transition from trapeze to T-stiffeners, ref. drw. SBJ-33C5-OON-22-DR144.

Bridge girder connection to abutment

The fixed end restrain of the bridge deck is obtained by means of post-tensioned tendons closely arranged along the periphery of box girder and anchored directly into the girder end frame. In order not to interfere with the assumptions for the dynamic behaviour, the joint is designed to remain in compression in the ultimate limit state. The necessary post-tensioning level has been determined from the simplified assumption of plain strain distribution over the interface.

As can be seen from Figure S-2 a high level of post-tensioning is required to compress the joint at abutment north under full loading at ultimate. The post-tensioning level is lower for the abutment south connection, see Figure S-3. For the north abutment, the assumption of a rigid end frame yields a total post-tensioning force of 1 173 MN (before losses), which is achieved by 124 post-tensioning tendons, varying from 6-53 tendons in the upper corner to 6-22 in the lower mid. For the south abutment a total of 84 post-tensioning tendons is needed to suppress tensile stresses over the joint, with a total post-tensioning force equal to approximately 410 MN (before losses). The tendon size varies from 6-31 in the upper corner to 0 in the lower mid.

The tendons and anchors are distributed with constant center distance 600 mm, arranged in between each stiffener.

The shear is transferred by means of multiple steel keys welded to the back of the end frame and arranged in the same pattern as the stiffeners. The shear capacity of the joint is a function of the net force normal to the joint and development of friction on the joint face. The shear resistance at the interface is predicted according to the construction joint provisions in EC2 6.2.5 [1] with the beveled shear keys configured in compliance with the indented surface specifications.

The end frame plate has a general width of 800 mm. The net contact area is 53.1 m^2 for abutment north when accounting for the holes for the PT trumpets (net-to-gross ratio ~0.92). A high strength concrete with a concrete grade of B85 (f_{cd} = 48 MPa) is required to resist the bearing stresses in the joint in ULS. The compressive stresses at service load level is well within the limits to avoid longitudinal cracks, micro-cracks and excessive creep.

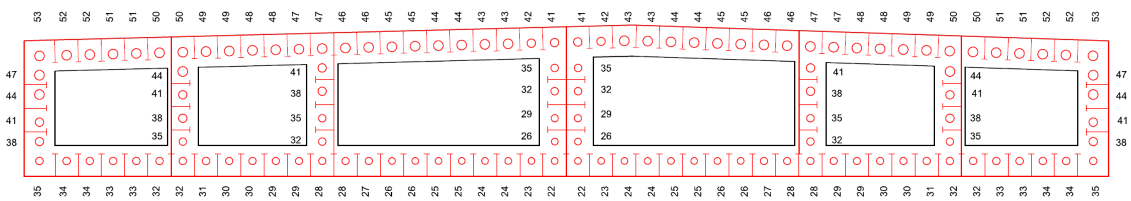

Figure S-2: Post-tensioning arrangement at the joint in abutment North (showing number of 0.6" strands per tendon). Center distances are 600 mm for PT as well as for stiffeners.

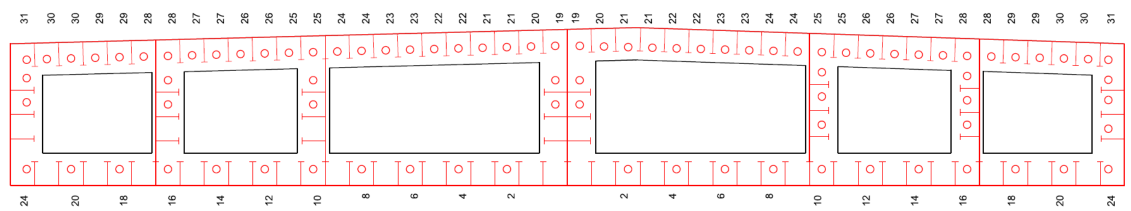

Figure S-3 Post-tensioning arrangement at the joint in abutment South (showing number of 0.6" strands per tendon). Center distances are 600 mm (or multiples of) for PT as well as for stiffeners.

The caisson is designed as a box composed of slabs and walls which are predominantly subjected to membrane action. In the front part the cells are concrete filled, to distribute the post-tensioning forces into the structure. The bonded PT tendons are anchored in the first open cell row as shown in Figure S-4. A fraction of the PT-tendons continues over the entire abutment length (joint by couplers) in order to reduce the amount of reinforcement needed to cover up for the tension behind the PT-anchors.

Foundation

Both abutments follow the same design principle. However, with the current overall dimensions, rock anchors are not necessary for abutment south. The abutments are founded directly on the bedrock. A level base is established whereby weathered and fissured rock is removed/excavated by blasting. To assure a predictable transfer of base shear and normal pressure, only the walls in limited areas in the front and rear parts of the abutment are cast directly onto bedrock whereas the base slab is cast onto a sand/gravel layer. The sliding capacity is determined from base friction only.

As for the joint, to conform with the boundary conditions assumed for the global dynamic analysis, no uplift at any point within the foundation footprint is accepted for the ultimate limit state. The contribution from post-tensioned rock anchors to the base friction capacity and to the overturning resistance is well within the limits prescribed by N400 11.6.2.2 [2]. The rock anchors (north abutment only) are distributed in the front part of the abutment.

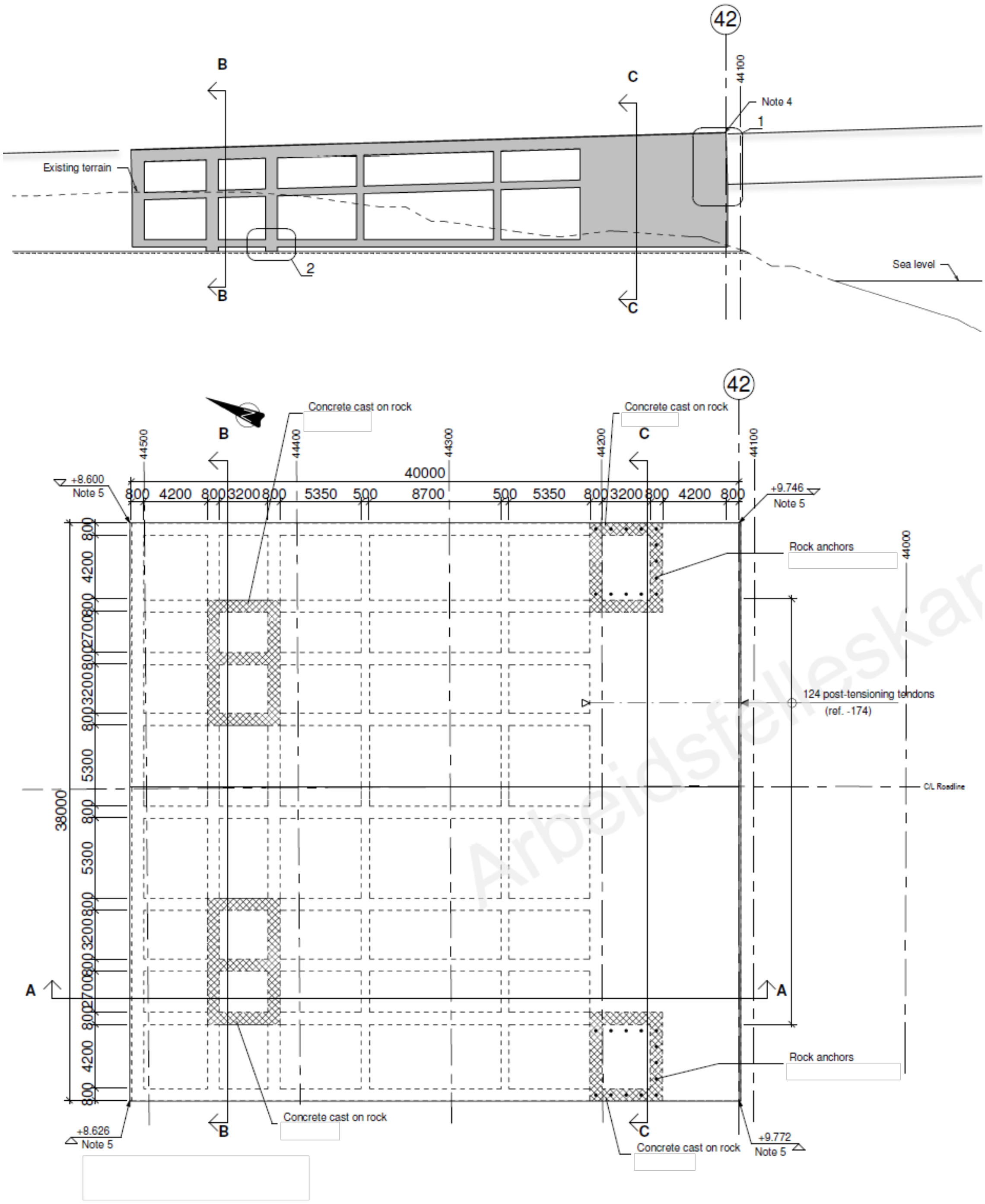

Figure S-4: Elevation and plan of north abutment. The shaded areas show the foot print, i.e. concrete cast on rock. The principles are the same for abutment south.

To get enough capacity for both sliding and overturning at the north abutment the size of the gravity base structure is 40 m x 38 (length x width) with an average height of approximately 7.5 m. Generally, the forces at abutment south is somewhat smaller than for abutment north, except for the axial force which is more than the double. The size of the gravity base structure is 35.5 m x 38 (length x width) with an average height of approximately 15 m. The large height is generated as a consequence of the abutment location in the terrain. Placing this abutment some 10 meters further south will reduced the height, as the ground forms a slope towards the sea. This is recommended to do in a later design phase and will be esthetically as well as economically beneficial.

Depending on the location of the abutment, there may also be an opportunity to provide anchorage by post-tensioning directly into the splay chamber for the cable-stayed bridge. It may then be possible to further reduce the abutment dimensions, since such arrangement may be higher utilized compared to rock anchors.

Table of Content

1 INTRODUCTION

1.1 Current report

This report covers the design of the connection of the bridge girder end to the abutment north as well as abutment south. This includes design of the bridge girder end section and the stiffener arrangement, the steel end frame and the post-tensioning of the connection. It also covers the abutment concrete design and global stability checks, which are performed in ShellDesign.

1.2 Project context

Statens vegvesen (SVV) has been commissioned by the Norwegian Ministry of Transport and Communications to develop plans for a ferry free coastal highway E39 between Kristiansand and Trondheim. The 1100 km long coastal corridor comprise today 8 ferry connections, most of them wide and deep fjord crossings that will require massive investments and longer spanning structures than previously installed in Norway. Based on the choice of concept evaluation (KVU) E39 Aksdal Bergen, the Ministry of Transport and Communications has decided that E39 shall cross Bjørnafjorden between Reksteren and Os.

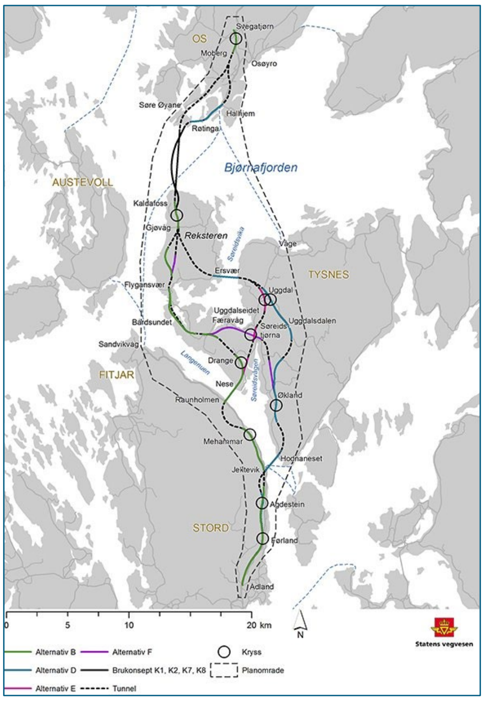

SVV is finalizing the work on a governmental regional plan with consequence assessment for E39 Stord-Os. This plan recommends a route from Stord to Os, including crossing solution for Bjørnafjorden, and shall be approved by the ministry of Local Government and Modernisation. In this fifth phase of the concept development, only floating bridge alternatives remain under consideration.

1.3 Project team

Norconsult AS and Dr.techn.Olav Olsen AS have a joint work collaboration for execution of this project. Norconsult is the largest multidiscipline consultant in Norway, and is a leading player within engineering for transportation and communication. Dr.techn.Olav Olsen is an independent structural engineering and marine technology consultant firm, who has a specialty in design of large floating structures. The team has been strengthened with selected subcontractors who are all highly qualified within their respective areas of expertise:

- Prodtex AS is a consultancy company specializing in the development of modern production and design processes. Prodtex sits on a highly qualified staff who have experience from design and operation of automated factories, where robots are used to handle materials and to carry out welding processes.
- Pure Logic AS is a consultancy firm specializing in cost- and uncertainty analyses for prediction of design effects to optimize large-scale constructs, ensuring optimal feedback for a multidisciplinary project team.
- Institute for Energy Technology (IFE) is an independent nonprofit foundation with 600 employees dedicated to research on energy technologies. IFE has been working

on high-performance computing software based on the Finite-Element-Method for the industry, wind, wind loads and aero-elasticity for more than 40 years.

- Buksér og Berging AS (BB) provides turn-key solutions, quality vessels and maritime personnel for the marine operations market. BB is currently operating 30 vessels for harbour assistance, project work and offshore support from headquarter at Lysaker, Norway.
- Miko Marine AS is a Norwegian registered company, established in 1996. The company specializes in products and services for oil pollution prevention and in-water repair of ship and floating rigs, and is further offering marine operation services for transport, handling and installation of heavy construction elements in the marine environment.
- Heyerdahl Arkitekter AS has in the last 20 years been providing architect services to major national infrastructural projects, both for roads and rails. The company shares has been sold to Norconsult, and the companies will be merged by 2020.
- Haug og Blom-Bakke AS is a structural engineering consultancy firm, who has extensive experience in bridge design.
- FORCE Technology AS is engineering company supplying assistance within many fields, and has in this project phase provided services within corrosion protection by use of coating technology and inspection/maintenance/monitoring.
- Swerim is a newly founded Metals and Mining research institute. It originates from Swerea-KIMAB and Swerea-MEFOS and the metals research institute IM founded in 1921. Core competences are within Manufacturing of and with metals, including application technologies for infrastructure, vehicles / transport, and the manufacturing industry.

In order to strengthen our expertise further on risk and uncertainties management in execution of large construction projects Kåre Dybwad has been seconded to the team as a consultant.

1.4 Project scope

The objective of the current project phase is to develop 4 nominated floating bridge concepts, document all 4 concepts sufficiently for ranking, and recommend the best suited alternative. The characteristics of the 4 concepts are as follows:

- K11: End-anchored floating bridge. In previous phase named K7.
- K12: End-anchored floating bridge with mooring system for increase robustness and redundancy.
- K13: Straight side-anchored bridge with expansion joint. In previous phase named K8.
- K14: Side-anchored bridge without expansion joint.

In order to make the correct recommendation all available documentation from previous phases have been thoroughly examined. Design and construction premises as well as selection criteria have been carefully considered and discussed with the Client. This form basis for the documentation of work performed and the conclusions presented. Key tasks are:

- Global analyses including sensitivity studies and validation of results
- Prediction of aerodynamic loads
- Prediction of hydrodynamic loads
- Ship impact analyses, investigation of local and global effects
- Fatigue analyses

- Design of structural elements
- Marine geotechnical evaluations
- Steel fabrication
- Bridge assembly and installation
- Architectural design
- Risk assessment

2 ABUTMENT NORTH

2.1 General description

The abutment that forms the restraint of the superstructure north end is a concrete gravity-based structure with a box-shaped, cellular configuration founded on prepared bedrock base. Solid ballast and post-tensioned rock anchors are used to enhance the abutments overturning and sliding resistance. The bridge box girder is monolithically connected to the abutment by horizontal post-tensioning.

The caisson that forms the abutment is designed as a box composed of slabs and walls which are predominantly subjected to membrane action. The first 9 meters (in front) consist of massive concrete, as shown in Figure 2-1. The horizontal post-tensioning is limited to the concrete-filled front cells of the abutment, with the stressing anchors inside the first row of empty cells (post-tensioning through the entire length of the abutment, with stressing anchors in the rear end, would create uplift in the front- and rear parts of the abutment). A portion of the post-tensioning strands may be spliced and continue through the entire abutment structure. This will reduce the amount longitudinal reinforcement needed to cover up for the tie-back tension behind the stressing zone.

To assure a predictable transfer of base shear and normal pressure, only the walls in the front corner parts and the rear part of the abutment are cast directly onto bed rock whereas the base slab is cast onto a sand/gravel layer (see Figure 2-23). The sliding capacity is determined from base friction only. The contribution from post-tensioned rock anchors to the base friction capacity and to the overturning resistance is well within the limits prescribed by N400 11.6.2.2 [2]. The rock anchors are distributed in the front part of the abutment. See Figure 2-25 for an overview.

The fixed end restrain of the bridge is obtained by means of post-tensioned tendons closely arranged along the periphery of the bridge box end girder and anchored directly into the girder end frame. The level of post-tensioning necessary is given by the criterion that the joint shall remain in compression at ultimate state condition in order not to interfere with the assumptions for the dynamic behavior.

A high level of post-tensioning is required to fully compress the joint. The assumption of a rigid end frame yields a PT intensity with 124 tendons (with varying no. of strands) arranged at center distances 600 mm. The post-tensioning arrangement is shown in Figure 2-1 and Figure 2-54. Vertically, there are 26 pcs. of 6-19 rock anchors.

The stressing anchors will be located within the walls and slabs and in special brackets, to achieve necessary space for the stressing anchors and jacks. The anchors within the girder end frame are passive, and the stressing anchors are located inside the first cells as shown in Figure 2-1. Stressing will be performed before casting the floor, intermediate walls and roof slab in this area.

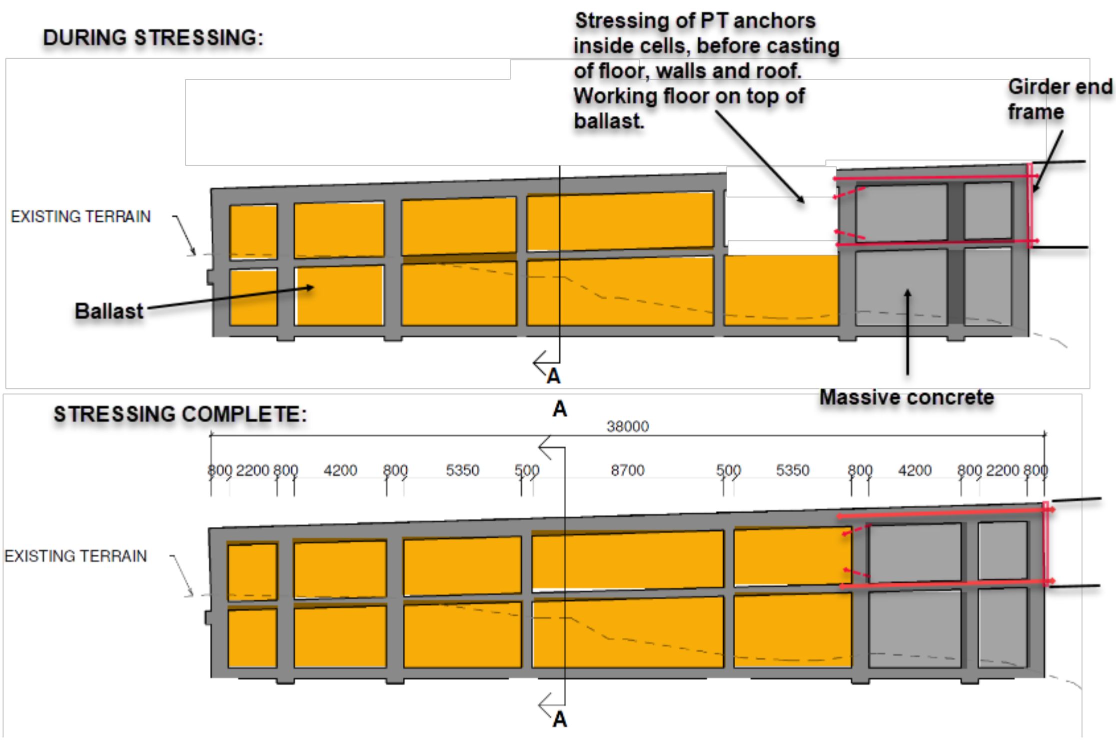

> *Figure 2-1: Stressing anchors inside the cells. Post-tensioning is performed before the floor, walls and roof is cast in the cells of concern. Tendons in walls not shown.*

The post-tensioned front part of the abutment is massive concrete, while the other cells are filled with ballast (olivine). A high strength concrete with a concrete grade of B85 is required in vicinty of the anchors, while the general concrete grade can be much lower.

2.2 Analytical model

A FE-model is generated with PatranPre with 20-noded volumetric elements. All tendon forces are added to the model via the program TenLoad that find the elements that the cables pass through and apply nodal forces from anchoring, losses and curvature. For the final analysis the contact surfaces to rock is modeled as fixed in all directions. The model stands on 4 local footings to maximize the axial force in these areas to eliminate uplift from the rock. Please refer to section 2.4 for more information.

Loads from ballast and from the bridge girder is applied as element pressure. The loads representing the loading from the bridge girder are described further in the next chapter.

The analytical model is fully parameterized with simple text input describing the distance and height between the cells, and thickness of walls. The position and the layout of the footing is also described as simple parametric input. This makes it easy to investigate different geometries and layouts of the footings as the whole analysis from PatranPre (geometry and loading), TenLoad (tendon forces), Sestra (FEA), GreenBox(fetching of loads) and ShellDesign (design calculation) is done automatically.

2.3 Design loads

The loads from the bridge girder is gathered from the latest database files from GeenBox and consist of combined dynamic loads from 3Dfloat and static loads from Sofistik. Because of statistics each DOF reaches its maximum and minimum amplitudes at different timestep. For that reason, max/min for each of the 6 DOF is stored together with simultaneous forces for the other DOFs.

The load cases from GreenBox and simultaneous forces for *min* and *max* for each DOF has its own load case in this report. The two first numbers represent the GreenBox load case and the two last the *min*/*max* DOF as described in the table below. Each load case has self-weight and post-tensioning appended. For SLS load case 24 and 25 is considered and for ULS 31-34.

> *Table 2-1: Extremal load case designation*

MAX						MIN					
Mxx	Myy	Mzz	Nx	Ny	Nz	Mxx	Myy	Mzz	Nx	Ny	Nz
01	02	03	04	05	06	07	08	09	10	11	12

When referring to load case 3409 in this report, this means GreenBox load case 34 with the minimum strong axis moment from the bridge girder. 3403 and 3409 which is the *min* and *max* strong axis moment from the bridge girder is fore the most part dimensioning for uplift of the footings.

The forces from the bridge girder (from GreenBox) are introduced into the abutment model by scaling of 6 unit loads – representing each of the DOF in the bridge girder. The axial load from the girder is shown in the figure below, where the load application area is equal to the bridge girder dimensions.

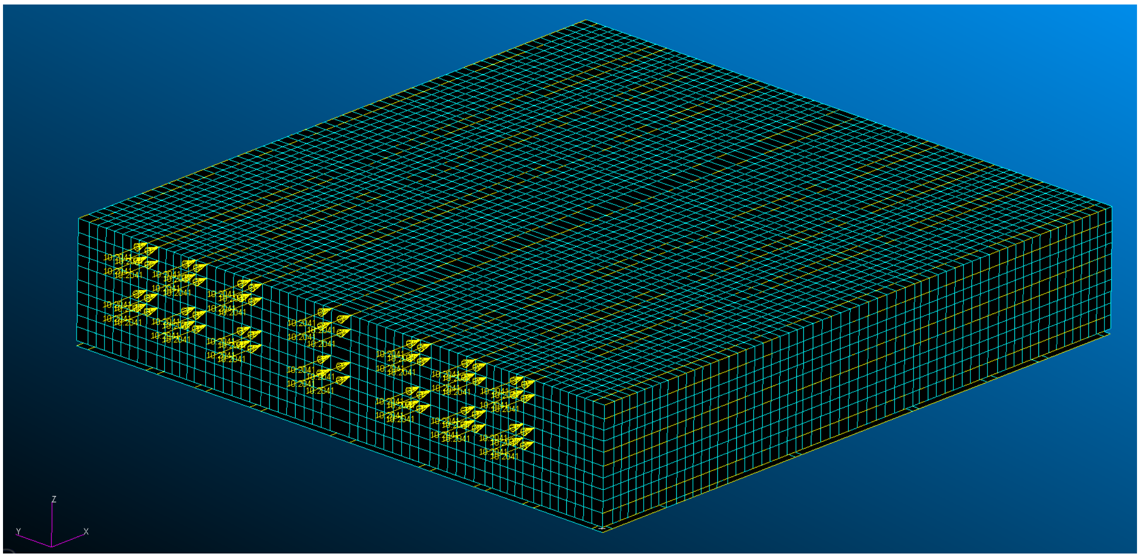

> *Figure 2-2: Illustration of load application area in PatranPre*

These 6 loads are scaled in accordance with the results from the GreenBox analysis (combined dynamic loads from 3Dfloat and static loads from Sofistik) in order to represent all the relevant actions from the bridge. The behavior of these load cases is described thoroughly below.

The base reactions and deformations for each of the 6 load cases 2 – 6 is shown in the figures below. The top figure describes the resulting forces in each of the 4 footing areass. The table in the middle shows each of the 6 beam forces for integration of each section (beam section bs=1 shows the integrated sum of all 4 footings). The figure at the bottom shows the deformations of the landfall structure.

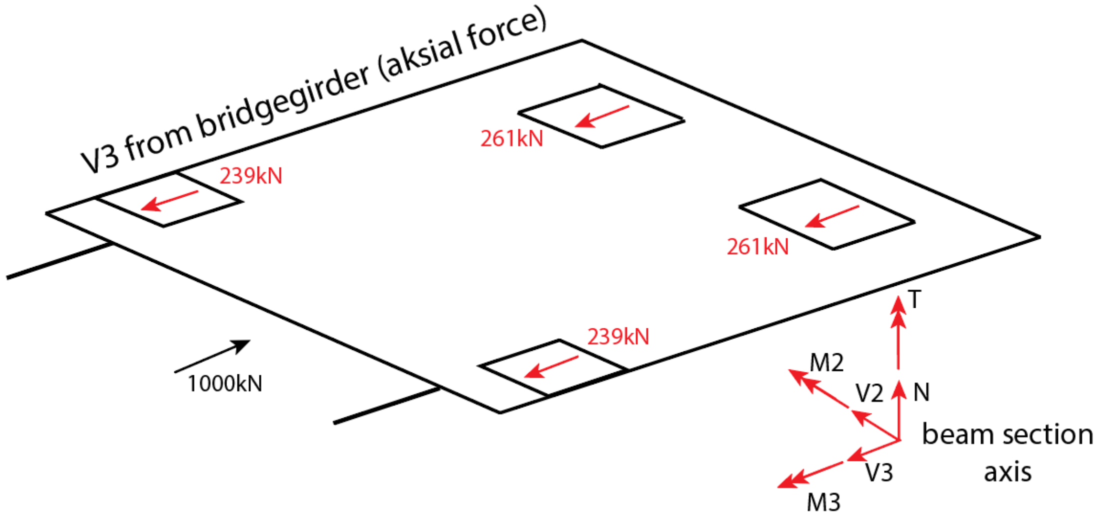

> *Figure 2-3:Distribution between the 4 footings*

de-case	bs	N [kN]	V2 [kN]	V3 [kN]	T [kNm]	M2 [kNm]	M3 [kNm]
2	1	0	0	-1000	0	5486	0
2	2	73	14	-239	355	648	-172
2	3	73	-14	-239	-355	648	172
2	4	-73	-13	-261	-3	245	-66
2	5	-73	13	-261	3	245	66

> *Figure 2-4: Table describing the beam section for each footing. Beam section nr 1 is the sum of each footing. For numbering of footing, please refer to Figure 2-37*

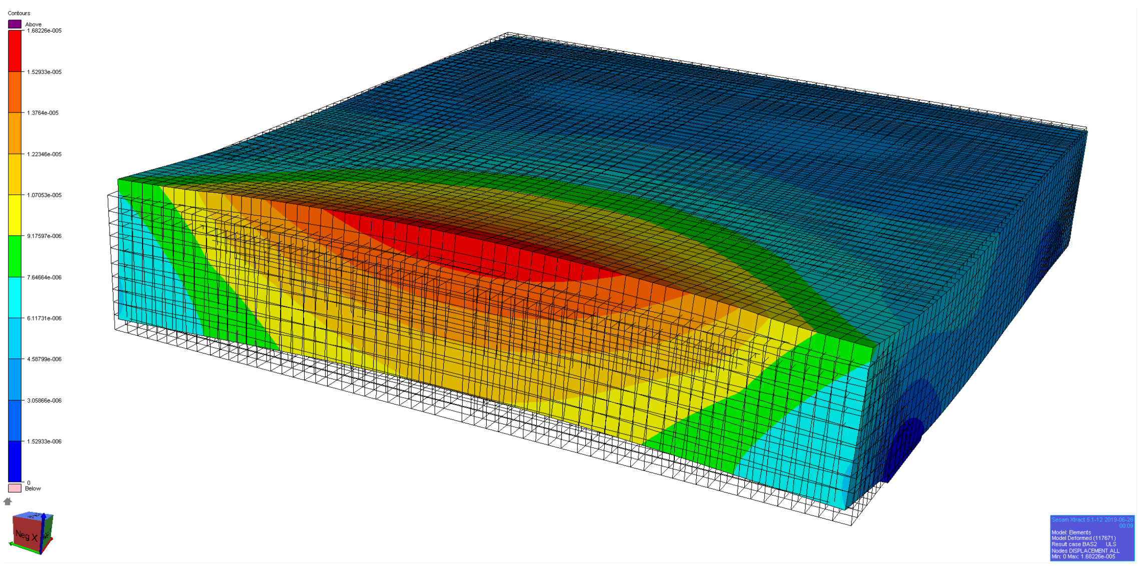

> *Figure 2-5: Deformation plot for unit bridge axial force (1000 kN)*

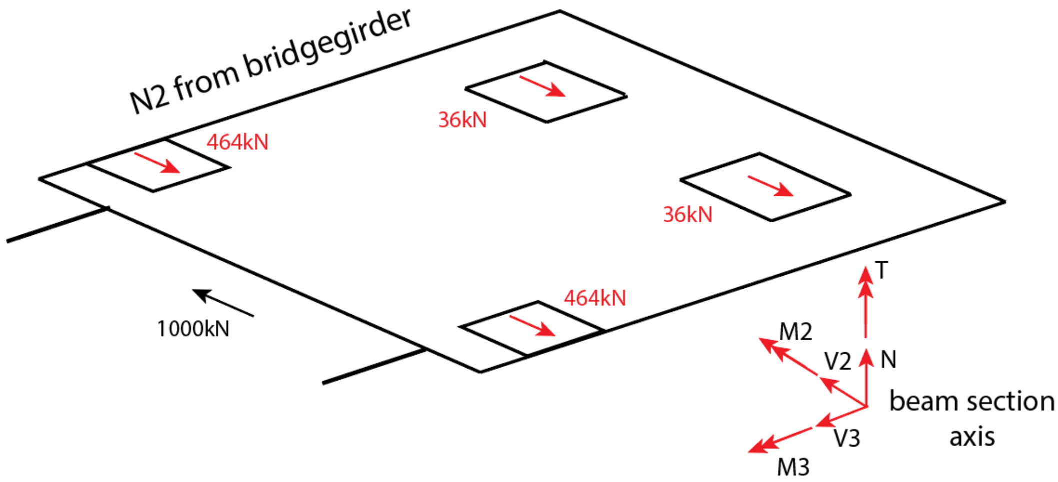

> *Figure 2-6:Distribution between the 4 footings*

de-case	bs	N [kN]	V2 [kN]	V3 [kN]	T [kNm]	M2 [kNm]	M3 [kNm]
3	1	0	1000	0	22334	0	5290
3	2	112	464	214	233	-213	515
3	3	-112	464	-214	233	213	515
3	4	25	36	75	167	-69	82
3	5	-25	36	-75	167	69	82

Figure 2-7: Table describing the beam section for each footing. Beam section nr 1 is the sum of each footing. For numbering of footing, please refer to Figure 2-37

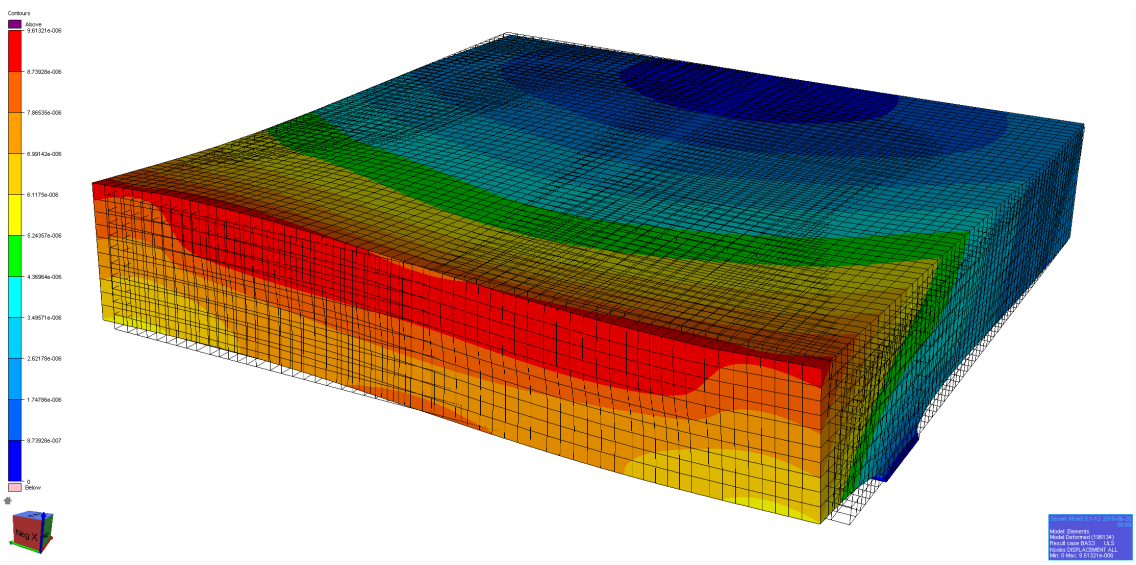

> *Figure 2-8: Deformation plot from pure horizontal shear 1000 kN from the bridge girder*

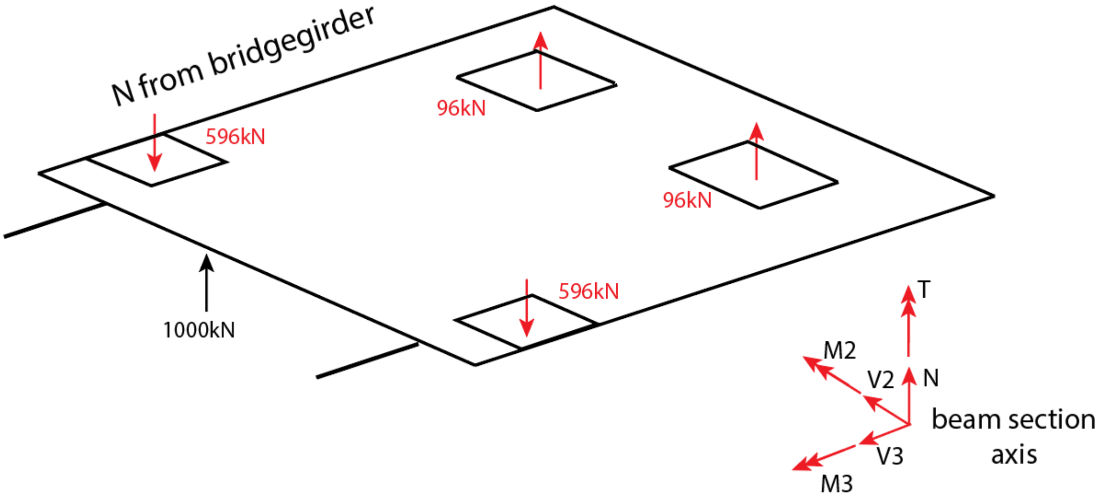

> *Figure 2-9:Distribution between the 4 footings*

de-case	bs	N [kN]	V2 [kN]	V3 [kN]	T [kNm]	M2 [kNm]	M3 [kNm]
4	1	1000	0	0	0	22337	0
4	2	596	377	167	-48	1152	-1252
4	3	596	-377	167	48	1152	1252
4	4	-96	33	-167	-84	137	-140
4	5	-96	-33	-167	84	137	140

Figure 2-10: Table describing the beam section for each footing. Beam section nr 1 is the sum of each footing. For numbering of footing, please refer to Figure 2-37

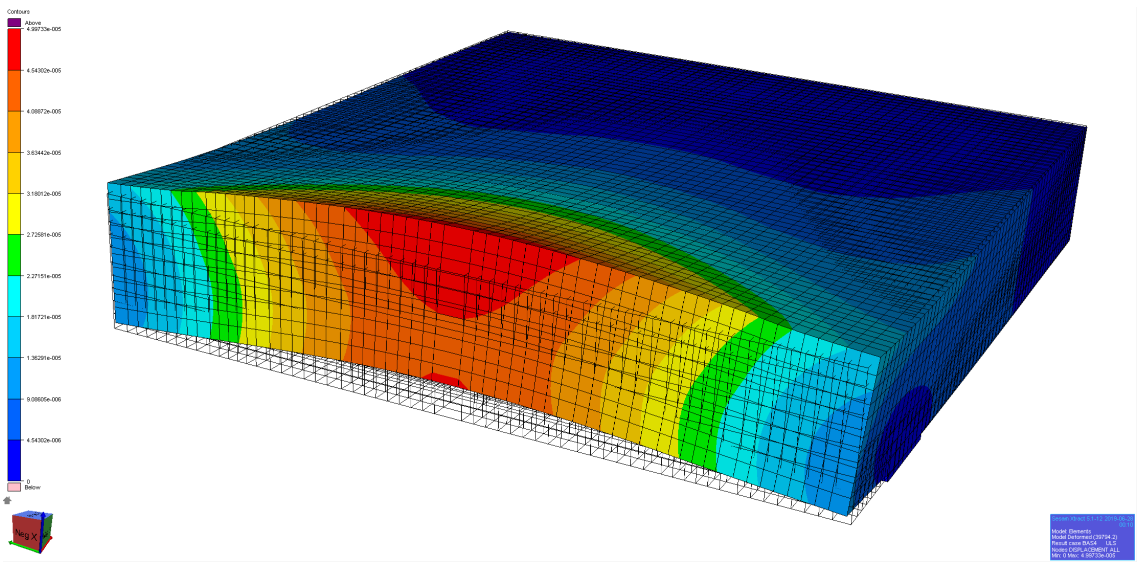

> *Figure 2-11: Vertical shear 1000 kN*

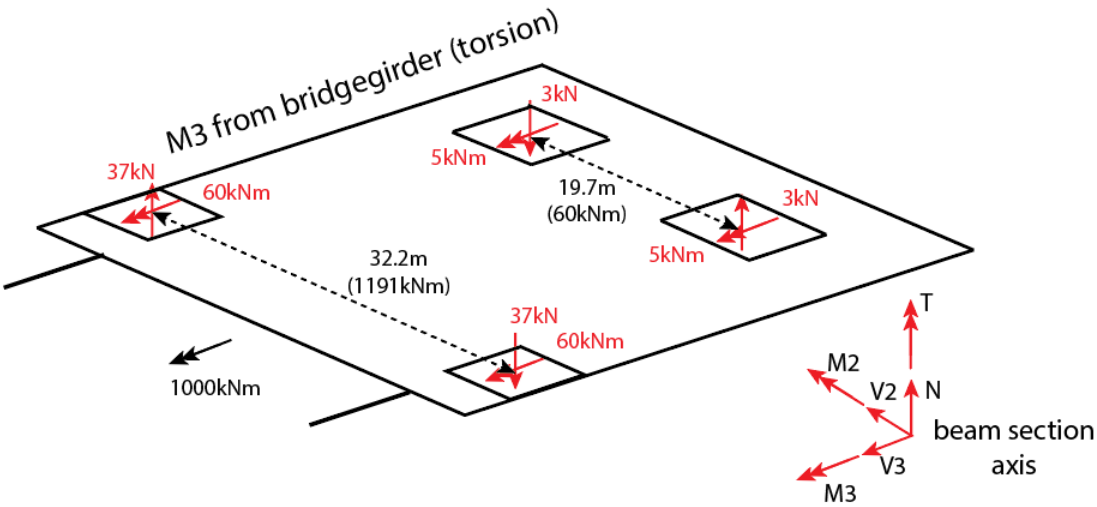

> *Figure 2-12:Distribution between the 4 footings*

dc-case	bs	N [kN]	V2 [kN]	V3 [kN]	T [kNm]	M2 [kNm]	M3 [kNm]
5	1	0	0	0	1	0	1003
5	2	37	-2	10	-14	75	-60
5	3	-37	-2	-10	-14	-75	-60
5	4	-3	2	-8	-12	3	-5
5	5	3	2	8	-12	-3	-5

Figure 2-13: Table describing the beam section for each footing. Beam section nr 1 is the sum of each footing. For numbering of footing, please refer to Figure 2-37

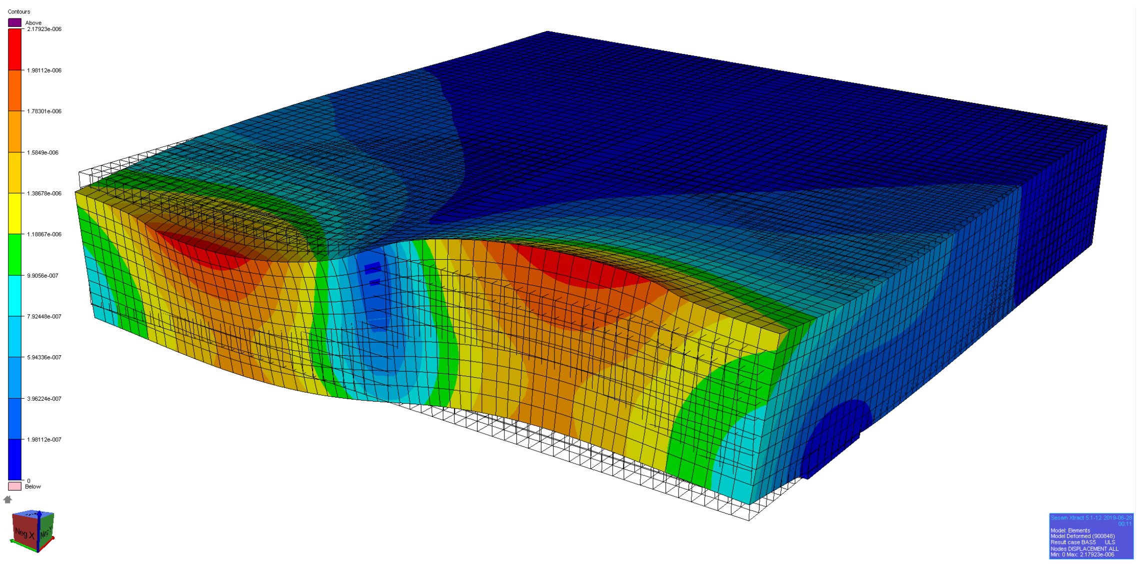

> *Figure 2-14: Torison 1000 kNm*

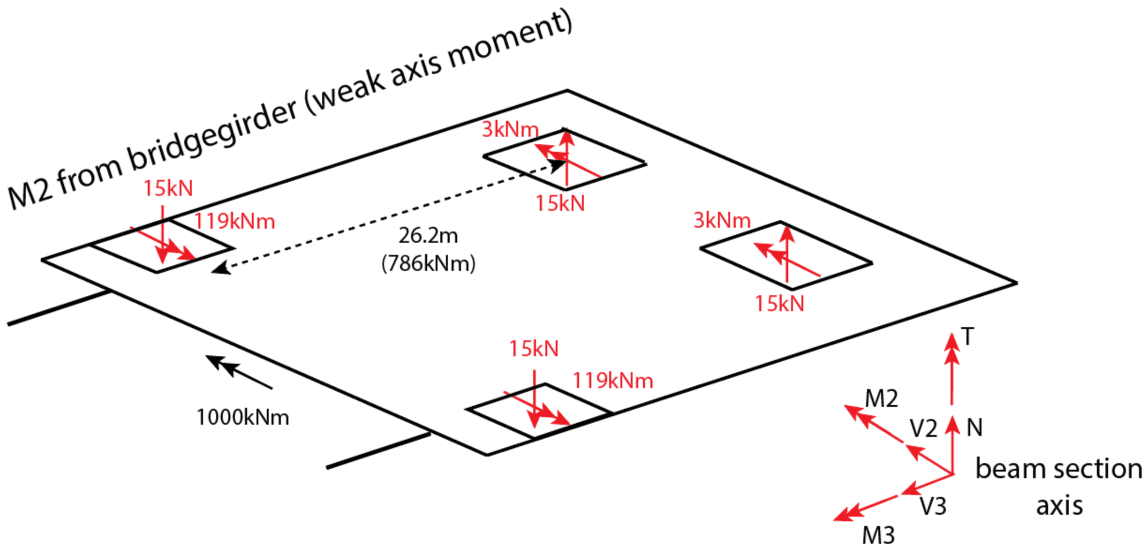

> *Figure 2-15:Distribution between the 4 footings*

de-case	bs	N [kN]	V2 [kN]	V3 [kN]	T [kNm]	M2 [kNm]	M3 [kNm]
6	1	0	0	0	0	1000	0
6	2	15	14	23	-14	119	-39
6	3	15	-14	23	14	119	39
6	4	-15	1	-23	-5	-3	-1
6	5	-15	-1	-23	5	-3	1

Figure 2-16: Table describing the beam section for each footing. Beam section nr 1 is the sum of each footing. For numbering of footing, please refer to Figure 2-37

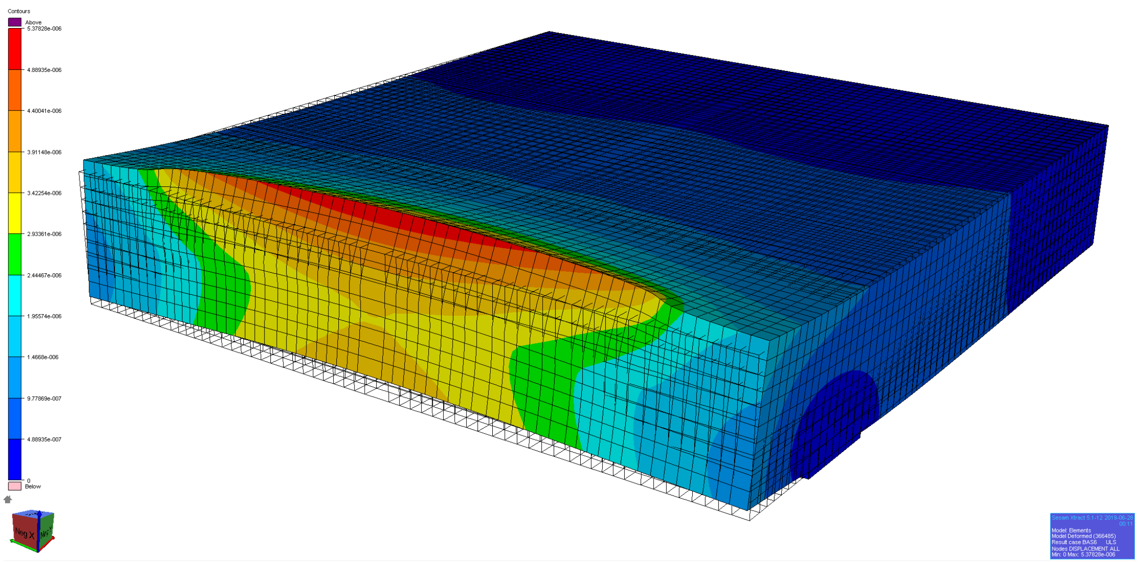

> *Figure 2-17: Weak axis moment 1000 kNm*

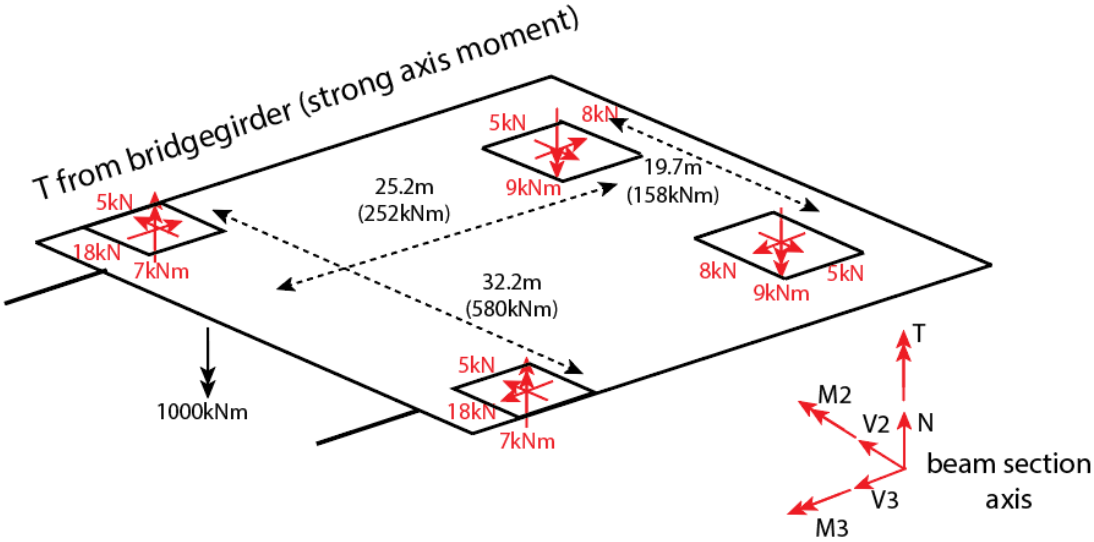

> *Figure 2-18:Distribution between the 4 footings*

de-case	bs	N [kN]	V2 [kN]	V3 [kN]	T [kNm]	M2 [kNm]	M3 [kNm]
7	1	0	0	0	1000	0	0
7	2	-2	5	18	-7	-44	7
7	3	2	5	-18	-7	44	7
7	4	2	-5	8	9	-4	-1
7	5	-2	-5	-8	9	4	-1

Figure 2-19: Table describing the beam section for each footing. Beam section nr 1 is the sum of each footing. For numbering of footing, please refer to Figure 2-37

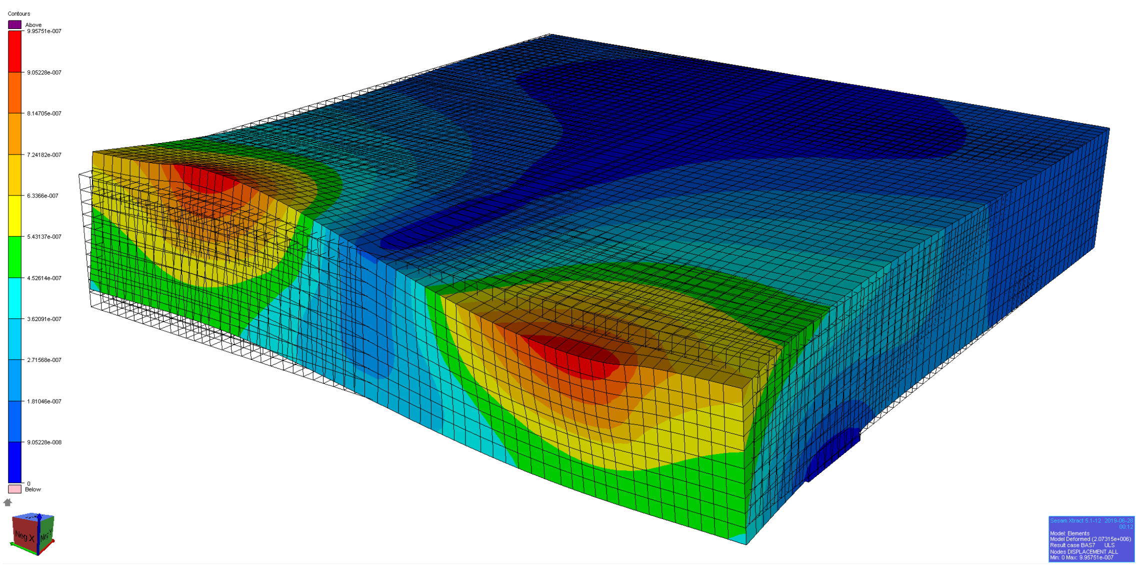

> *Figure 2-20: Strong axis moment 1000 kNm*

2.4 Foot print

The configuration of the foot print is developed based on the criteria that no uplift is allowed in SLS load conditions in areas with concrete to bed rock contact. The analytical model has been set up with the restriction that the boundary condition is removed upon tension in the vertical direction (uplifting).

Some iterations have been necessary to find an arrangement that eliminates uplifting in SLS while keeping the geometry of the abutment. Figure 2-21 to Figure 2-24 shows the development sequence and illustrates the philosophy behind the chosen foot print configuration. For the final analysis the contact surfaces to rock is modeled as fixed in all directions.

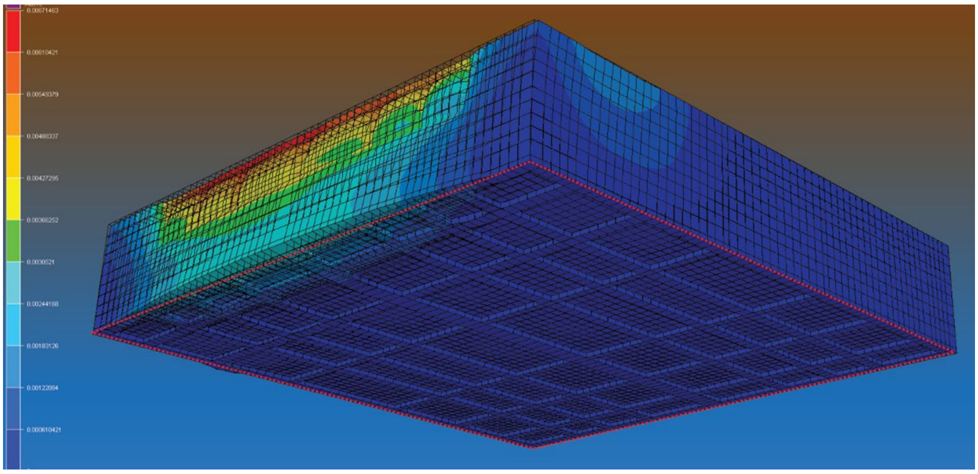

> *Figure 2-21: In previous design phases it was assumed foundation to bed rock for all walls. However, uplift will be present in several locations, most apparent in the front area.*

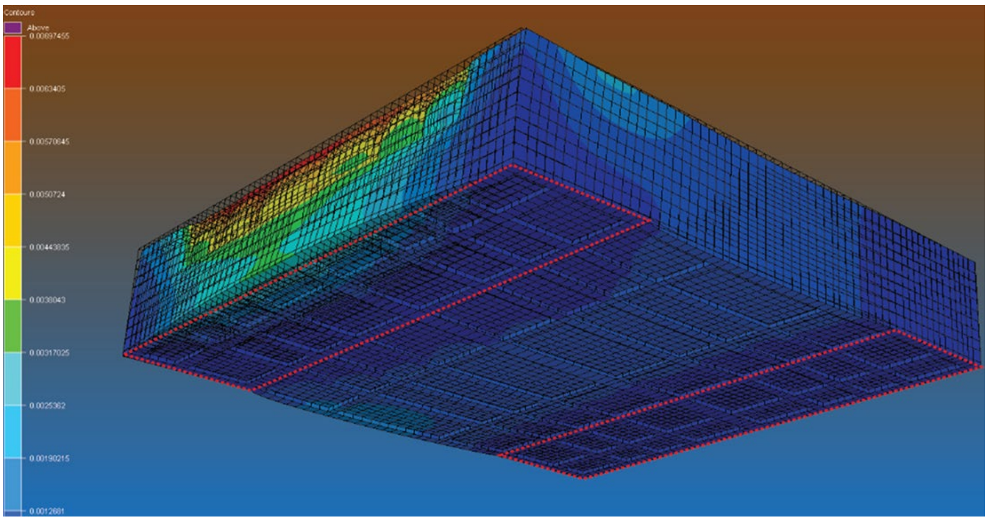

> *Figure 2-22: Assuming foot print concentrated to the front and rear areas still gives uplift in regions with concrete to bed rock contact.*

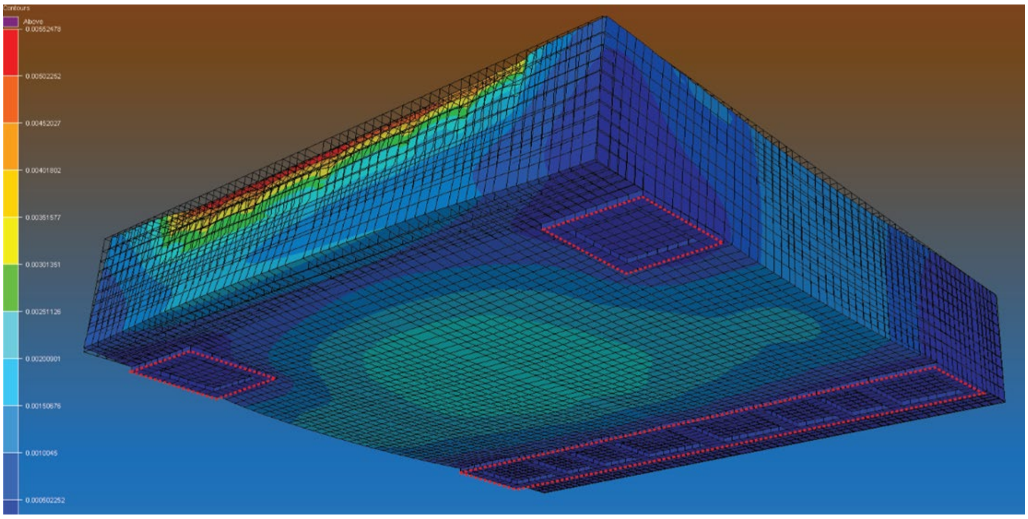

> *Figure 2-23: A more concentrated foot print configuration in the front that still gives uplift in regions with concrete to bed rock contact in the back.*

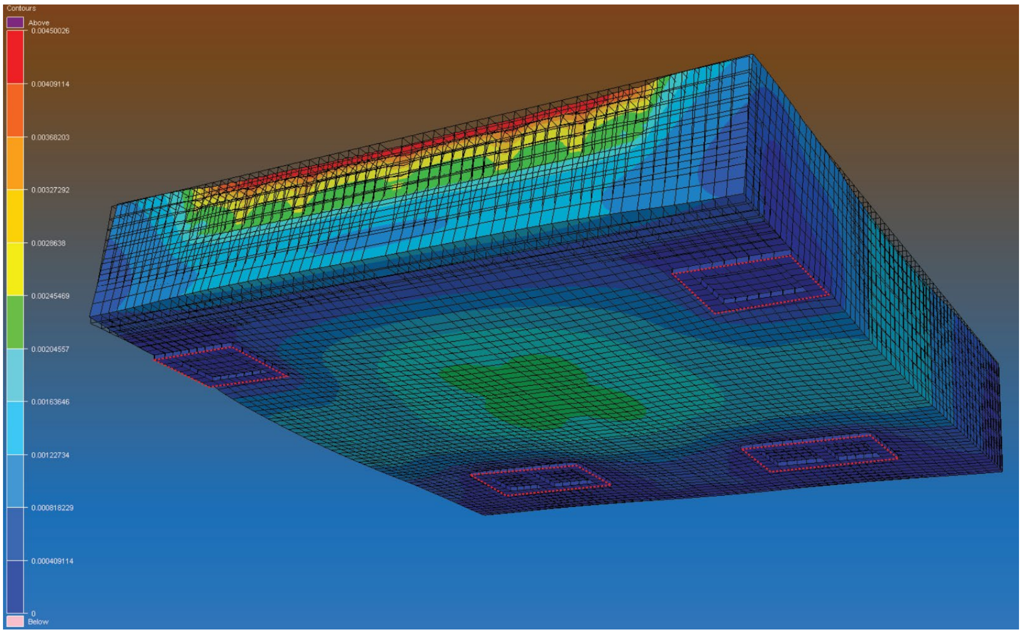

> *Figure 2-24: A more concentrated foot print configuration provides compression in all regions with concrete to bed rock contact.*

2.5 Caisson concrete structural design

2.5.1 General

The abutment structures and the distribution of the base reactions used in the global stability control is predicted by means of the 3-dimensional solid FE-model and the results are extracted by using ShellDesign. Ballast with density 30 kN/m^3 is assumed (olivine).

2.5.2 Structural configuration

A plan view and section of the cellular box configuration is shown in Figure 2-25. The front cells are filled with concrete, to be able to distribute the incoming forces from the bridge girder. Horizontal post-tensioning and vertical rock anchors are stressed within the areas shown in the figure.

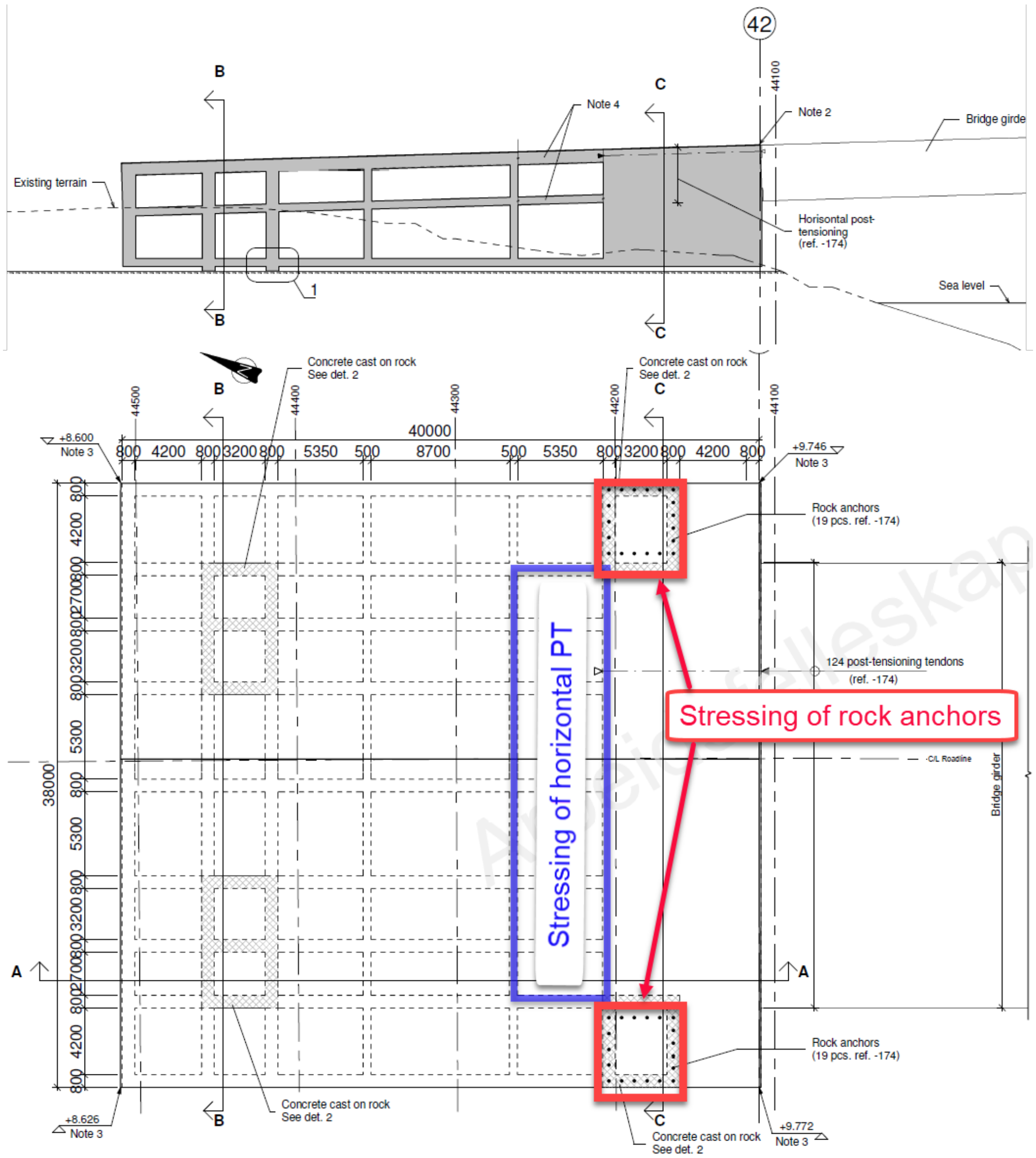

> *Figure 2-25: Cellular configuration of abutment, showing concrete filled cells in the front, and locations for stressing the horizontal and vertical post-tensioning.*

2.5.3 Concrete structural design

The solid concrete part towards the main span have a concrete material of grade B85 because of the post-tension anchoring. The lower section in this part could probably be of a lower concrete grade. The rest of the structure is set to grade B45.

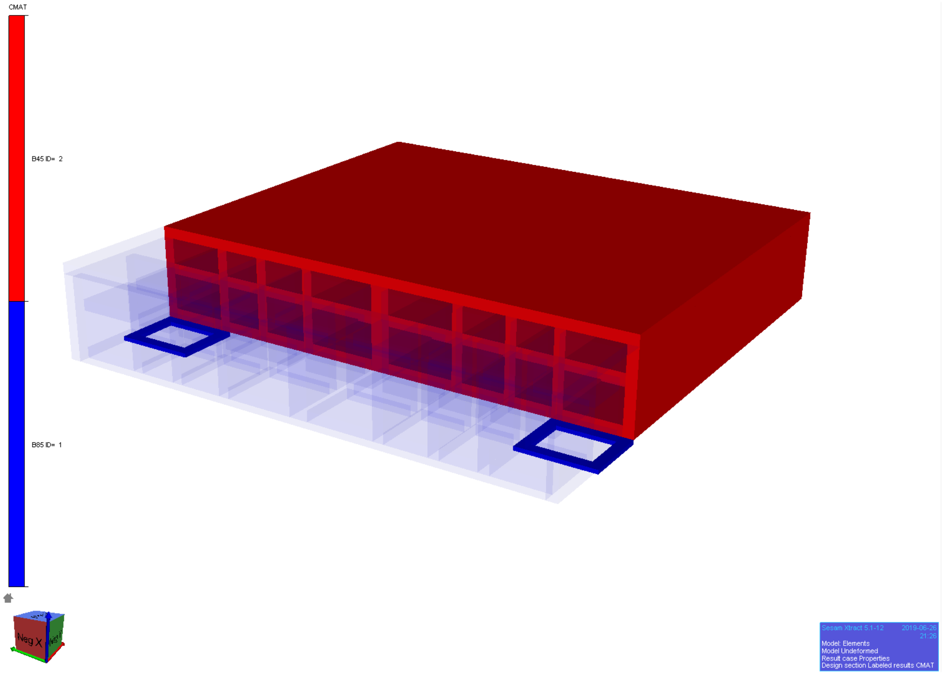

> *Figure 2-26 Concrete grade B85 in the front part and B45 in the rest of the structure.*

A small intensity of shear reinforcement (approximately ø12 c200c200) is necessary in about 1/3 of the abutment length (in blue areas in Figure 2-27).

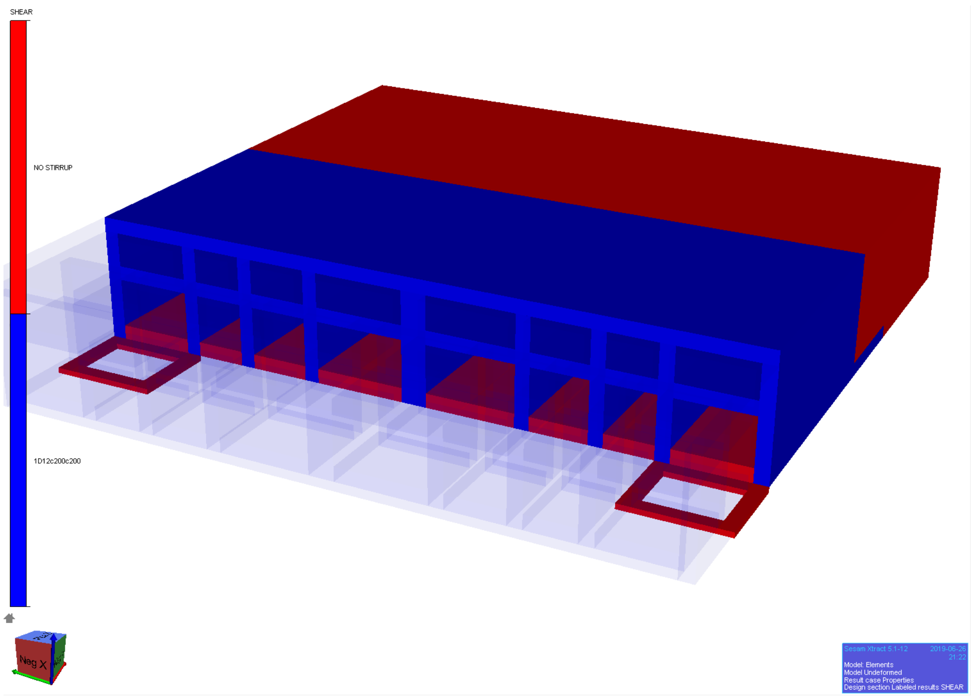

> *Figure 2-27 A small amount of shear reinforcement is necessary in the blue areas.*

Reinforcement in bridge direction, equal intensity at both faces. Yellow area indicates ø32 c100, dark blue is ø25 c100 and light blue is ø25 c200.

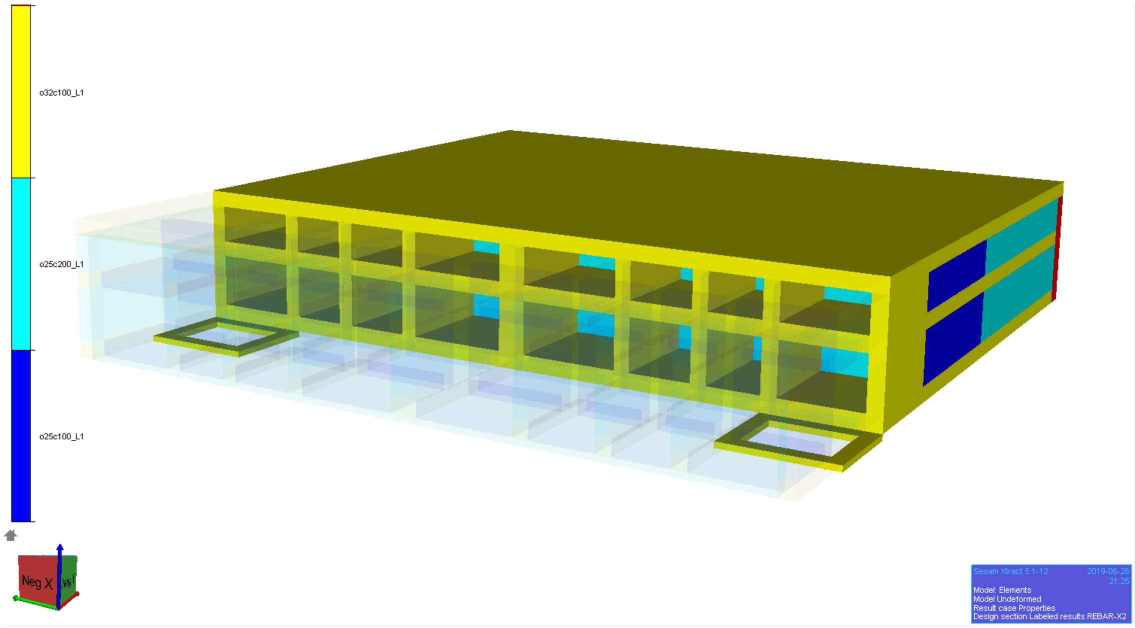

> *Figure 2-28 Reinforcement intensity in bridge (longitudinal) direction.*

Reinforcement normal to the bridge direction (slabs) and vertical (walls), equal intensity at both faces. Red color indicates ø32 c100, light blue is ø25 c100 and yellow is ø25 c200.

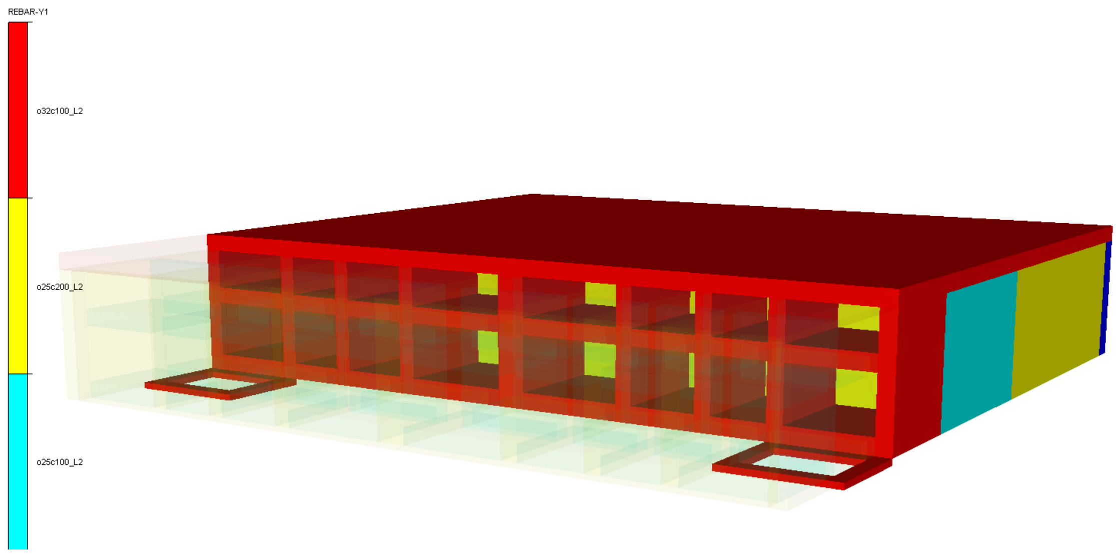

> *Figure 2-29 Reinforcement intensity in transverse direction (vertical for walls).*

The utilizations shown in the following figures are within acceptable limits except for local areas around the post-tensioning anchors. These areas should be evaluated in the next phase. Figure 2-30 shows utilization for compression of concrete.

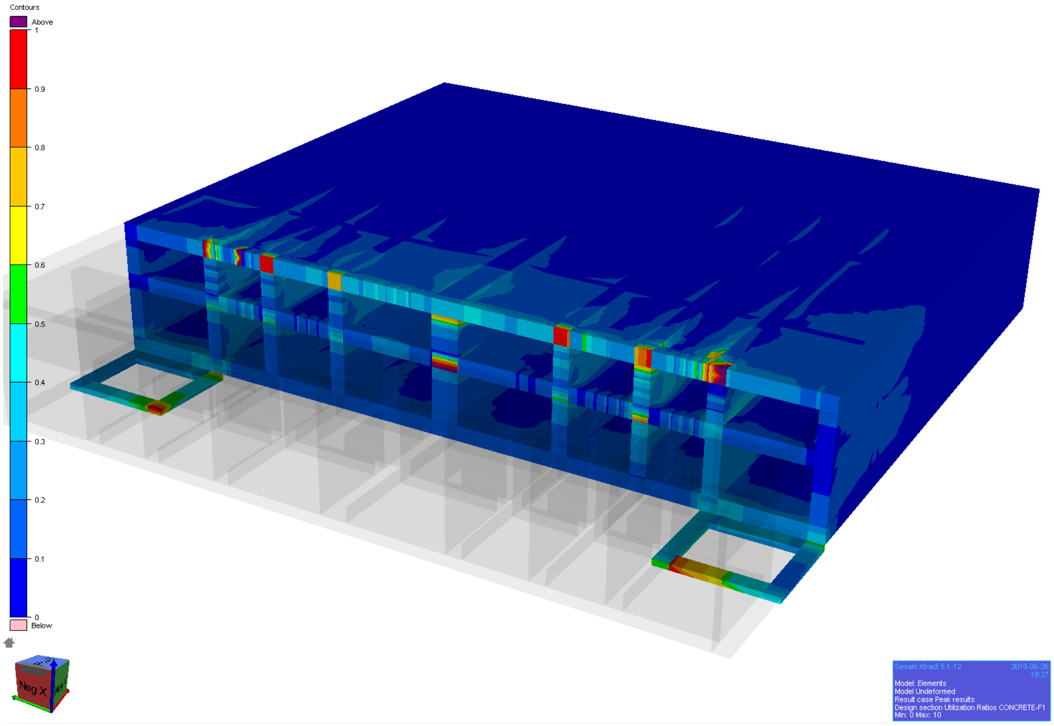

> *Figure 2-30 Concrete utilization, compression.*

Figure 2-31 shows utilization of shear reinforcement.

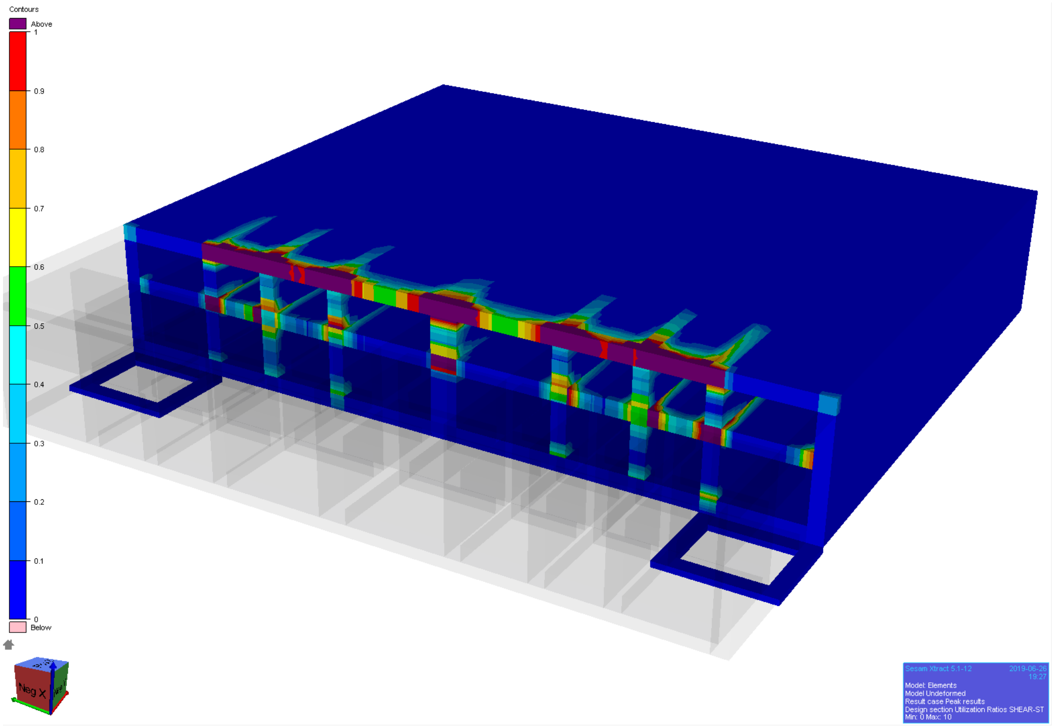

> *Figure 2-31 Utilization of shear reinforcement.*

Utilization of longitudinal (bridge direction) reinforcement is shown in Figure 2-32.

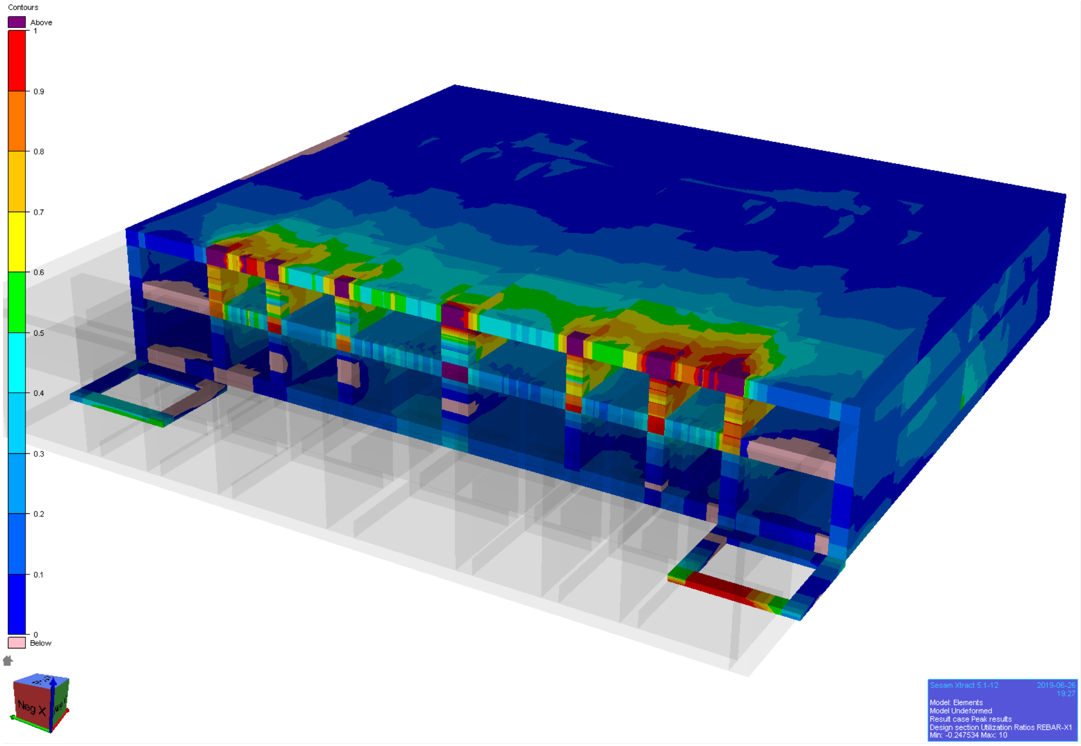

> *Figure 2-32 Utilization of longitudinal (bridge direction) reinforcement.*

Utilization of reinforcement in the normal/vertical direction is shown in Figure 2-33.

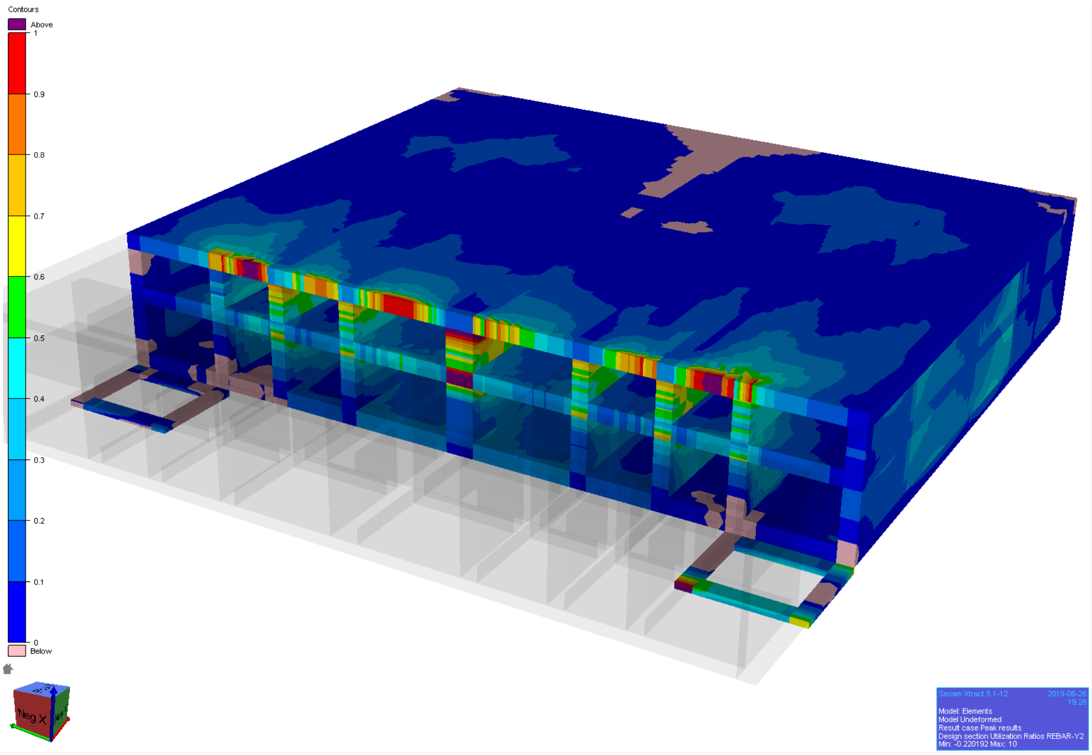

> *Figure 2-33 Utilization of transverse (normal to bridge direction) and vertical reinforcement.*

The SLS crack width utilization check is shown in Figure 2-34. Crack widths are checked for w_{max} = 0.30 mm, according to the requirements in table NA.7.1N in [1].

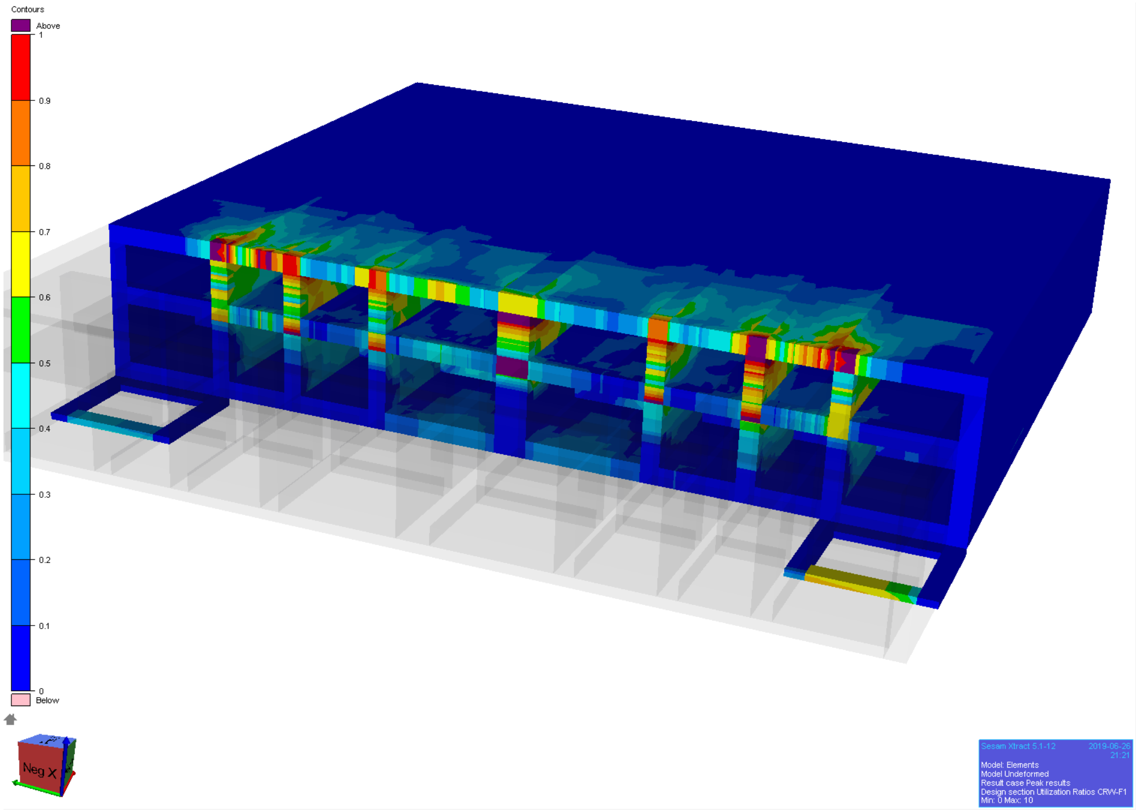

> *Figure 2-34 Crack width utilization.*

2.6 Foundation

2.6.1 Geological conditions

A geological map of the Røtinga area, issued by the Norwegian Geological Survey (NGU), is shown in Figure 2-35. The north abutment is located on Gullholmane, south-east of the island Røtinga. Trondhjemite is present on half of the island of Gulholmane, and in the continued axis of the road/bridge on to the island of Røtinga. The other half of Gulholmane is comprised of a metatuff, a fine-grained metamorphic rock of volcanic ash origins.
The bedrock is evaluated to be feasible regarding reaction forces from the abutment and any potential for land slide is not considered relevant with respect to landfall foundation at this location.

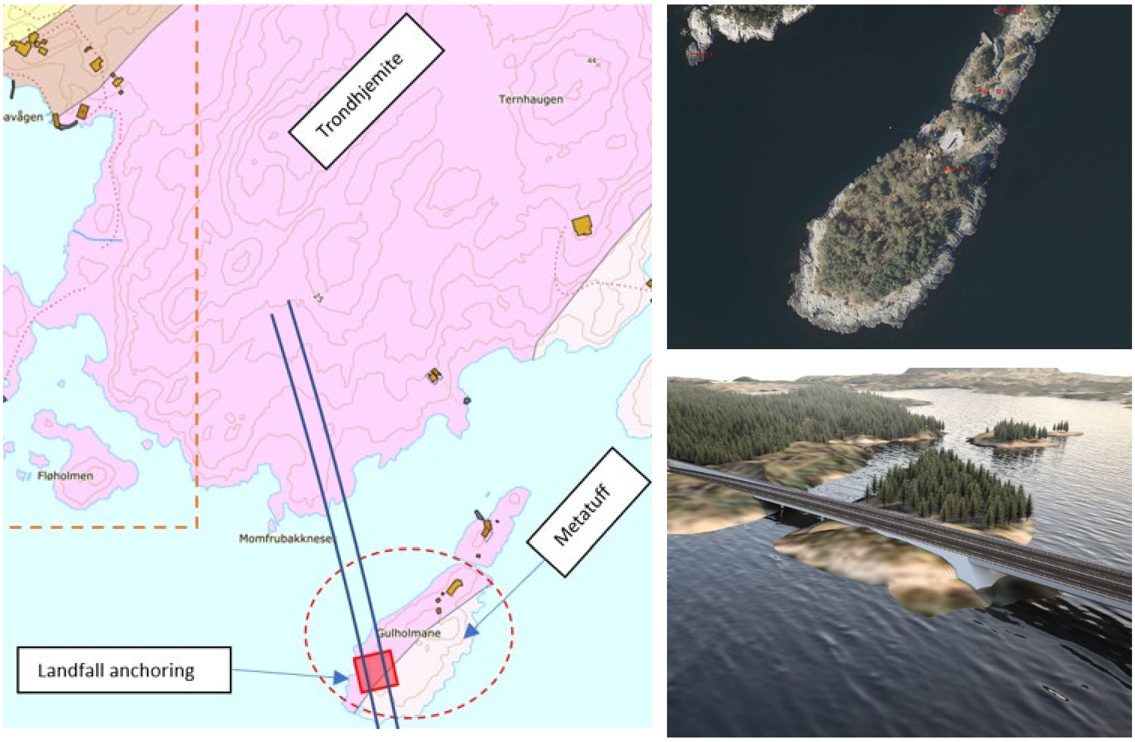

> *Figure 2-35: Extract from geological map showing Trondhjemite and Metatuff at Gullholmane. North shore approach is rendered (lower right) and a photo of the islet Gullholmane (upper right).*

> *Figure 2-36: Arial photo south of Gulholmane. Trondhjemite to the left and Metatuff to the right*

2.6.2 Base reactions

The caisson is supported in 4 limited areas localized as shown in the figure below. On the next pages (Figure 2-39 to Figure 2-46) the base reactions for GreenBox load cases 31-34 (ULS) is shown for each foundation area. Foundation area number 1 is the sum of areas 2 - 5, i.e. the total base reactions for the entire abutment. The load area with the lowest axial force is area 4 in load case 3409. The load area with the lowest value for axial force divided by shear force is area 4 in load case 3409 with a factor of 1.26.

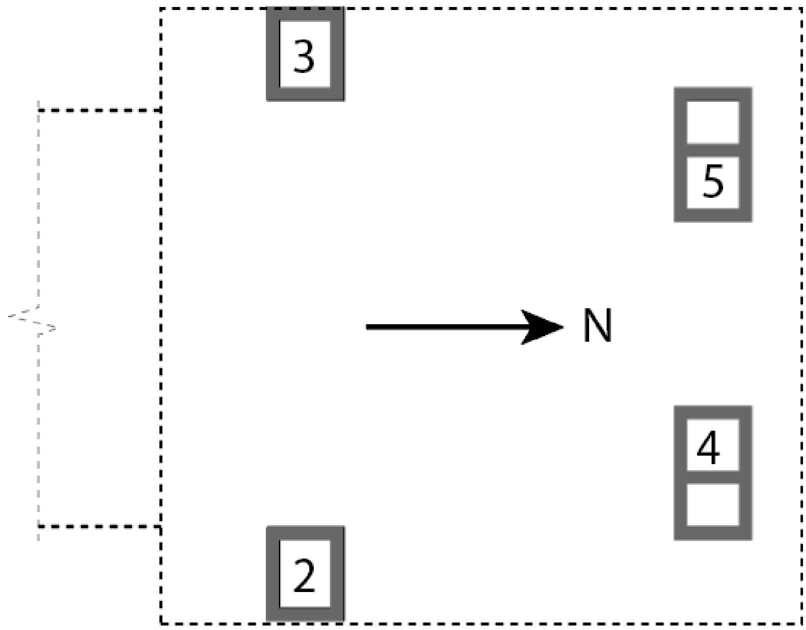

> *Figure 2-37: Numbering of foundation areas*

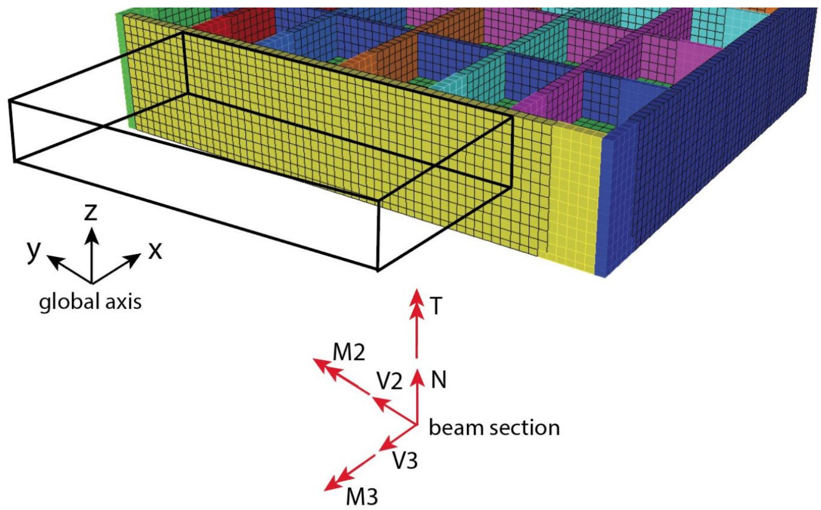

> *Figure 2-38: Definition of beam section forces.*

de-case	bs	N [kN]	V2 [kN]	V3 [kN]	T [kNm]	M2 [kNm]	M3 [kNm]	N/V
3101	1	-393086	798	-4794	-227674	-3096066	171545	33.06
3101	2	-131567	-63687	-14081	3817	-12970	80927	2.02
3101	3	-144832	61156	-8670	-5158	-59966	-103801	2.34
3101	4	-59268	1035	5964	-4243	-44534	12150	8.61
3101	5	-57419	2295	11993	-3426	-47369	-13018	4.46
3102	1	-381575	878	-5372	-267728	-2093942	19008	27.83
3102	2	-118947	-48665	2595	-4690	79093	46081	2.44
3102	3	-121031	46536	12620	8338	51334	-51208	2.49
3102	4	-71304	1689	-12445	-7199	-45367	10471	5.1
3102	5	-70293	1318	-8142	2409	-47449	-9890	8.06
3103	1	-382357	1018	-6218	-1624566	-2277292	8786	6.75
3103	2	-120266	-58080	-26824	7673	117809	44986	1.87
3103	3	-125720	42502	33467	15130	-28564	-67399	2.25
3103	4	-71179	8345	-18852	-18063	-39795	11681	2.98
3103	5	-65192	8250	5991	-10156	-51820	-9135	5.67
3104	1	-387997	-295	26290	91608	-3002096	-6466	13.32
3104	2	-135542	-58435	2058	-9782	-37199	86028	2.32
3104	3	-134761	59175	-1226	8111	-28466	-84754	2.28
3104	4	-58604	-472	13576	-438	-53663	13789	4.29
3104	5	-59090	-563	11882	2435	-52930	-13749	4.78
3105	1	-388056	-5218	1869	-17670	-2871092	-28082	67.48
3105	2	-134196	-60436	-4836	-2311	-20297	79178	2.22
3105	3	-132640	56588	-6125	-1791	-14268	-83496	2.33
3105	4	-60503	-969	6862	-1372	-47341	11765	8.41
3105	5	-60716	-400	5968	1627	-47316	-12571	9.63
3106	1	-379940	830	-4973	-265111	-2171237	-8936	28.72
3106	2	-120741	-49566	153	-2949	65245	50149	2.44
3106	3	-120752	47564	10625	7316	41938	-51973	2.47
3106	4	-69634	1595	-9790	-6471	-45018	10500	6.22
3106	5	-68813	1236	-5961	2378	-46889	-9683	10.5

> *Figure 2-39: Base reaction for GreenBox load case 31, part 1/2*

de-case	bs	N [kN]	V2 [kN]	V3 [kN]	T [kNm]	M2 [kNm]	M3 [kNm]	N/V
3107	1	-387578	-125	945	20194	-2593162	-135098	245.76
3107	2	-134121	-54228	-567	-2143	4210	78187	2.48
3107	3	-124015	55005	1478	5295	25757	-62327	2.26
3107	4	-64194	-577	1299	-866	-48352	12442	40.6
3107	5	-65248	-325	-1265	4641	-47261	-11104	29.43
3108	1	-392860	-173	1004	47881	-3311648	-51150	157.34
3108	2	-143355	-64778	-13974	5294	-68103	103593	2.16
3108	3	-139385	65387	-14678	-4969	-56641	-97429	2.08
3108	4	-54753	-1047	15678	1607	-47143	13393	3.42
3108	5	-55367	265	13978	682	-46425	-12861	3.93
3109	1	-388056	-294	1833	1485996	-2870867	-2268	8.09
3109	2	-135778	-51162	21881	-10768	-82987	91323	2.41
3109	3	-131052	65859	-32858	-10273	48476	-71337	1.76
3109	4	-57792	-7781	17847	11616	-52818	11222	2.68
3109	5	-63433	-7211	-5037	14615	-41821	-13110	5.91
3110	1	-384252	1017	-24944	-311866	-2261116	33110	11.1
3110	2	-121796	-52639	-8223	5630	66256	53477	2.28
3110	3	-125045	50101	3212	-1647	32375	-60706	2.49
3110	4	-69339	1485	-12571	-6588	-40108	9755	4.97
3110	5	-68072	2070	-7363	707	-42610	-9209	8.75
3111	1	-382357	5476	-6279	-214639	-2276916	32249	27.21
3111	2	-121767	-49440	-1746	-311	58930	56305	2.47
3111	3	-124209	51139	8362	7104	30403	-56056	2.39
3111	4	-68637	1935	-8545	-5882	-44926	11153	6.93
3111	5	-67745	1842	-4349	2026	-46660	-9654	13.29
3112	1	-395532	-125	624	46551	-3185659	49435	190.76
3112	2	-138395	-63423	-9272	1515	-41541	93671	2.16
3112	3	-141873	63563	-11946	-4005	-45293	-99455	2.19
3112	4	-57653	-774	10985	-206	-47606	13108	5.22
3112	5	-57611	510	10856	118	-47588	-13470	5.29

> *Figure 2-40: Base reaction for GreenBox load case 31, part 2/2*

de-case	bs	N [kN]	V2 [kN]	V3 [kN]	T [kNm]	M2 [kNm]	M3 [kNm]	N/V
3201	1	-388350	1422	-7345	-441295	-2860399	145668	18.41
3201	2	-127455	-61010	-15567	4962	15641	70490	2.02
3201	3	-139393	56920	-1448	-2036	-46851	-92377	2.45
3201	4	-61988	2319	358	-6724	-42904	11538	21.55
3201	5	-59514	3193	9313	-4024	-47131	-11732	5.61
3202	1	-381029	1351	-8283	-420517	-1902885	10818	17.82
3202	2	-116018	-46691	2748	-4632	107264	38240	2.48
3202	3	-117914	43417	18806	11062	66856	-43856	2.45
3202	4	-74311	2574	-18197	-9227	-44525	10234	3.68
3202	5	-72786	2052	-11640	1995	-47674	-9258	5.96
3203	1	-381836	1626	-10081	-3168829	-2201301	14901	3.52
3203	2	-116461	-64753	-55198	19253	195031	31380	1.33
3203	3	-127020	34110	62166	25260	-89338	-74975	1.69
3203	4	-75059	16173	-32796	-31843	-33189	12401	1.78
3203	5	-63296	16096	15747	-23426	-56648	-7670	2.44
3204	1	-388526	-507	52994	160095	-3203134	-3642	6.71
3204	2	-138460	-59349	8718	-19223	-63070	93117	2.29
3204	3	-137699	60607	2747	16330	-48540	-91524	2.27
3204	4	-55822	-523	22123	444	-60382	15584	2.52
3204	5	-56545	-1242	19407	2667	-59165	-15714	2.84
3205	1	-388526	-10553	3160	-64290	-2929710	-56789	33.08
3205	2	-135922	-63324	-5368	-3894	-28652	79383	2.14
3205	3	-132916	55248	-7035	-3682	-18409	-88143	2.39
3205	4	-59736	-1546	8383	-1394	-47499	11475	6.79
3205	5	-59953	-932	7179	1139	-47676	-13247	8.04
3206	1	-377836	1351	-8283	-420517	-2047878	10819	17.67
3206	2	-117415	-48542	-1731	-1681	85271	42759	2.42
3206	3	-119311	45267	14327	8111	44863	-48375	2.49
3206	4	-71318	2553	-13718	-8496	-43451	10008	4.57
3206	5	-69793	2073	-7160	1265	-46600	-9032	9.07

> *Figure 2-41: Base reaction for GreenBox load case 32, part 1/2*

de-case	bs	N [kN]	V2 [kN]	V3 [kN]	T [kNm]	M2 [kNm]	M3 [kNm]	N/V
3207	1	-382073	-450	3090	128321	-2289182	-142146	53.9
3207	2	-128469	-49020	7338	-6734	26611	65017	2.59
3207	3	-117544	50678	5380	8294	59026	-47268	2.3
3207	4	-67280	-853	-2636	-1198	-49108	11537	22.44
3207	5	-68780	-1255	-6992	7002	-47174	-10360	8.11
3208	1	-389351	-354	2140	114704	-3270406	-1582	68.15
3208	2	-140077	-63759	-12051	3910	-67776	97994	2.16
3208	3	-139592	64664	-16315	-6094	-57687	-97065	2.09
3208	4	-54571	-1171	16241	1454	-46924	12718	3.3
3208	5	-55112	-87	14264	827	-46054	-12767	3.82
3209	1	-388526	-507	3160	3002809	-2929709	-4566	4.03
3209	2	-139171	-44407	49139	-21163	-156610	104198	2.01
3209	3	-129666	74165	-61542	-20951	109550	-63328	1.31
3209	4	-54199	-15439	30813	25103	-58691	10373	1.39
3209	5	-65490	-14825	-15250	27636	-36485	-14348	2.57
3210	1	-381836	1626	-48104	-498715	-1992683	14034	6.01
3210	2	-117775	-50840	-15127	14315	101480	43296	2.19
3210	3	-120120	46967	3885	-6643	53464	-50000	2.55
3210	4	-72889	2280	-22345	-8653	-33748	8087	3.02
3210	5	-71052	3220	-14516	0	-37493	-6967	4.78
3211	1	-381836	10720	-10081	-295614	-2201300	62139	17.33
3211	2	-119552	-47144	-4074	2952	74915	54511	2.53
3211	3	-123930	51718	11042	8959	30779	-51844	2.33
3211	4	-69867	3111	-11754	-7012	-43677	11339	5.17
3211	5	-68488	3034	-5295	1405	-46160	-8733	10.79
3212	1	-393710	-354	2140	114704	-3114527	-1582	68.92
3212	2	-138812	-61828	-6911	486	-42745	93481	2.24
3212	3	-138327	62732	-11175	-2670	-32655	-92552	2.17
3212	4	-58015	-1167	11101	651	-48266	13070	5.14
3212	5	-58556	-91	9124	1630	-47397	-13119	6.2

> *Figure 2-42: Base reaction for GreenBox load case 32, part 2/2*

de-case	bs	N [kN]	V2 [kN]	V3 [kN]	T [kNm]	M2 [kNm]	M3 [kNm]	N/V
3301	1	-396074	895	-5349	-257447	-3262182	172809	29.62
3301	2	-134780	-66369	-17648	5861	-26761	88391	1.96
3301	3	-148220	63604	-11117	-6738	-76654	-111694	2.29
3301	4	-57521	1032	8452	-3792	-44395	12661	6.21
3301	5	-55553	2628	14964	-4420	-47457	-13477	3.46
3302	1	-381404	996	-5945	-308867	-1989297	19260	24.5
3302	2	-117248	-47377	3965	-5563	93138	41704	2.47
3302	3	-119464	44920	15560	9881	61612	-47269	2.48
3302	4	-72929	1968	-15209	-8024	-45338	10351	4.31
3302	5	-71764	1485	-10262	2518	-47724	-9688	6.61
3303	1	-382186	1136	-6791	-1665705	-2172648	9038	6.53
3303	2	-118566	-56792	-25453	6801	131853	40609	1.89
3303	3	-124153	40887	36407	16673	-18287	-63459	2.18
3303	4	-72804	8624	-21616	-18888	-39766	11560	2.72
3303	5	-66663	8417	3871	-10047	-52095	-8932	6.5
3304	1	-390990	-277	26134	87043	-3170735	-6002	13.56
3304	2	-138856	-61027	-943	-8075	-52485	93743	2.28
3304	3	-138120	61733	-4060	6471	-44239	-92563	2.23
3304	4	-56774	-609	16376	242	-53716	14305	3.46
3304	5	-57241	-373	14761	1665	-53020	-14259	3.8
3305	1	-391049	-5200	1713	-22235	-3039732	-27618	68.27
3305	2	-137510	-63028	-7837	-604	-35583	86893	2.17
3305	3	-136000	59146	-8959	-3431	-30041	-91305	2.27
3305	4	-58673	-1106	9662	-692	-47394	12281	5.95
3305	5	-58867	-211	8846	857	-47406	-13080	6.53
3306	1	-379769	948	-5546	-306250	-2066591	-8683	25.18
3306	2	-119041	-48278	1524	-3822	79290	45772	2.47
3306	3	-119185	45949	13566	8858	52216	-48033	2.47
3306	4	-71259	1874	-12554	-7296	-44989	10380	5.05
3306	5	-70284	1403	-8082	2488	-47164	-9481	8.09

> *Figure 2-43: Base reaction for GreenBox load case 33, part 1/2*

de-case	bs	N [kN]	V2 [kN]	V3 [kN]	T [kNm]	M2 [kNm]	M3 [kNm]	N/V
3307	1	-387412	-85	771	4286	-2491041	-135638	426.63
3307	2	-132521	-52851	1369	-3353	16759	74062	2.51
3307	3	-122419	53501	4031	6777	36949	-58303	2.28
3307	4	-65737	-432	-1152	-1462	-48517	12326	43.61
3307	5	-66735	-302	-3477	4974	-47538	-10952	14.89
3308	1	-395853	-155	848	43316	-3480288	-50686	180.05
3308	2	-146668	-67371	-16975	7001	-83390	111308	2.11
3308	3	-142745	67945	-17511	-6610	-72414	-105237	2.03
3308	4	-52923	-1184	18478	2287	-47197	13909	2.79
3308	5	-53517	455	16856	-88	-46514	-13371	3.18
3309	1	-391049	-276	1677	1481431	-3039508	-1804	8.21
3309	2	-139092	-53755	18880	-9061	-98274	99038	2.42
3309	3	-134411	68418	-35692	-11913	32703	-79146	1.72
3309	4	-55963	-7917	20647	12296	-52871	11738	2.3
3309	5	-61584	-7022	-2158	13846	-41911	-13619	7.18
3310	1	-384081	1135	-25517	-353004	-2156472	33363	10.53
3310	2	-120097	-51351	-6852	4758	80301	49100	2.32
3310	3	-123478	48485	6152	-105	42653	-56766	2.53
3310	4	-70964	1764	-15334	-7413	-40079	9635	4.2
3310	5	-69543	2237	-9483	817	-42886	-9006	7.03
3311	1	-382185	5594	-6852	-255777	-2172249	32501	24.17
3311	2	-120066	-48151	-375	-1183	72975	51927	2.5
3311	3	-122641	49523	11302	8647	40682	-52115	2.4
3311	4	-70262	2214	-11309	-6707	-44897	11033	5.48
3311	5	-69215	2009	-6469	2135	-46935	-9451	9.64
3312	1	-398525	-106	468	42009	-3354299	49905	224.43
3312	2	-141708	-66016	-12273	3223	-56827	101387	2.11
3312	3	-145233	66121	-14780	-5645	-61067	-107263	2.14
3312	4	-55823	-911	13785	475	-47660	13624	4.02
3312	5	-55761	699	13735	-652	-47678	-13979	4.02

> *Figure 2-44: Base reaction for GreenBox load case 33, part 2/2*

de-case	bs	N [kN]	V2 [kN]	V3 [kN]	T [kNm]	M2 [kNm]	M3 [kNm]	N/V
3401	1	-391337	1518	-7900	-471091	-3026494	146927	17.34
3401	2	-130668	-63691	-19134	7006	1852	77952	1.96
3401	3	-142781	59367	-3894	-3616	-63538	-100270	2.4
3401	4	-60241	2316	2845	-6273	-42764	12049	12.8
3401	5	-57648	3526	12284	-5018	-47219	-12192	4.2
3402	1	-380858	1469	-8856	-461656	-1798240	11071	16.39
3402	2	-114318	-45404	4119	-5504	121308	33863	2.51
3402	3	-116347	41801	21747	12604	77134	-39916	2.41
3402	4	-75936	2853	-20961	-10052	-44496	10114	3.29
3402	5	-74257	2219	-13760	2105	-47949	-9056	5.18
3403	1	-381665	1744	-10653	-3209968	-2096657	15154	3.46
3403	2	-114762	-63465	-53827	18380	209075	27003	1.35
3403	3	-125453	32495	65106	26802	-79060	-71035	1.62
3403	4	-76684	16452	-35560	-32668	-33160	12281	1.7
3403	5	-64767	16263	13627	-23316	-56923	-7468	2.65
3404	1	-391519	-489	52838	155529	-3371774	-3178	6.79
3404	2	-141773	-61942	5716	-17516	-78356	100832	2.27
3404	3	-141059	63165	-87	14690	-64314	-99333	2.24
3404	4	-53992	-659	24923	1124	-60435	16100	2.15
3404	5	-54695	-1053	22285	1897	-59255	-16223	2.42
3405	1	-391519	-10534	3003	-68833	-3098346	-56320	33.41
3405	2	-139235	-65916	-8369	-2187	-43938	87098	2.1
3405	3	-136275	57807	-9868	-5323	-34182	-95951	2.32
3405	4	-57906	-1683	11183	-713	-47552	11991	5.06
3405	5	-58103	-743	10057	370	-47766	-13756	5.72
3406	1	-377665	1469	-8856	-461656	-1943233	11071	16.26
3406	2	-115715	-47254	-360	-2554	99316	38382	2.45
3406	3	-117744	43651	17267	9654	55141	-44435	2.47
3406	4	-72943	2832	-16482	-9322	-43423	9887	3.93
3406	5	-71263	2240	-9281	1374	-46875	-8830	7.27

> *Figure 2-45: Base reaction for GreenBox load case 34, part 1/2*

de-case	bs	N [kN]	V2 [kN]	V3 [kN]	T [kNm]	M2 [kNm]	M3 [kNm]	N/V
3407	1	-381908	-410	2916	112413	-2187083	-142687	59.49
3407	2	-126870	-47644	9274	-7944	39159	60893	2.6
3407	3	-115949	49174	7933	9775	70217	-43244	2.32
3407	4	-68822	-708	-5087	-1793	-49273	11421	12.54
3407	5	-70267	-1232	-9204	7336	-47451	-10209	6.55
3408	1	-392344	-335	1984	110162	-3439046	-1112	72.45
3408	2	-143390	-66352	-15052	5618	-83063	105709	2.1
3408	3	-142952	67223	-19148	-7734	-73460	-104873	2.04
3408	4	-52741	-1308	19041	2135	-46977	13234	2.71
3408	5	-53262	102	17143	57	-46144	-13277	3.11
3409	1	-391519	-489	3003	2998244	-3098344	-4102	4.08
3409	2	-142484	-47000	46138	-19456	-171896	111912	2.08
3409	3	-133026	76723	-64375	-22592	93777	-71137	1.3
3409	4	-52369	-15576	33612	25784	-58744	10889	1.26
3409	5	-63640	-14636	-12372	26867	-36575	-14858	2.77
3410	1	-381665	1744	-48676	-539854	-1888038	14287	5.84
3410	2	-116075	-49552	-13756	13443	115524	38919	2.23
3410	3	-118553	45352	6825	-5101	63741	-46060	2.58
3410	4	-74514	2558	-25109	-9478	-33720	7966	2.75
3410	5	-72523	3387	-16637	110	-37769	-6765	4.27
3411	1	-381665	10838	-10654	-336753	-2096656	62392	16.09
3411	2	-117852	-45856	-2703	2080	88959	50134	2.57
3411	3	-122363	50103	13982	10502	41056	-47904	2.33
3411	4	-71492	3390	-14518	-7837	-43648	11219	4.35
3411	5	-69959	3201	-7415	1515	-46435	-8531	8.38
3412	1	-396703	-335	1984	110161	-3283167	-1113	73.26
3412	2	-142125	-64420	-9912	2193	-58031	101197	2.18
3412	3	-141687	65291	-14008	-4310	-48429	-100360	2.12
3412	4	-56185	-1304	13901	1332	-48320	13586	3.95

> *Figure 2-46: Base reaction for GreenBox load case 34, part 2/2*

2.6.3 Sliding resistance

The figure below shows the axial force divided by the shear force (x and y direction) for each gauss point in the foundation. For the local foundation area 2-4 there are areas with lower axial force than shear, but each foundation (i.e. foot print) area has an individual total axial force that is greater than the shear. The lowest factor is 1.26 for area 4 in load case 3409. The shear force is transferred to the rock due to friction and axial force. The friction coefficient is assumed to be 1.0.

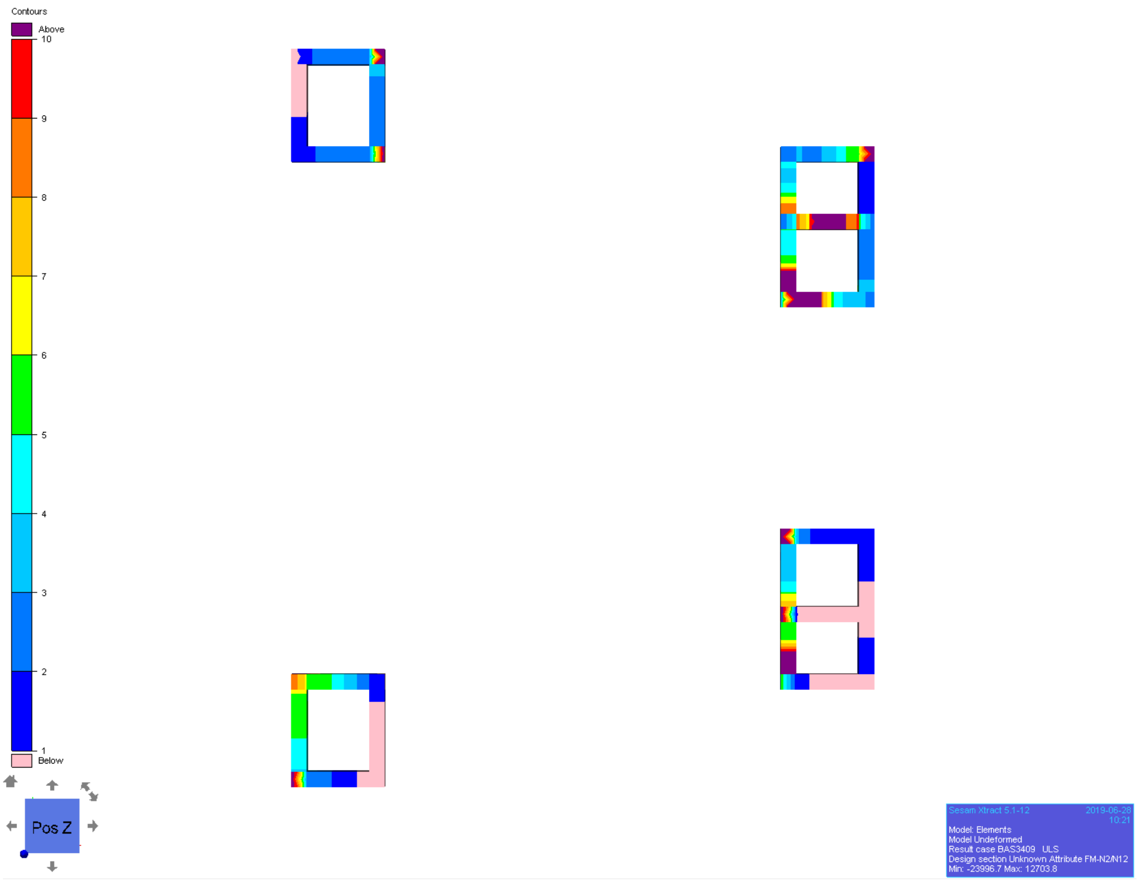

> *Figure 2-47: Axial force divided by shear force for each footing section in foundation, load case 3409*

de-case	bs	N [kN]	V2 [kN]	V3 [kN]	T [kNm]	M2 [kNm]	M3 [kNm]	N/V
3409	1	-391519	-489	3003	2998244	-3098344	-4102	4.08
3409	2	-142484	-47000	46138	-19456	-171896	111912	2.08
3409	3	-133026	76723	-64375	-22592	93777	-71137	1.3
3409	4	-52369	-15576	33612	25784	-58744	10889	1.26
3409	5	-63640	-14636	-12372	26867	-36575	-14858	2.77

> *Figure 2-48: Corresponding integrated beam forces for each local area, load case 3409*

2.6.4 Overturning stability

There are two load cases (3203 and 3403) that are resulting in tensile forces in the foundation for ULS loads. 3403 has the lowest ratio of axial force to shear force, and its axial force in the transition to the rock is shown below, tension is indicated by purple color. In SLS there are no points with uplift in the abutment.

With compression in almost the entire foundation there is no risk of overturning.

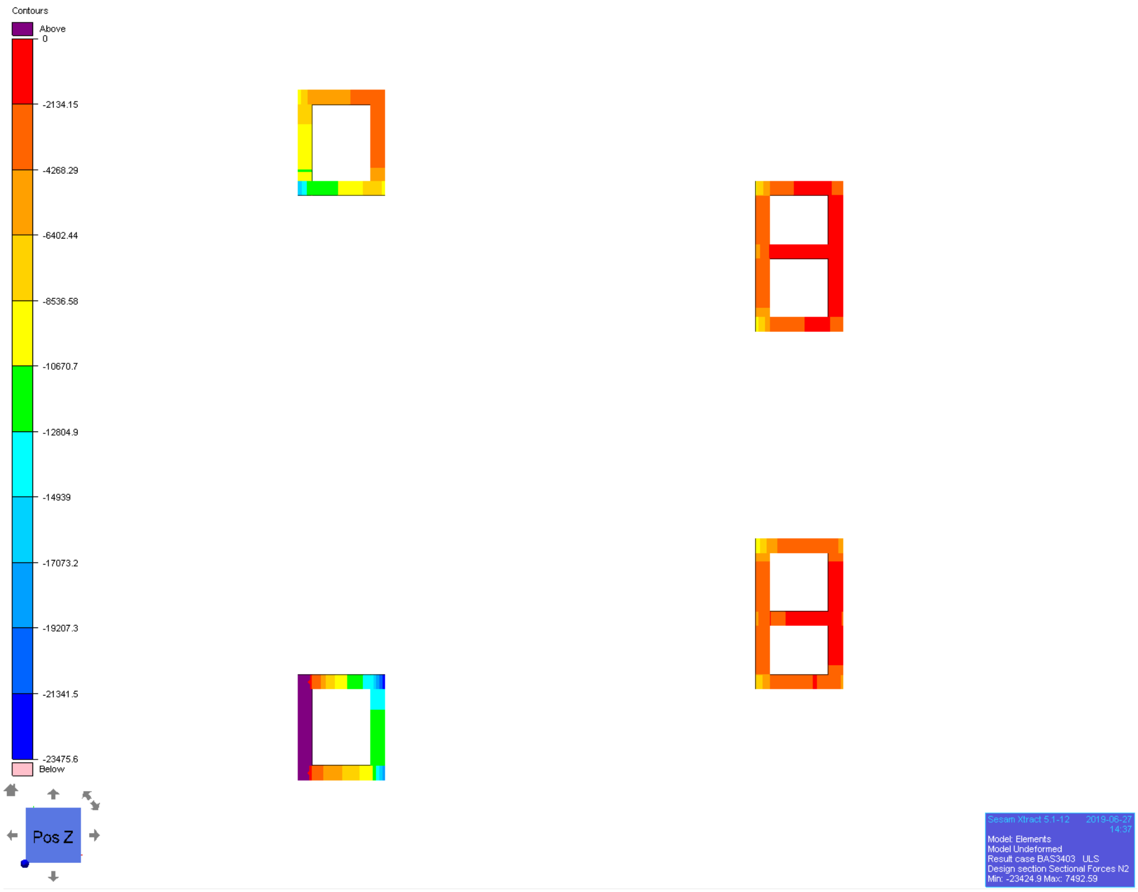

> *Figure 2-49: Axial force in foundation, load case 3403*

2.6.5 Rock anchor design

There is applied totally 38 pcs. of 6-19 vertical rock anchors, with total stressing force 92.6 MN (after losses). The vertical stressing force corresponds to 92.63 / 325.38 => 28% of the permanent vertical force, which complies with the requirements in N400 11.6.2.2 [2]. See Table 2-2. The abutment has good capability for redistribution of forces. The model plot in Figure 2-50 shows the configuration of rock anchors, within in the front foot print area.

> *Table 2-2: Permanent vertical force and rock anchor force.*

Load	Vertical component (MN)
Selfweight	161.07
Ballast, lower cells	42.08
Ballast, upper cells	29.61
Post-tensioning (rock anchors)	92.63
Sum vertical component	325.38

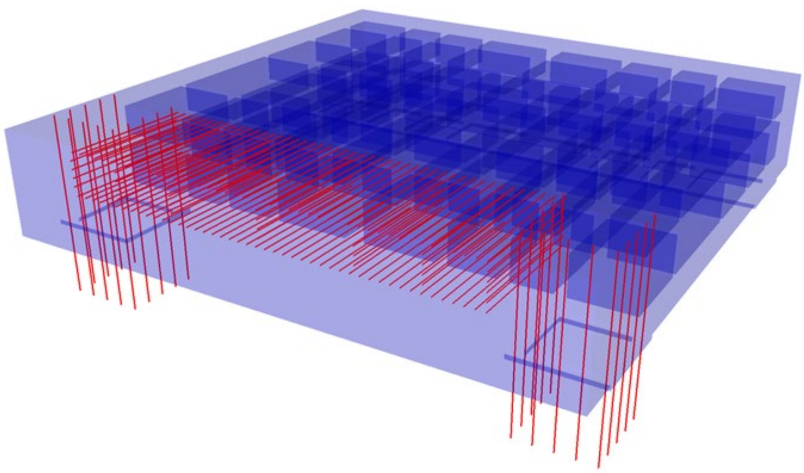

> *Figure 2-50: Rock anchor configuration and longitudinal post-tensioning. (The figure shows 2 x 13 rock anchors, but it is included 2 x 19 rock anchors in the current calculations).*

2.7 Bridge girder end section

2.7.1 Design loads for the post-tensioned connection

The design of the post-tensioned connection between abutment and bridge end girder is based on the ULS loads from the global analysis model 16. These loads are summarized in Table 2-3. The loads represent one of four ULS combinations. All combinations are run and the LC34 is governing.

> *Table 2-3 ULS design loads (LC34 in Greenbox) at bridge girder end. Extreme value for each load effect (red) together with coincident values (black).*

	Nx		Ny		Nz		Mx		My		Mz	
	Max	Min	Max	Min	Max	Min	Max	Min	Max	Min	Max	Min
Fx	51	-57	7	-20	-14	6	-19	7	-14	6	-20	7
Fy	1	-3	10	-11	-2	1	-3	1	-2	1	-3	1
Fz	-19	-9	-19	-9	-5	-24	-15	-13	-9	-20	-9	-19
Mx	-5	10	-5	10	6	-4	147	-140	6	-4	10	-5
My	-657	40	-657	40	106	-727	-477	-141	335	-948	40	-657
Mz	-380	893	-380	893	662	-320	858	-344	662	-320	3 291	-2 719

2.7.2 Cross section properties

The stiffness of the bridge girder is increasing towards the abutment. The end section is connected to the steel end frame, with holes for the post-tensioning anchors. The stiffeners and the holes are arranged in a system with center distance 600 mm. Figure 2-51 below shows the cross-section geometry of the girder end section at the connection to the end frame. The end frame plate has a general width of 800 mm. The net contact area is 53.1 m^2 when accounting for the holes for the PT trumpets (net-to-gross ratio ~0.92)

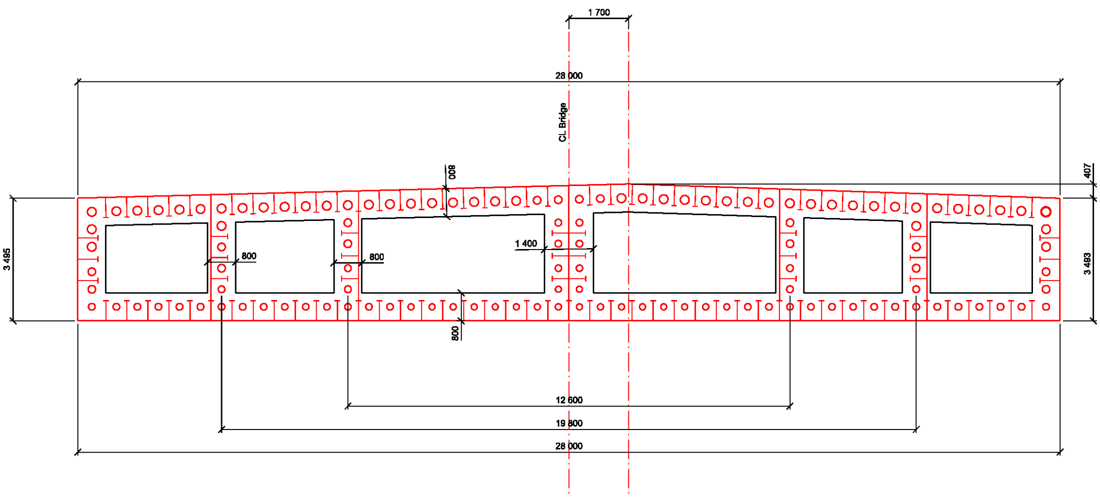

> *Figure 2-51 Cross section of bridge girder end section at the connection to the end steel frame.*

For information regarding bridge girder cross section properties and utilization, reference is made to [3].
The center distance between the trapeze stiffeners in the bridge girder end section matches the T-stiffeners in the general bridge girder section. The transition from T-stiffeners to trapeze stiffeners is shown in Figure 2-52.

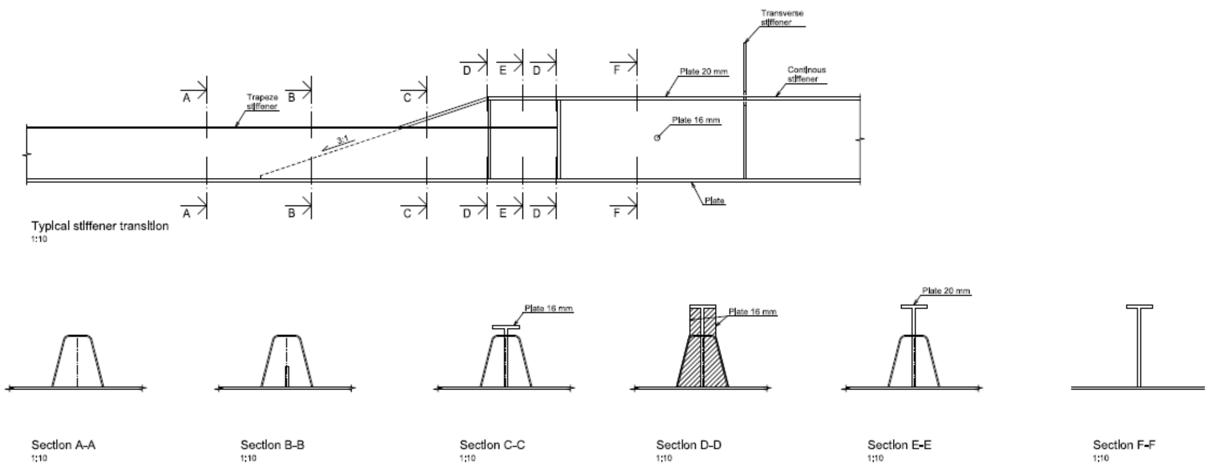

> *Figure 2-52 Stiffener transition from trapeze stiffener to T-stiffener*

2.8 Bridge girder connection

2.8.1 General

In the girder-to-abutment connection the bridge terminal end is coupled to the abutment front face. The bridge girder is cast integrally with the abutment by the pre-installation of a bridge girder transition segment, as outlined in Figure 2-53. A cast-in-place joint is deemed necessary to assure uniform distribution of the contact forces and to allow ample time (> 8 weeks) for placement and stressing of the PT tendons.

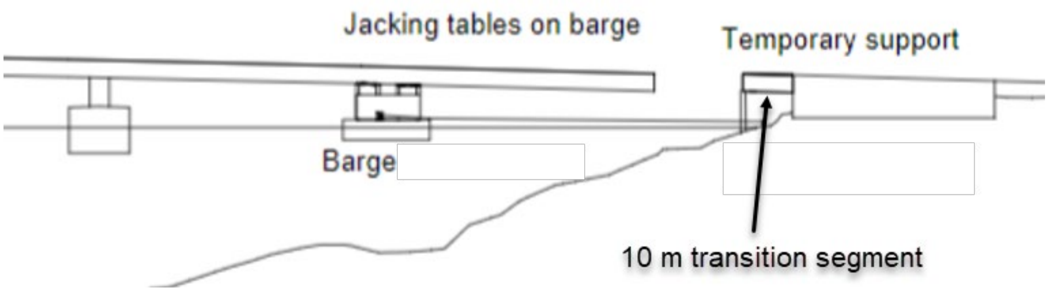

> *Figure 2-53 A 10 m long bridge girder transition element is installed and connected to the abutment.*

The post-tensioning arrangement at the girder end frame is shown in Figure 2-54, where the numbers indicates number of strands in each tendon.

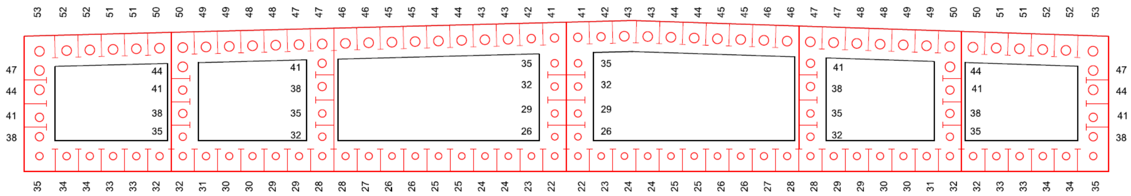

> *Figure 2-54 Arrangement of the post-tensioning at connection to abutment* (showing *number of 0.6" strands per tendon).*

2.8.2 Verification of axial force and flexural resistance

Because of the bridge segment installation procedure, where the bridge segment dead load is applied before it is connected to the transition segment, the weak axis design moment due to dead load is somewhat reduced when designing the post-tensioned connection. The reduced moment is approximately 75 % of the green box design moment.
The design criteria for the post-tensioning cables in the intersection between the bridge and the abutment is that tension across the joint interface is not allowed for any ULS load combination. The maximum allowed utilization of the concrete compression capacity is set to approximately 80% to have some reserves for stress concentrations that may occur locally behind the plate stiffeners.

The normal stress on the concrete is calculated according to linear-elastic theory from the following expression:

$$\sigma = \frac{N}{A} + \frac{Mz}{Iz}y + \frac{My}{Iy}z$$

Due to the high compression stress level concrete grade B85 with a design compressive strength f_{cd} of 48.2 MPa is required in the areas closest to the PT anchors. The rest of the abutment can have much lower concrete grade.

For the north abutment a total of 124 post-tensioning tendons is needed to suppress tensile stresses over the joint, with a total post-tensioning force equal to 1 173 MN (before losses). The tendon size varies from 6-53 in the upper corner to 6-22 in the lower mid, with strand intensity varying according to the linear stress distribution. See Figure 2-54.

The average concrete compressive stress resulting from post-tensioning varies from approximately 8 to 20 MPa. The compressive stresses at service load level is well within the limits to avoid longitudinal cracks, micro-cracks and excessive creep. The highest compressive stress is found in the upper corner where the combination of large M_y and M_z governs the design.

The post-tensioning forces and stresses from bridge end forces and post-tensioning, together with an overview of the calculation points are summarized in the figure below. The figure shows values for load case $M_{z,min}$ according to Table 2-3, which is governing for post tensioning in the top slab.

Calc. point	Strands	PT-force			tresses due to bridge end force			Stresses due to PT			Resulting stresses			Necessary f_{ck}	
c_0	38	F_{p0}	-88.76	MN	$\sigma_{c.0}$	9.77	MPa	$\sigma_{c.0}$	-14.73	MPa	$\sigma_{res.0}$	-4.97	MPa	49.0	MPa
c_4	17	F_{p4}	-39.71	MN	$\sigma_{c.4}$	-9.50	MPa	$\sigma_{c.4}$	-6.59	MPa	$\sigma_{res.4}$	-16.09	MPa	31.0	MPa
c_5	35	F_{p5}	-46.93	MN	$\sigma_{c.5}$	0.91	MPa	$\sigma_{c.5}$	-13.57	MPa	$\sigma_{res.5}$	-12.66	MPa	30.9	MPa
c_{5b}	27	F_{p5b}	-35.44	MN	$\sigma_{c.5b}$	-1.84	MPa	$\sigma_{c.5b}$	-10.47	MPa	$\sigma_{res.5b}$	-12.31	MPa	25.8	MPa
c_{5c}	22	F_{p5c}	-51.39	MN	$\sigma_{c.5c}$	-4.52	MPa	$\sigma_{c.5c}$	-8.53	MPa	$\sigma_{res.5c}$	-13.05	MPa	26.4	MPa
c_7	53	F_{p7}	-71.07	MN	$\sigma_{c.7}$	20.18	MPa	$\sigma_{c.7}$	-20.55	MPa	$\sigma_{res.7}$	-0.37	MPa	79.9	MPa
c_{7b}	47	F_{p7b}	-61.69	MN	$\sigma_{c.7b}$	17.43	MPa	$\sigma_{c.7b}$	-18.22	MPa	$\sigma_{res.7b}$	-0.80	MPa	70.1	MPa
c_{7c}	39	F_{p7c}	-91.10	MN	$\sigma_{c.7c}$	14.75	MPa	$\sigma_{c.7c}$	-15.12	MPa	$\sigma_{res.7c}$	-0.37	MPa	58.6	MPa

> *Figure 2-55 Post-tensioning forces, and stresses from bridge end forces and post-tensioning. Shown load case is $M_{z,min}$ with corresponding forces and moments.*

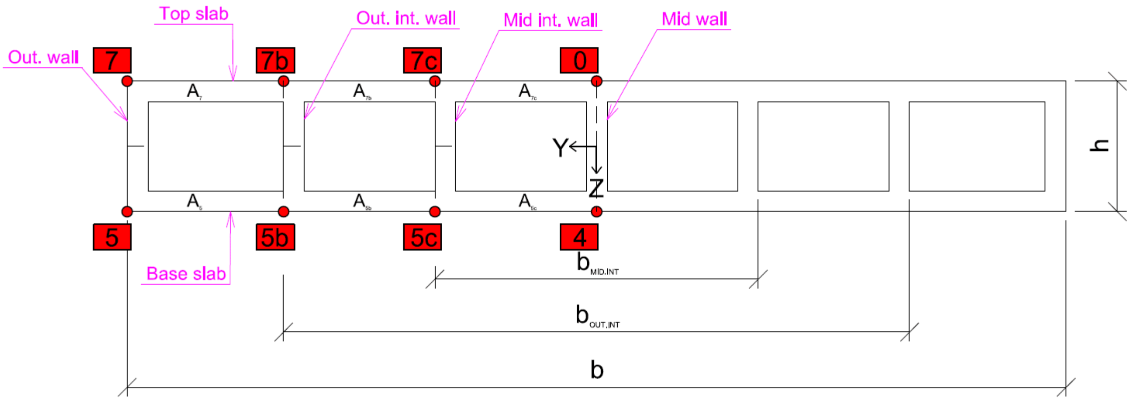

> *Figure 2-56: The calculation points applied*

2.8.3 Verification of shear and torsion resistance

The shear forces are transferred from the steel bridge girder to the concrete by means of steel shear keys welded to the back of the end plate. Typical arrangement and layout are shown in Figure 2-57.
Although this is not a typical casting joint, the shear resistance at the interface is calculated according to the provisions for ordinary construction joints in EC2. The design requirement for the post-tensioning crossing the joint is that there should always be contact between the steel and the concrete. Therefore, there will always be contact pressure and friction between the surfaces.

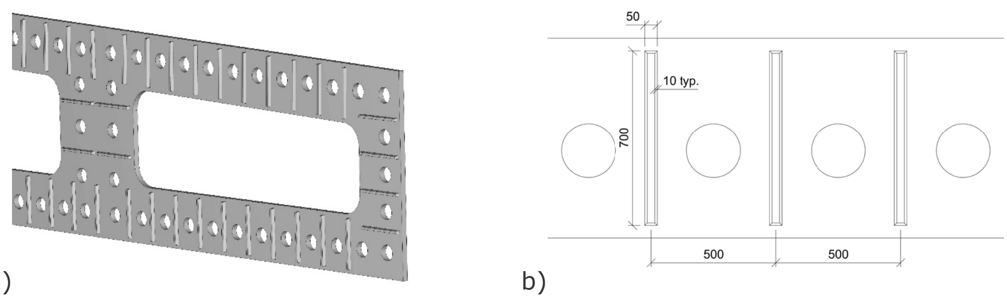

a) b)

> *Figure 2-57 Shear keys; (a) arrangement and (b) typical configuration.*

With concrete grade B85 and with the size and spacing of the key satisfying an indented interface the formula according to 6.2.5 in NS-EN1992 [1] can be expressed as:

$$v_{Rdi} = 0.5 * f_{ctd} + 0.9 * \sigma_n$$

The contribution from the post-tensioning steel to the shear resistance is neglected.

The shear and torsion resistance is summarized in Table 2-4 below, for load case $M_{z,min}$. τ_{res} = 1.297 MPa, includes resulting shear stress from V_y, V_z and torsion.

> *Table 2-4: Shear and torsion resistance summary, for $M_{z,min}$.*

$v_{Rd,i} = -0.5 \times f_{ctd} + 0.9 \times \sigma_{res,i}$			$v_{Rd,i} - \tau_{res}$	
$v_{Rd.0}$	5.45	MPa	4.15	MPa
$v_{Rd.4}$	15.46	MPa	14.16	MPa
$v_{Rd.5}$	12.37	MPa	11.07	MPa
$v_{Rd.5b}$	12.05	MPa	10.76	MPa
$v_{Rd.5c}$	12.72	MPa	11.42	MPa
$v_{Rd.7}$	1.31	MPa	0.02	MPa
$v_{Rd.7b}$	1.70	MPa	0.40	MPa
$v_{Rd.7c}$	1.31	MPa	0.02	MPa

2.9 Bill of Quantities

Table 2-5: Material quantities for abutment north.

Item	Quantity	Unit
Concrete	6 753	m^3
Ballast[1)]	2 496	m^3
Reinforcement	1 553	t
Post-tensioning	11 727	MNm
Rock anchors	1 992	MNm
Formwork (walls)	5 245	m^2
Lean concrete (under top/mid slabs)	83	m^3
EPS (under base slab)	1 500	m^2
Rock blasting and excavation	4 500	m^3

Note 1: Ballast with density 30 kN/m^3.

3 ABUTMENT SOUTH

3.1 General description

In general, the south abutment structure follows the same design principles as the north abutment, and for a general description reference is made to abutment north as described in section 2.1.

Generally, the bridge girder end forces at abutment south is somewhat smaller than for abutment north, except for the axial force (compression) which is more than the double. With the current location the abutment will have a height of approximately 15 m. This generates a significant mass, and rock anchors will not be necessary. Normal ballast with density 20 kN/m^3 is assumed in the chambers.

The post-tensioning level is lower compared to the north abutment. The total amount of horizontal post-tensioning is 84 horizontal tendons (with varying no. of strands) arranged with 600 mm center distances.

Placing the abutment some 10 meters further south will reduce the height, as the ground forms a slope towards the sea. This is recommended to do in a later design phase and will be esthetically as well as economically beneficial. The southern span of the cable stayed bridge will then be correspondingly longer.
Depending on the location of the abutment, there may also be an opportunity to provide anchorage by post-tensioning directly into the splay chamber. It may then be possible to further reduce the abutment dimensions, since such arrangement may be higher utilized compared to rock anchors.

3.2 Analytical model

Reference is made to the description regarding abutment north in section 2.2. The same parametric system with loads fetched from the latest GreenBox results are used here.

3.3 Design loads

Reference is made to the description regarding abutment north in section 2.3.

Loads effects related to the cable-stayed bridge construction phase will have an impact on the abutment. This is not considered in the design at this stage, but stresses in the bridge girder end is checked for 50-year wind combination on bridge tower. The observation is that the stresses are lower than for the included combinations. Hence this is no further investigated in current design phase.

3.4 Caisson concrete structural design

3.4.1 General

The abutment structures and the distribution of the base reactions used in the global stability control is predicted by means of the 3-dimensional solid FE-model and the results are extracted by using ShellDesign.
Ballast with density 20 kN/m^3 is assumed.

3.4.2 Structural configuration

The principle with the cellular box configuration is the same as for abutment north (as described in section 2.5.2), but with different dimensions. Abutment south is higher and slightly shorter but the width is equal, compared to abutment north. Section and plan are shown in Figure 2-25. There are no rock anchors in abutment south.

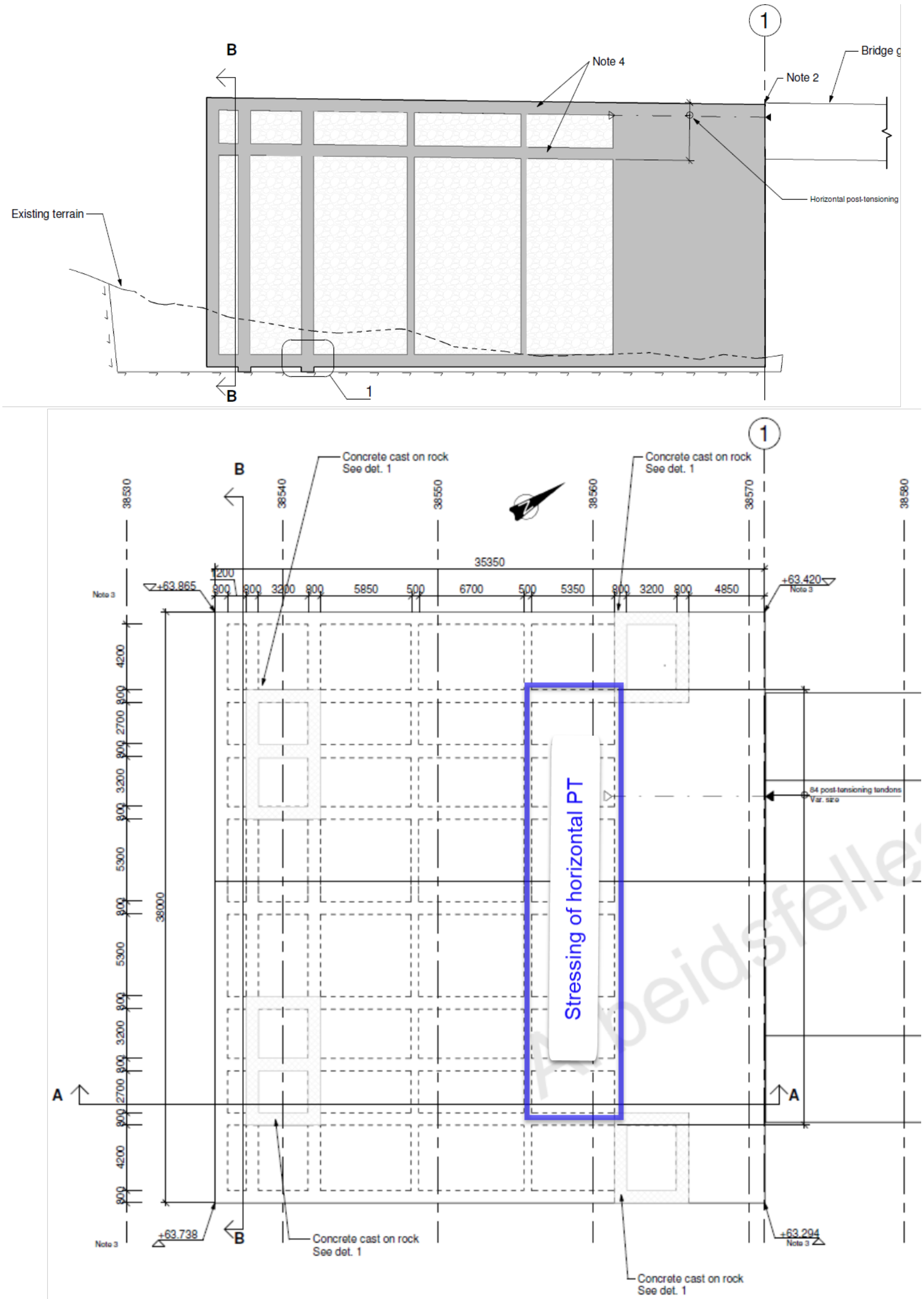

> *Figure 3-1 Cellular configuration of abutment, showing concrete filled cells in the front, and locations for stressing the horizontal post-tensioning.*

3.4.3 Concrete structural design

The solid concrete part towards the main span have a concrete material of B85 because of the post-tension anchoring. The lower section in this part could be of a lower concrete grade. The rest of the structure is set to B45.

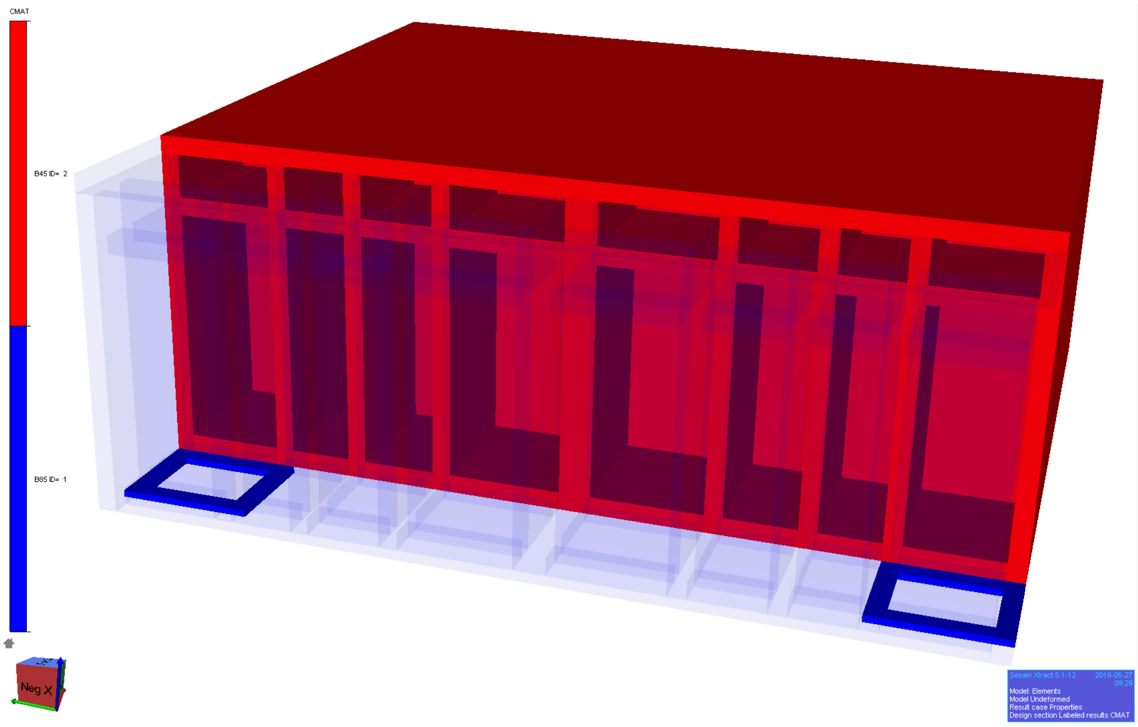

> *Figure 3-2 Concrete grade B85 in the front part (not needed over the entire height) and B45 in the rest of the structure*

A small intensity of shear reinforcement (approximately ø12 c200c200) is necessary in about 1/3 of the length. For wall in the lower chamber it is assumed that most of the stirrups can be removed. The rest of the shear reinforcement has a low utilization, but there need to be some of it present.

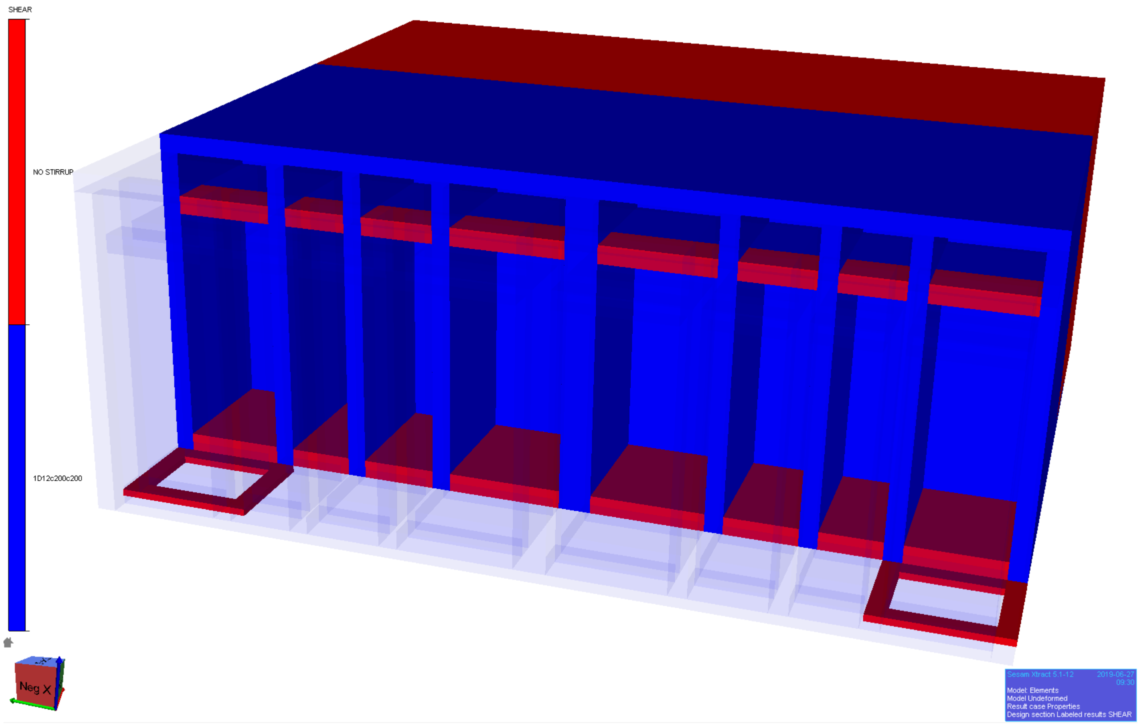

> *Figure 3-3 A small amount of shear reinforcement is necessary in the blue areas.*

Reinforcement in bridge direction, equal intensity at both faces. Green areas indicates ø32 c100, dark blue is ø25 c100 and red is ø25 c200.

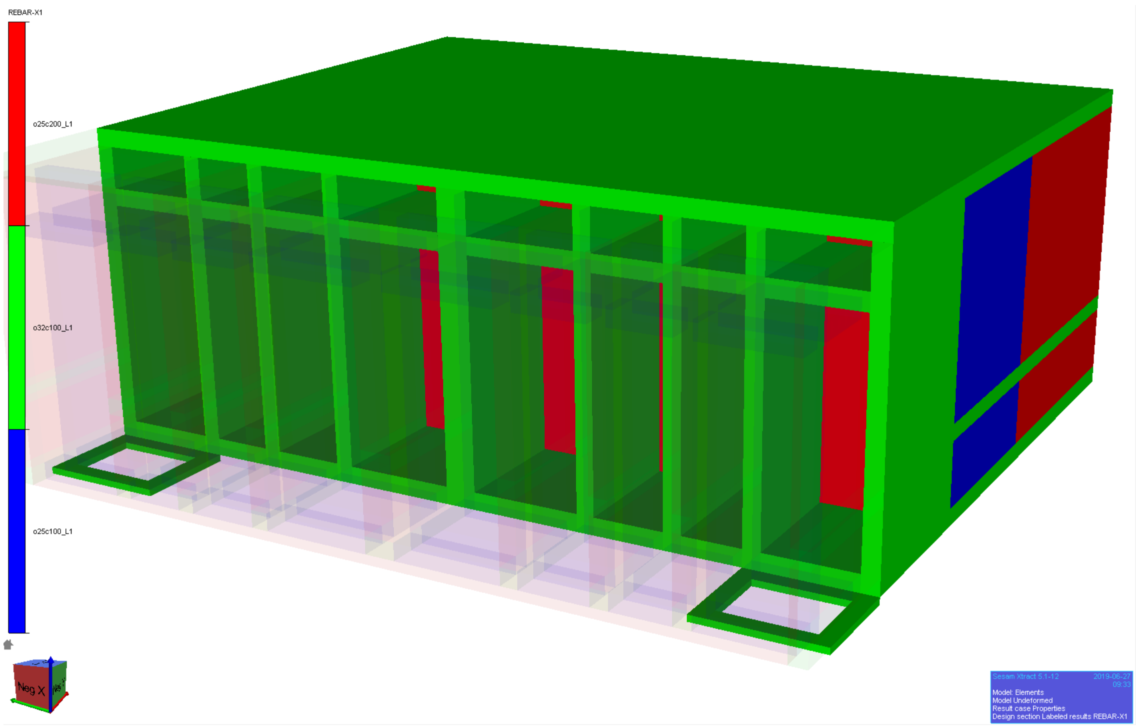

> *Figure 3-4 Reinforcement intensity in bridge (longitudinal) direction.*

Reinforcement normal to the bridge direction (slabs) and vertical (walls), equal intensity at both faces. Green color indicates ø32 c100, blue is ø25 c100 and red is ø25 c200.

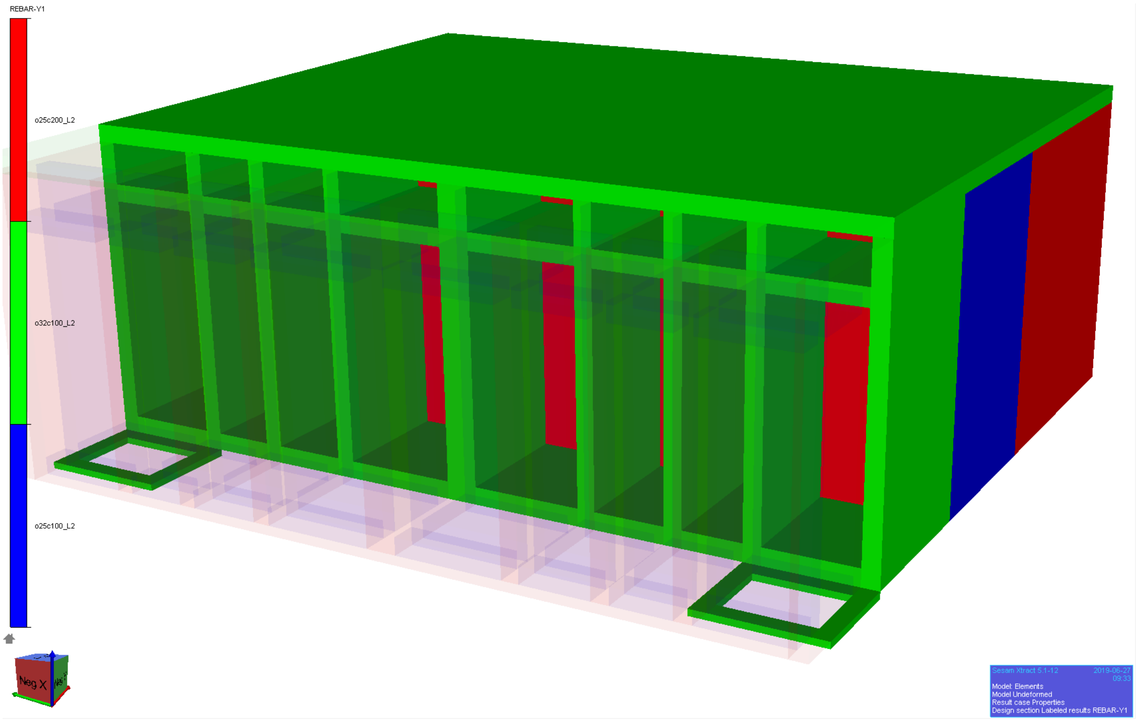

> *Figure 3-5 Reinforcement intensity in transverse direction (vertical for walls).*

The utilizations shown in the following figures are within acceptable limits except for local areas around the post-tensioning anchors. These areas should be evaluated in the next phase. Figure 2-30 shows utilization for compression of concrete

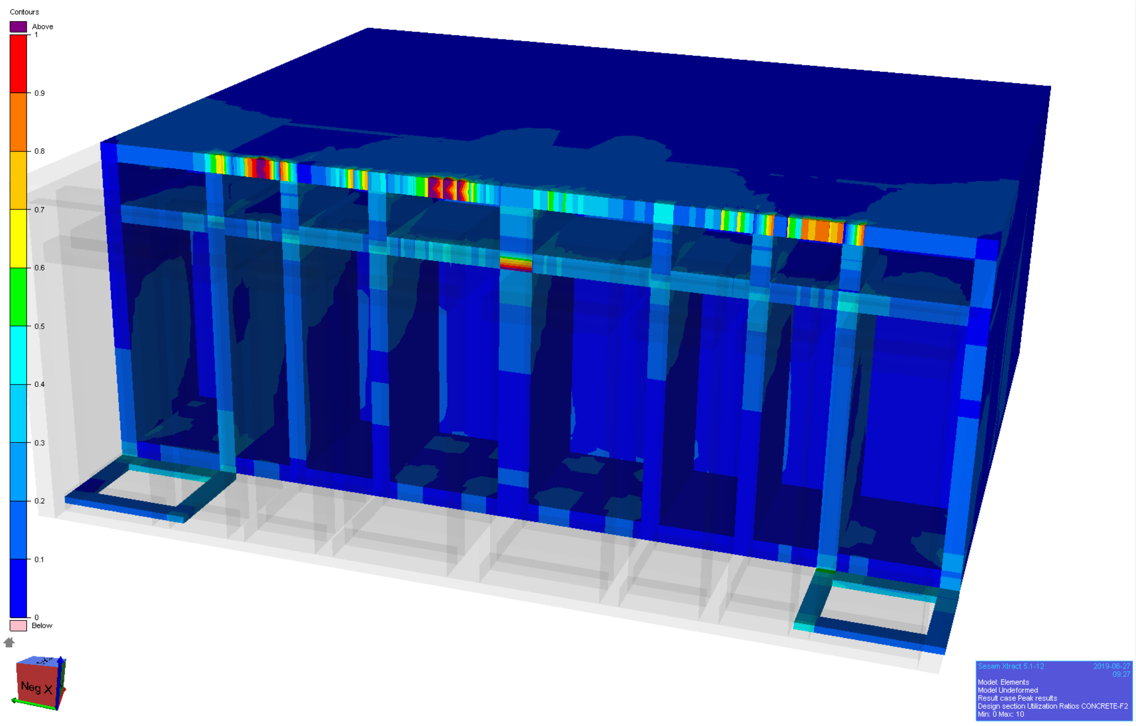

> *Figure 3-6 Concrete utilization, compression.*

Figure 2-31 shows utilization of shear reinforcement.

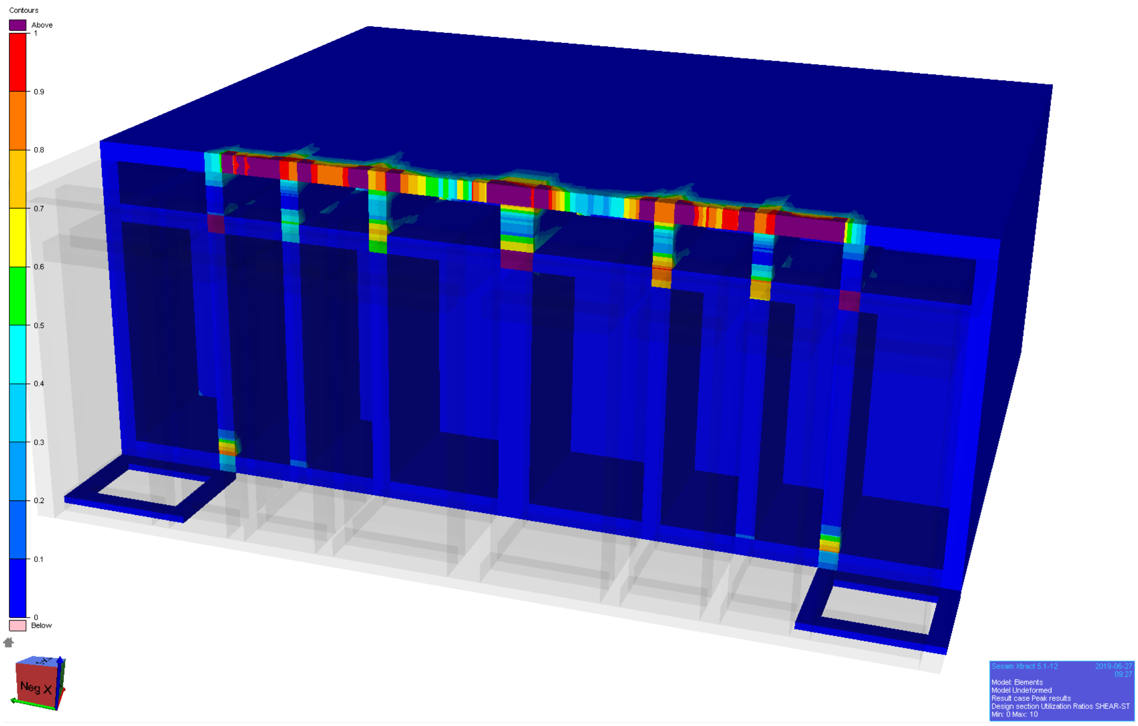

> *Figure 3-7 Utilization of shear reinforcement.*

Utilization of longitudinal (bridge direction) reinforcement is shown in Figure 2-32.

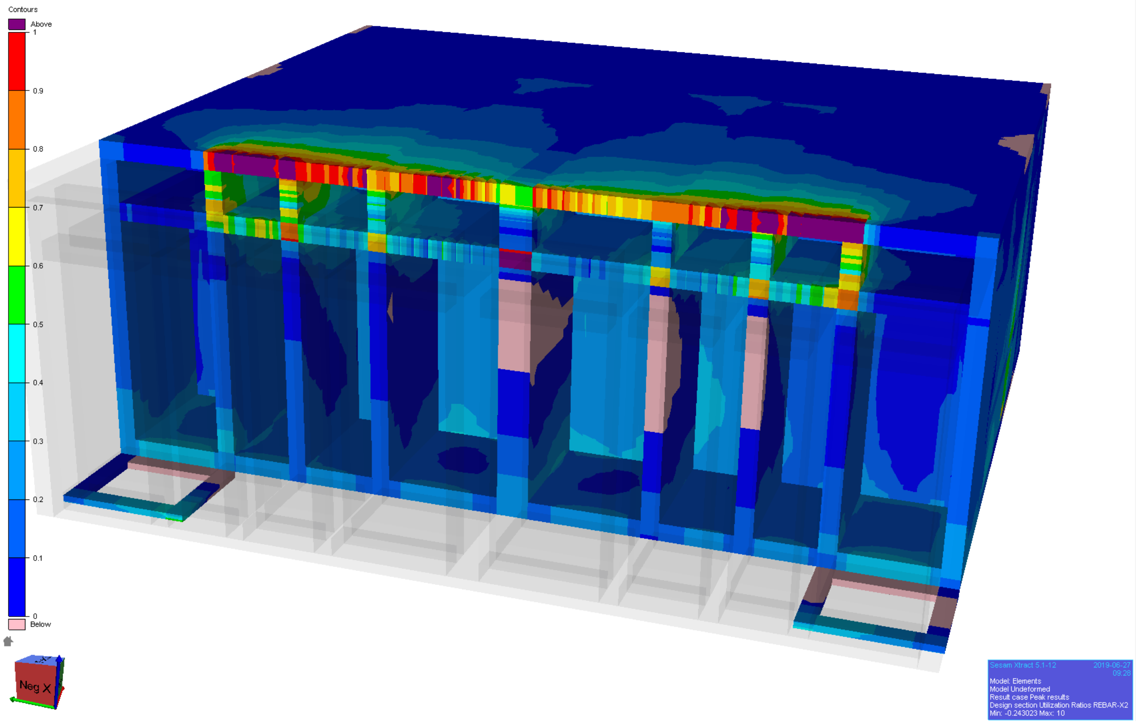

> *Figure 3-8 Utilization of longitudinal (bridge direction) reinforcement.*

Utilization of reinforcement in the normal/vertical direction is shown in Figure 2-33.

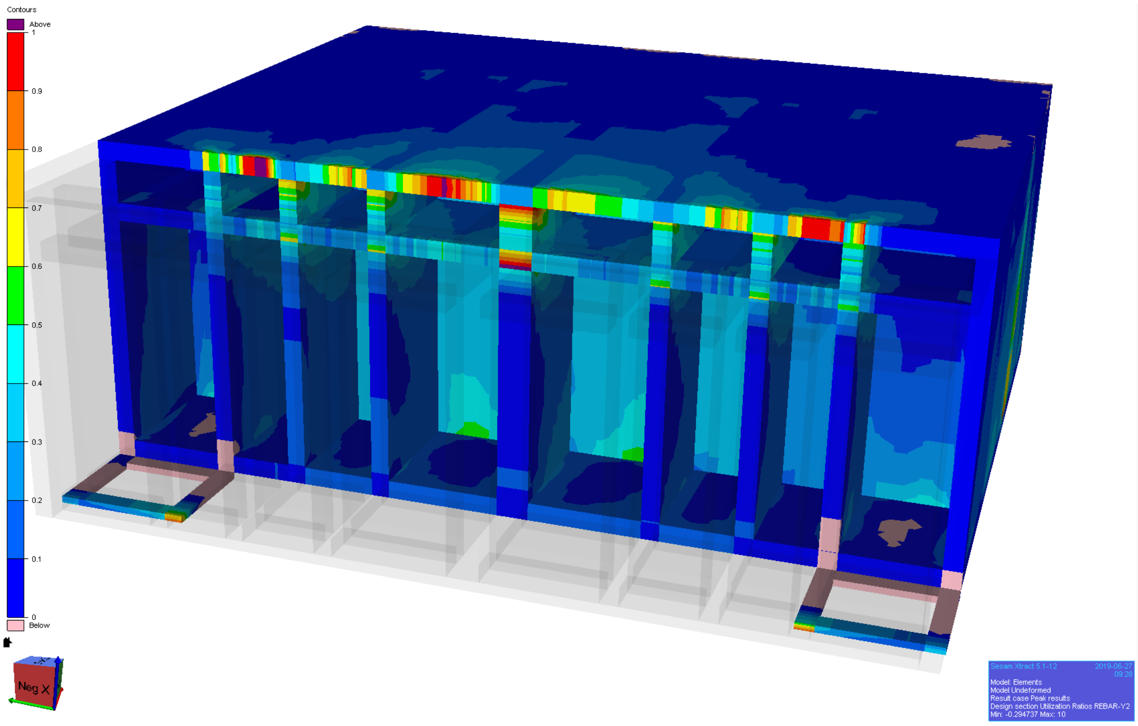

> *Figure 3-9 Utilization of transverse (normal to bridge direction) and vertical reinforcement.*

The SLS crack width utilization check is shown in Figure 2-34. Crack widths are checked for w_{max} = 0.30 mm, according to the requirements in table NA.7.1N in [1].

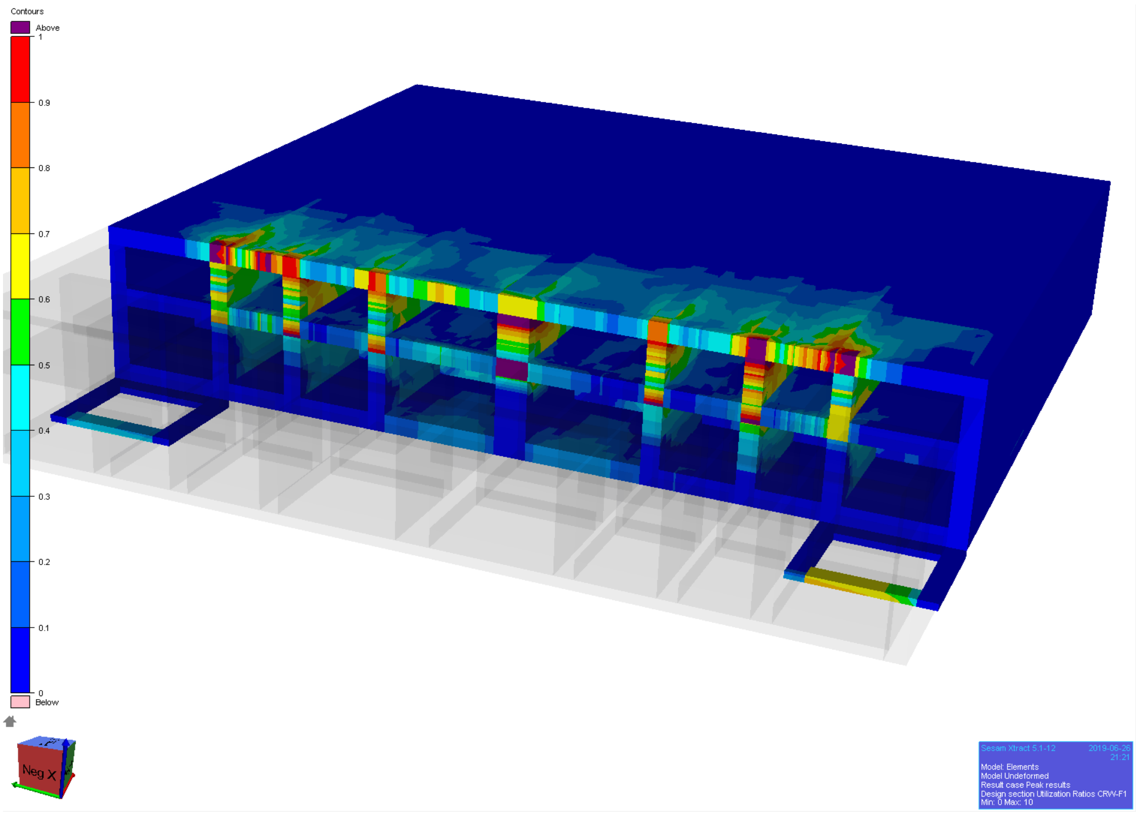

> *Figure 3-10 Crack width utilization.*

3.5 Foundation

3.5.1 General

The design principles for abutment south follows the same principles as for abutment north, see section 3.5. However, rock anchors are not necessary.

The southern abutment is located on approximately elevation +46 m on blasted bedrock, in the north facing slope of Reksteren. The abutment localization shows in Figure 3-11 and Figure 3-12.

> *Figure 3-11: Arial photo of Reksteren from east, Svarvhelleholmen island to the right. The red circle indicates the abutment localization.*

> *Figure 3-12: Arial photo (downwards), approximate location of abutment in center.*

3.5.2 Base reactions

The caisson is supported in 4 limited areas localized as shown in the figure below. On the next pages (Figure 3-15 to Figure 3-22) the base reactions for GreenBox load cases 31-34 (ULS) is shown for each foundation area. Foundation area number 1 is the sum of areas 2-5 i.e. the total base reactions for the whole abutments. The load area with the lowest axial force is area 3 in load case 3310. The load area with the lowest value for axial force divided by shear force is area 3 in load case 3403 with a factor of 1.27.

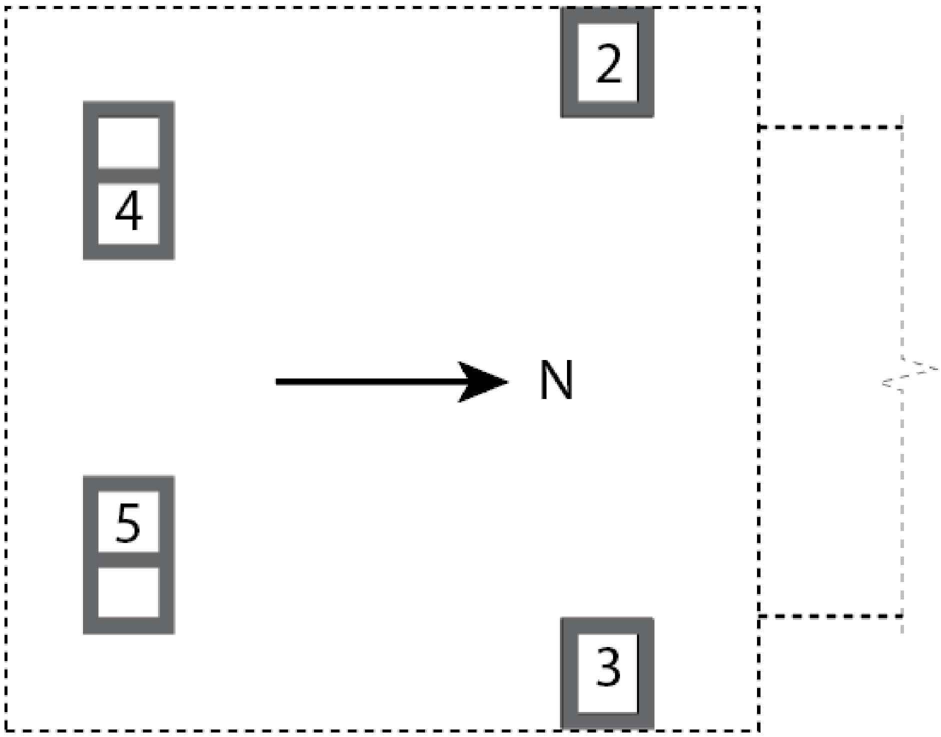

> *Figure 3-13: Numbering of foundation areas*

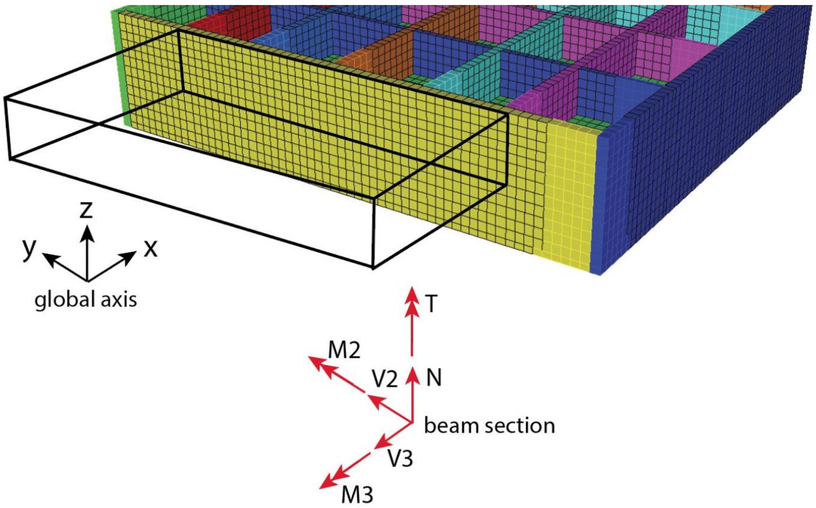

> *Figure 3-14: Definition of beam section forces.*

de-case	bs	N [kN]	V2 [kN]	V3 [kN]	T [kNm]	M2 [kNm]	M3 [kNm]	N/V
3101	1	-453429	-989	-69825	-412970	104302	74026	5.49
3101	2	-88496	-27932	-7646	10597	62304	31843	3
3101	3	-96250	20831	1282	-9913	33720	-43757	4.57
3101	4	-136293	348	-36611	-9132	8296	4126	3.55
3101	5	-132391	5763	-26850	-5591	2126	-4461	4.64
3102	1	-447464	841	-83603	111891	696393	7317	5.14
3102	2	-79889	-18158	-1640	9880	61079	30719	4.32
3102	3	-79460	20376	-4124	-10127	67329	-28188	3.74
3102	4	-143487	-3129	-37704	-781	12163	3008	3.78
3102	5	-144629	1753	-40135	4466	13646	-2598	3.53
3103	1	-452667	1407	-85893	1697177	322566	-39037	3.27
3103	2	-95571	-9828	13602	11476	2347	52752	5.12
3103	3	-80878	36242	-26237	-18731	112222	-18093	1.72
3103	4	-129950	-15297	-16765	27800	-1564	4178	4.81
3103	5	-146269	-9710	-56495	30229	22430	-2556	2.32
3104	1	-454082	-385	-27972	-233431	-625071	25599	12.9
3104	2	-104444	-31153	735	504	28313	43022	3.36
3104	3	-107752	27314	5976	150	12373	-48981	3.86
3104	4	-122034	-863	-20088	-6687	-7961	6778	5.7
3104	5	-119852	4317	-14594	-1463	-11367	-6924	7.74
3105	1	-452102	6014	-75610	481526	186933	22297	4.99
3105	2	-91865	-18176	523	12306	37916	43880	4.99
3105	3	-89297	29406	-9341	-12070	64807	-29594	2.82
3105	4	-133082	-5335	-28402	6274	3976	5001	4.42
3105	5	-137858	118	-38390	9396	10273	-2828	3.43
3106	1	-458531	-391	-61907	-98619	-265489	11693	7.06
3106	2	-99873	-28587	-4475	10497	41607	41802	3.41
3106	3	-101332	26803	-2340	-10349	34788	-44683	3.74
3106	4	-129110	-2200	-28683	-2922	1269	5210	4.4
3106	5	-128216	3593	-26408	-496	-162	-5291	4.8

> *Figure 3-15: Base reaction for GreenBox load case 31, part 1/2*

de-case	bs	N [kN]	V2 [kN]	V3 [kN]	T [kNm]	M2 [kNm]	M3 [kNm]	N/V
3107	1	-454200	1311	-85145	384711	279753	-89701	4.68
3107	2	-93700	-20014	-2264	14868	43081	42225	4.53
3107	3	-85050	26962	-10286	-15102	69447	-30168	2.83
3107	4	-135853	-5644	-31752	5822	7008	3766	4.07
3107	5	-139597	7	-40843	8137	12850	-3249	3.29
3108	1	-456050	-347	-61108	-86746	-374655	16367	7.15
3108	2	-101405	-29267	-5377	12164	38568	42941	3.35
3108	3	-103077	27675	-3554	-12107	32363	-45743	3.65
3108	4	-126173	-2320	-27100	-2365	164	5294	4.56
3108	5	-125394	3566	-25078	-702	-1129	-5344	4.93
3109	1	-451760	-1056	-70542	-1602845	149286	29896	3.76
3109	2	-84476	-36270	-22094	13878	101237	20747	1.93
3109	3	-97823	11528	15670	-6841	-3117	-53205	4.76
3109	4	-142382	9171	-50833	-29183	17045	3482	2.49
3109	5	-127079	14514	-13285	-25513	-5594	-4811	5.43
3110	1	-448651	805	-118990	235610	1022404	2633	3.56
3110	2	-75005	-15842	-8113	21760	74330	29247	3.73
3110	3	-73401	19897	-13528	-22580	88741	-24250	2.74
3110	4	-148960	-4392	-45994	3061	21551	1300	3.19
3110	5	-151285	1142	-51356	4883	24800	-821	2.9
3111	1	-452332	-4701	-80793	-484499	283911	-18844	4.72
3111	2	-87498	-28347	-10271	13442	69230	28975	2.81
3111	3	-90129	17955	34	-13101	40674	-42376	4.97
3111	4	-139688	107	-40447	-9417	12237	2776	3.3
3111	5	-135017	5585	-30110	-6442	5801	-4427	4.24
3112	1	-446259	817	-83567	105492	631436	7388	5.14
3112	2	-80904	-18711	-2444	11056	59803	31359	4.2
3112	3	-80527	20817	-4783	-11285	65649	-28976	3.67
3112	4	-141874	-3122	-37027	-632	11687	3036	3.81
3112	5	-142955	1833	-39313	4101	13080	-2638	3.56

> *Figure 3-16: Base reaction for GreenBox load case 31, part 2/2*

de-case	bs	N [kN]	V2 [kN]	V3 [kN]	T [kNm]	M2 [kNm]	M3 [kNm]	N/V
3201	1	-450037	-166	-53093	-308107	-18289	77625	7.19
3201	2	-90165	-27065	-2826	4979	51464	33623	3.3
3201	3	-97331	22081	3815	-4460	29112	-42855	4.32
3201	4	-132712	-97	-30781	-8260	2990	4961	4.1
3201	5	-129829	4916	-23301	-3002	-1774	-4979	5.33
3202	1	-449347	-160	-60672	-242846	318077	5561	6.59
3202	2	-86054	-23714	-1767	4353	57662	31332	3.61
3202	3	-88119	19959	3944	-3310	41548	-36420	4.31
3202	4	-138723	-576	-34270	-7332	6640	4168	3.89
3202	5	-136451	4171	-28579	-942	3203	-4305	4.7
3203	1	-450986	-5	-75818	2711001	248666	-4829	2.82
3203	2	-98898	-2951	28359	5020	-35015	61117	3.36
3203	3	-79360	43399	-36474	-18354	140330	-10364	1.35
3203	4	-123362	-22902	-1990	44383	-11405	4812	4.87
3203	5	-149367	-17551	-65713	47862	26725	-2765	1.94
3204	1	-450254	-162	-9360	-302275	-612762	7558	24.02
3204	2	-103356	-30444	5228	-7383	24919	41306	3.32
3204	3	-105970	25794	12343	8695	4902	-47589	3.61
3204	4	-121884	-14	-17012	-9256	-11464	7332	6.47
3204	5	-119044	4502	-9918	-1060	-15747	-7508	10.74
3205	1	-450489	9351	-63712	229504	83217	119663	6.31
3205	2	-89468	-19416	-15	9268	42576	41962	4.59
3205	3	-94638	28839	-3669	-7325	48572	-32819	3.24
3205	4	-131971	-2638	-28502	764	2714	6025	4.59
3205	5	-134413	2567	-31526	5025	4725	-2868	4.12
3206	1	-455506	14	-68562	40315	25667	-1104	6.53
3206	2	-94530	-24863	-2758	10166	44963	39451	3.74
3206	3	-94143	25475	-3711	-10359	47273	-38789	3.61
3206	4	-133196	-3061	-30571	-935	4025	4571	4.31
3206	5	-133637	2464	-31522	2344	4596	-4466	4.17

> *Figure 3-17: Base reaction for GreenBox load case 32, part 1/2*

de-case	bs	N [kN]	V2 [kN]	V3 [kN]	T [kNm]	M2 [kNm]	M3 [kNm]	N/V
3207	1	-450986	-5	-75818	82599	248665	-76308	5.76
3207	2	-91891	-22430	-3400	11921	49076	37979	3.97
3207	3	-86366	23921	-4715	-11452	56238	-33502	3.47
3207	4	-135949	-3424	-32743	86	6863	3766	4.13
3207	5	-136780	1927	-34960	3566	8457	-3811	3.83
3208	1	-451633	14	-68562	40315	-94613	-1104	6.47
3208	2	-96119	-25678	-4344	12739	42129	40537	3.62
3208	3	-95733	26289	-5297	-12932	44439	-39875	3.49
3208	4	-129670	-3116	-28985	-417	3077	4568	4.44
3208	5	-130111	2519	-29936	1826	3648	-4464	4.28
3209	1	-450037	-166	-53093	-2701849	-18290	9475	3.29
3209	2	-83882	-44799	-31763	11282	128005	12612	1.5
3209	3	-103614	4347	32752	1843	-47429	-63866	3.11
3209	4	-144176	17636	-58783	-48586	19618	4005	2.04
3209	5	-118365	22649	4701	-43328	-18402	-5935	4.51
3210	1	-450769	-9	-125481	76768	921332	-2735	3.53
3210	2	-77161	-18600	-12581	26019	79062	29421	3
3210	3	-76414	19745	-14400	-26384	83790	-28035	2.75
3210	4	-148203	-3537	-48341	1270	23235	1070	3.05
3210	5	-148991	2383	-50159	1398	24329	-949	2.96
3211	1	-450490	-7559	-64552	-431688	142492	-88889	5.76
3211	2	-91885	-29295	-5953	7638	57876	30324	3.04
3211	3	-89902	17972	2819	-8110	36285	-42911	4.86
3211	4	-136467	-691	-34835	-8815	6937	3051	3.73
3211	5	-132236	4454	-26583	-4267	1806	-5632	4.76
3212	1	-446890	-160	-60672	-242845	186642	5561	6.56
3212	2	-88158	-24722	-3272	6753	54691	32776	3.51
3212	3	-90222	20967	2438	-5710	38577	-37864	4.25
3212	4	-135391	-652	-32764	-6806	5601	4234	3.97
3212	5	-133119	4247	-27074	-1468	2165	-4370	4.81

> *Figure 3-18: Base reaction for GreenBox load case 32, part 2/2*

de-case	bs	N [kN]	V2 [kN]	V3 [kN]	T [kNm]	M2 [kNm]	M3 [kNm]	N/V
3301	1	-454150	-996	-77368	-426502	188230	74360	5.02
3301	2	-87080	-27640	-9307	12910	66780	30999	2.9
3301	3	-94952	20332	-60	-12167	37314	-43188	4.64
3301	4	-138075	386	-39040	-9060	10695	3749	3.38
3301	5	-134043	5927	-28961	-6125	4333	-4096	4.36
3302	1	-448124	832	-91679	99652	792592	7572	4.73
3302	2	-78236	-17766	-3348	12289	65923	29735	4.19
3302	3	-77911	19793	-5544	-12483	71378	-27453	3.65
3302	4	-145477	-3100	-40321	-686	14766	2593	3.59
3302	5	-146501	1905	-42466	3953	16075	-2194	3.39
3303	1	-454602	1399	-99185	1691745	427915	-38976	3
3303	2	-94141	-9598	10593	15949	8773	52129	5.61
3303	3	-79492	35925	-29119	-23182	118299	-17582	1.62
3303	4	-132351	-15405	-20528	28378	2194	3599	4.36
3303	5	-148618	-9523	-60131	29466	26113	-1982	2.23
3304	1	-455023	-388	-34348	-241014	-574566	25808	10.88
3304	2	-103738	-31081	-766	2659	31560	42675	3.34
3304	3	-107114	27126	4653	-1972	15124	-48788	3.89
3304	4	-123213	-878	-21954	-6495	-6123	6499	5.3
3304	5	-120958	4445	-16281	-1915	-9636	-6651	7.02
3305	1	-453044	6012	-81985	473962	237419	22518	4.68
3305	2	-91160	-18103	-978	14461	41163	43534	4.93
3305	3	-88659	29219	-10664	-14191	67559	-29401	2.76
3305	4	-134261	-5349	-30267	6466	5814	4723	4.2
3305	5	-138964	246	-40077	8945	12003	-2555	3.32
3306	1	-460527	-397	-74664	-105343	-172439	11834	5.91
3306	2	-98682	-28458	-7437	14875	47663	41319	3.26
3306	3	-100198	26569	-5144	-14698	40408	-44338	3.61
3306	4	-131303	-2299	-32258	-2367	4823	4668	4.01
3306	5	-130344	3791	-29825	-1280	3297	-4756	4.3

> *Figure 3-19: Base reaction for GreenBox load case 33, part 1/2*

de-case	bs	N [kN]	V2 [kN]	V3 [kN]	T [kNm]	M2 [kNm]	M3 [kNm]	N/V
3307	1	-456136	1303	-98436	379279	385069	-89639	4.14
3307	2	-92272	-19784	-5274	19342	49506	41602	4.24
3307	3	-83665	26646	-13168	-19553	75523	-29658	2.65
3307	4	-138254	-5752	-35515	6400	10767	3186	3.72
3307	5	-141946	194	-44480	7374	16532	-2676	3.09
3308	1	-458046	-352	-73865	-93453	-281604	16520	5.97
3308	2	-100214	-29138	-8338	16541	44624	42459	3.2
3308	3	-101944	27441	-6357	-16456	37983	-45398	3.51
3308	4	-128366	-2419	-30674	-1811	3719	4753	4.13
3308	5	-127523	3764	-28495	-1486	2330	-4809	4.4
3309	1	-452480	-1063	-78084	-1616377	233219	30229	3.53
3309	2	-83061	-35978	-23755	16191	105712	19903	1.85
3309	3	-96525	11029	14329	-9094	477	-52635	4.94
3309	4	-144163	9208	-53262	-29112	19443	3106	2.42
3309	5	-128731	14678	-15396	-26048	-3387	-4446	5.09
3310	1	-450366	792	-133448	224211	1161162	2807	3.21
3310	2	-72866	-15393	-11281	26392	81985	28126	3.23
3310	3	-71356	19268	-16429	-27164	95660	-23363	2.45
3310	4	-151964	-4448	-50320	3519	25870	623	2.97
3310	5	-154180	1365	-55417	4037	28959	-156	2.75
3311	1	-454046	-4714	-95251	-495899	422689	-18671	4.1
3311	2	-85359	-27898	-13440	18074	76885	27853	2.62
3311	3	-88083	17326	-2867	-17685	47593	-41488	4.77
3311	4	-142692	51	-44773	-8960	16556	2099	3.07
3311	5	-137912	5807	-34170	-7288	9960	-3761	3.83
3312	1	-446919	807	-91644	93235	727649	7631	4.73
3312	2	-79250	-18319	-4152	13466	64647	30374	4.06
3312	3	-78977	20234	-6204	-13641	69699	-28241	3.58
3312	4	-143865	-3093	-39645	-537	14290	2621	3.61
3312	5	-144828	1985	-41643	3588	15510	-2234	3.42

> *Figure 3-20: Base reaction for GreenBox load case 33, part 2/2*

de-case	bs	N [kN]	V2 [kN]	V3 [kN]	T [kNm]	M2 [kNm]	M3 [kNm]	N/V
3401	1	-450757	-173	-60636	-321639	65658	77959	6.39
3401	2	-88749	-26774	-4487	7292	55940	32779	3.24
3401	3	-96033	21582	2474	-6714	32706	-42285	4.39
3401	4	-134494	-60	-33210	-8189	5389	4584	3.86
3401	5	-131481	5079	-25412	-3536	434	-4614	4.95
3402	1	-450007	-169	-68749	-255085	414290	5816	5.87
3402	2	-84401	-23322	-3475	6762	62507	30348	3.55
3402	3	-86569	19377	2523	-5666	45598	-35685	4.4
3402	4	-140713	-548	-36887	-7237	9243	3754	3.68
3402	5	-138324	4323	-30910	-1455	5633	-3901	4.4
3403	1	-452922	-13	-89109	2705570	353996	-4767	2.62
3403	2	-97469	-2721	25349	9494	-28589	60494	3.56
3403	3	-77974	43083	-39356	-22805	146406	-9853	1.27
3403	4	-125763	-23010	-5753	44961	-7646	4233	4.61
3403	5	-151716	-17364	-69350	47099	30407	-2192	1.89
3404	1	-451196	-164	-15735	-309839	-562276	7779	17.8
3404	2	-102651	-30371	3727	-5228	28165	40960	3.34
3404	3	-105333	25606	11020	6573	7654	-47395	3.71
3404	4	-123063	-28	-18877	-9064	-9626	7054	5.95
3404	5	-120150	4629	-11605	-1511	-14017	-7235	9.41
3405	1	-451431	9348	-70087	221921	133691	119873	5.83
3405	2	-88763	-19344	-1516	11423	45821	41616	4.51
3405	3	-94001	28651	-4991	-9447	51323	-32627	3.2
3405	4	-133149	-2653	-30367	956	4551	5746	4.35
3405	5	-135519	2694	-33212	4574	6455	-2595	3.96
3406	1	-457502	8	-81318	33590	118717	-964	5.56
3406	2	-93339	-24734	-5719	14544	51019	38968	3.57
3406	3	-93010	25241	-6515	-14708	52893	-38443	3.46
3406	4	-135389	-3160	-34146	-381	7579	4030	3.94
3406	5	-135765	2662	-34939	1560	8055	-3931	3.85

> *Figure 3-21: Base reaction for GreenBox load case 34, part 1/2*

de-case	bs	N [kN]	V2 [kN]	V3 [kN]	T [kNm]	M2 [kNm]	M3 [kNm]	N/V
3407	1	-452922	-13	-89109	77168	353995	-76246	4.95
3407	2	-90462	-22199	-6409	16395	55502	37356	3.74
3407	3	-84981	23604	-7597	-15904	62315	-32991	3.28
3407	4	-138350	-3532	-36506	665	10622	3187	3.76
3407	5	-139129	2114	-38597	2803	12139	-3238	3.55
3408	1	-453629	8	-81318	33591	-1563	-964	5.51
3408	2	-94928	-25549	-7305	17117	48185	40055	3.43
3408	3	-94599	26055	-8100	-17281	50059	-39530	3.32
3408	4	-131863	-3216	-32560	137	6631	4027	4.03
3408	5	-132239	2717	-33353	1042	7107	-3929	3.93
3409	1	-450757	-173	-60636	-2715381	65657	9809	3.11
3409	2	-82466	-44508	-33424	13595	132481	11768	1.44
3409	3	-102316	3848	31410	-411	-43835	-63296	3.23
3409	4	-145957	17674	-61212	-48515	22017	3628	2
3409	5	-120018	22813	2590	-43862	-16194	-5570	4.71
3410	1	-452483	-21	-139939	65387	1060109	-2549	3.19
3410	2	-75022	-18150	-15750	30651	86717	28300	2.64
3410	3	-74368	19117	-17301	-30968	90710	-27147	2.46
3410	4	-151207	-3593	-52667	1728	27554	393	2.85
3410	5	-151886	2606	-54220	552	28488	-284	2.8
3411	1	-452205	-7571	-79010	-443069	281250	-88702	4.86
3411	2	-89746	-28845	-9121	12270	65530	29203	2.89
3411	3	-87857	17344	-83	-12694	43204	-42023	5.01
3411	4	-139470	-747	-39161	-8357	11257	2374	3.42
3411	5	-135131	4677	-30644	-5113	5964	-4966	4.23
3412	1	-447551	-169	-68749	-255085	282837	5816	5.84
3412	2	-86505	-24330	-4981	9163	59536	31792	3.43
3412	3	-88673	20385	1018	-8067	42627	-37129	4.32
3412	4	-137381	-623	-35381	-6711	8204	3819	3.75

> *Figure 3-22: Base reaction for GreenBox load case 34, part 2/2*

3.5.3 Sliding resistance

The figure below shows the axial force divided by the shear force (x and y direction) for each gauss point in the foundation. For the local foundation area 3 there are areas that have a lover axial force than shear, but each foundation (i.e. foot print) area has an individual total axial force that is greater than the shear. The lowest factor is 1.27 in load case 3403. The shear force is transferred to the rock because of friction. The friction coefficient is assumed to be 1.0.

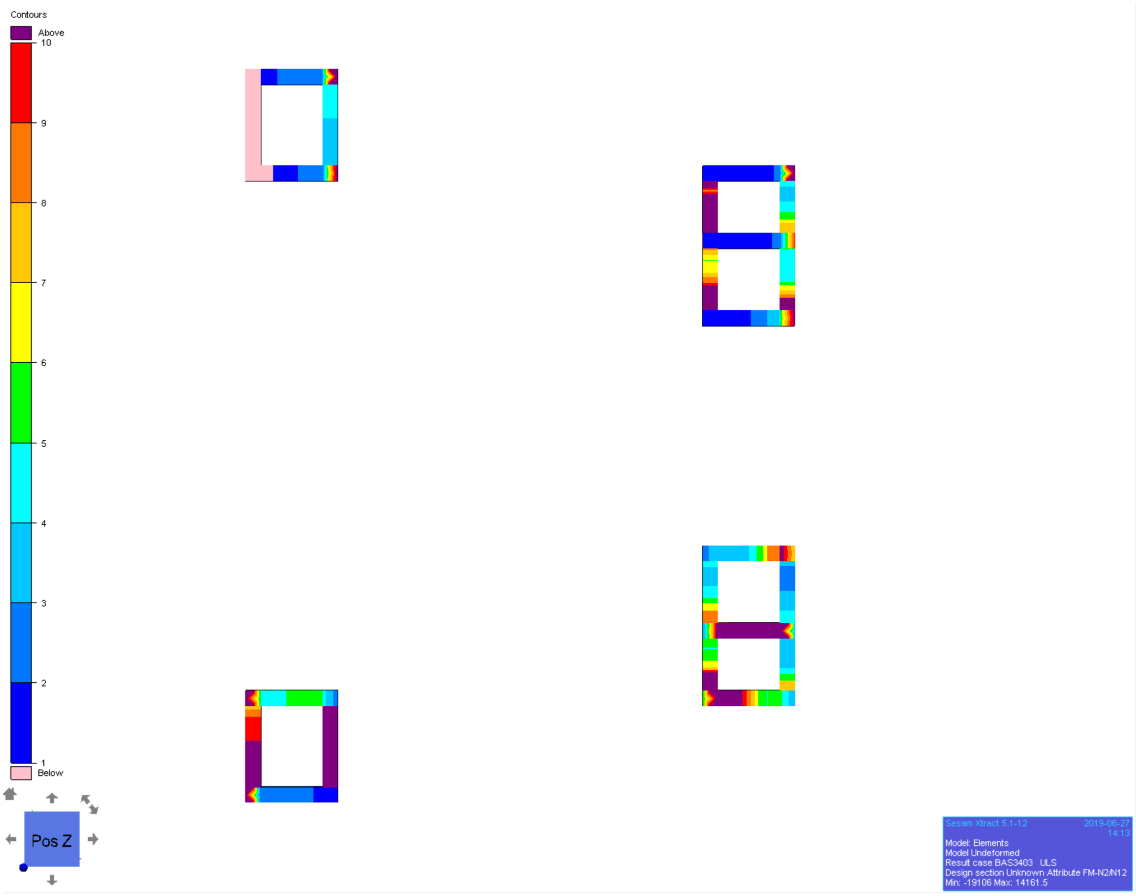

> *Figure 3-23: Axial force divided with shear force for each section in foundation, load case 3403*

de-case	bs	N [kN]	V2 [kN]	V3 [kN]	T [kNm]	M2 [kNm]	M3 [kNm]	N/V
3403	1	-452922	-13	-89109	2705570	353996	-4767	2.62
3403	2	-97469	-2721	25349	9494	-28589	60494	3.56
3403	3	-77974	43083	-39356	-22805	146406	-9853	1.27
3403	4	-125763	-23010	-5753	44961	-7646	4233	4.61
3403	5	-151716	-17364	-69350	47099	30407	-2192	1.89

> *Figure 3-24: Corresponding integrated beam forces for each local area, load case 3403*

3.5.4 Overturning stability

There are 4 load cases (3203, 3209, 3403 and 3409) that are resulting in tensile forces in the foundation. 3403 har the lowest ratio of axial force to shear force, and is shown below, tension is indicated by purple color. In SLS there are no points with uplift in the abutment.

With compression in almost the entire foundation there is no risk of overturning the abutment.

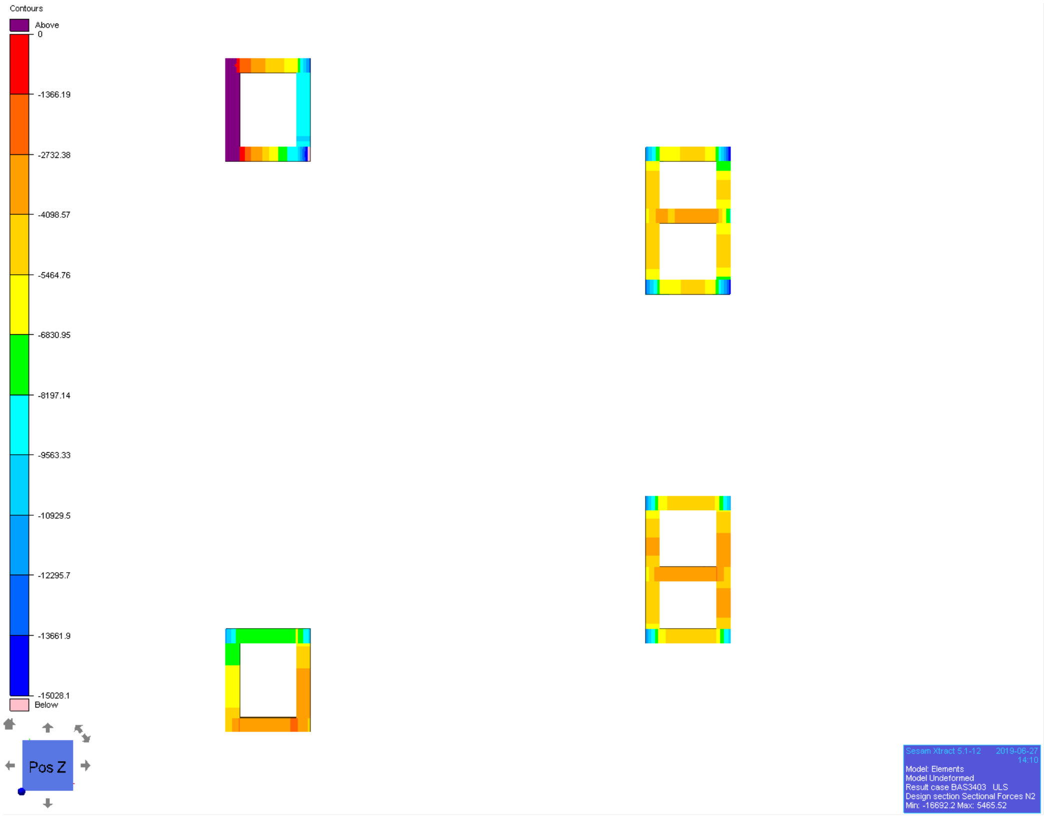

> *Figure 3-25: Axial force in foundation, load case 3403*

3.5.5 Rock anchor design

There are no rock anchors in abutment south because of the large height (and hence weight) of the abutment.

3.6 Bridge girder end section

3.6.1 Design loads for the post-tensioned connection

The design of the post-tensioned connection between abutment and bridge end girder is based on the ULS loads from the global analysis model 16. These loads are summarized in Table 3-1.
The loads represent one of four ULS combinations. All combinations are run and the LC34 is governing.

> *Table 3-1: ULS design loads (LC34 in Greenbox) at bridge girder end. Extreme value for each load effect (red) together with coincident values (black).*

	Nx		Ny		Nz		Mx		My		Mz	
	Max	Min	Max	Min	Max	Min	Max	Min	Max	Min	Max	Min
Fx	-48	-200	-94	-141	-130	-115	-94	-141	-115	-130	-141	-94
Fy	0	0	9	-7	0	0	0	0	0	0	0	0
Fz	11	13	11	13	17	8	11	13	10	14	13	11
Mx	15	-5	15	-5	-4	2	89	-80	2	-4	-5	15
My	-208	-218	-178	-248	-275	-149	-178	-246	-24	-453	-246	-178
Mz	-339	107	-340	104	86	-51	-340	116	-51	86	2 297	-2 289

3.6.2 Cross section properties

The stiffness of the bridge girder is increasing towards the abutment. The end section is connected to the steel end frame, with holes for the post-tensioning anchors. The stiffeners and the holes are arranged in a system with center distance 600 mm. Figure 2-51 below shows the cross-section geometry of the girder end section at the connection to the end frame. The end frame plate has a general width of 800 mm. The net contact area is 54.7 m^2 when accounting for the holes for the PT trumpets (net-to-gross ratio ~0.96) The thickness of the end frame is 80 mm.

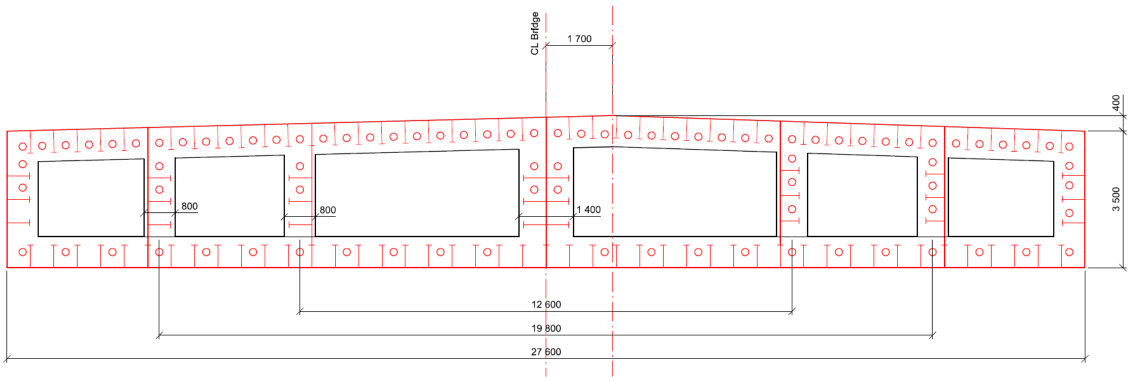

> *Figure 3-26: Cross section of bridge girder end section at the connection to the end steel frame.*

For information regarding bridge girder cross section properties and utilization, a general reference is made to [3].

The center distance between the trapeze stiffeners in the bridge girder end section matches the T-stiffeners in the general bridge girder section. The transition from T-stiffeners to trapeze stiffeners is shown in Figure 2-52.

3.7 Bridge girder connection

3.7.1 General

In the girder-to-abutment connection the bridge terminal end is coupled to the abutment front face. The bridge girder is cast integrally with the abutment by the pre-installation of a bridge girder transition segment. A cast-in-place joint is deemed necessary to assure uniform distribution of the contact forces and to allow ample time (> 8 weeks) for placement and stressing of the PT tendons. The post-tensioning arrangement at the girder end frame is shown in Figure 3-27, where the numbers indicates number of strands in each tendon.

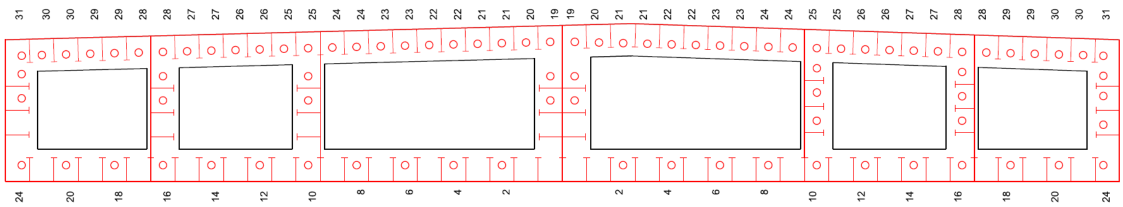

> *Figure 3-27: Arrangement of the post-tensioning at connection to abutment (*showing *number of 0.6" strands per tendon).*

3.7.2 Verification of axial force and flexural resistance

The design criteria for the post-tensioning cables in the intersection between the bridge and the abutment south follows the same principle as for the abutment north, as described in section 2.8.2.

For the south abutment a total of 84 post-tensioning tendons is needed to suppress tensile stresses over the joint, with a total post-tensioning force equal to approximately 410 MN (before losses). This is significantly lower than for the north abutment. The tendon size varies from 6-31 in the upper corner to 0 in the lower mid, with strand intensity varying according to the linear stress distribution. See Figure 3-27.

The average concrete compressive stress resulting from post-tensioning varies from approximately 0 to 12 MPa. The compressive stresses at service load level is well within the limits to avoid longitudinal cracks, micro-cracks and excessive creep. The highest compressive stress is found in the upper corner where the combination of high M_y and M_z governs the design.

The post-tensioning forces and stresses from bridge end forces and post-tensioning, together with an overview of the calculation points are summarized in the figure below. The figure shows values for load case $M_{z,max}$ according to Table 3-1, which is governing for post tensioning in the top slab.

Calc. point	Strands	PT-force			Stresses due to bridge end forces			Stresses due to PT			Resulting stresses			Necessary fck	
c0	19	Fp0	-44.38	MN	σc.0	2.11	MPa	σc.0	-7.37	MPa	σres.0	-5.26	MPa	19.6	MPa
c4	0	Fp4	0.00	MN	σc.4	-7.65	MPa	σc.4	0.00	MPa	σres.4	-7.65	MPa	13.5	MPa
c5	24	Fp5	-15.41	MN	σc.5	1.34	MPa	σc.5	-4.65	MPa	σres.5	-3.32	MPa	12.4	MPa
c5b	12	Fp5b	-7.88	MN	σc.5b	-0.94	MPa	σc.5b	-2.33	MPa	σres.5b	-3.27	MPa	6.7	MPa
c5c	0	Fp5c	0.00	MN	σc.5c	-3.29	MPa	σc.5c	0.00	MPa	σres.5c	-3.29	MPa	5.8	MPa
c7	31	Fp7	-39.82	MN	σc.7	11.09	MPa	σc.7	-12.02	MPa	σres.7	-0.93	MPa	45.5	MPa
c7b	25	Fp7b	-32.82	MN	σc.7b	8.81	MPa	σc.7b	-9.69	MPa	σres.7b	-0.88	MPa	36.5	MPa
c7c	19	Fp7c	-44.38	MN	σc.7c	6.47	MPa	σc.7c	-7.37	MPa	σres.7c	-0.90	MPa	27.3	MPa

> *Figure 3-28 Post-tensioning forces, and stresses from bridge end forces and post-tensioning. Shown load case is $M_{z,min}$ with corresponding forces and moments.*

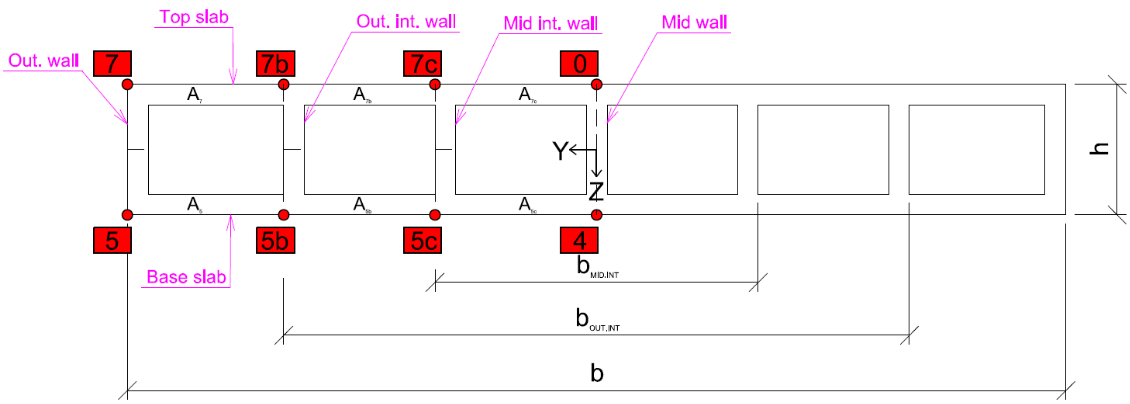

> *Figure 3-29: Calculation points applied in the design of the post-tensioning arrangement.*

3.7.3 Verification of shear and torsion resistance

The design principles are described in section 2.8.3.
The shear and torsion resistance is summarized in Table 2-4 below, for load case $M_{z,max}$. τ_{res} = 0.901 MPa, includes resulting shear stress from V_y, V_z and torsion.

> *Table 3-2: Shear and torsion resistance summary, for $M_{z,max}$*

$v_{Rd,i} = -0.5 \times f_{ctd} + 0.9 \times \sigma_{res,i}$			$v_{Rd,i} - \tau_{res}$	
vRd.0	5.713	MPa	4.811	MPa
$v_{Rd.4}$	7.860	MPa	6.959	MPa
$v_{Rd.5}$	3.962	MPa	3.060	MPa
$v_{Rd.5b}$	3.919	MPa	3.017	MPa
$v_{Rd.5c}$	3.934	MPa	3.033	MPa
$v_{Rd.7}$	1.814	MPa	0.913	MPa
$v_{Rd.7b}$	1.771	MPa	0.870	MPa
$v_{Rd.7c}$	1.787	MPa	0.886	MPa

3.8 Bill of Quantities

> *Table 3-3 Material quantities for abutment south.*

Item	Quantity	Unit
Concrete	10 127	m^3
Ballast[1)]	9 454	m^3
Reinforcement	2 025	t
Post-tensioning	3 690	MNm
Rock anchors	0	MNm
Formwork (walls)	14 081	m^2
Lean concrete (under top/mid slabs)	69	m^3
EPS (under base slab)	1 345	m^2
Rock blasting and excavation	3 500	m^3

Note 1: *Ballast with density 20 kN/m^3*

4 REFERENCES

[1] NS-EN 1992-1-1:2004+A1:2014+NA:2018, Eurocode 2: Design of concrete structures - Part 1-1: General rules and rules for buildings, Standard Norge, 2004.

[2] Håndbok N400 , "Bruprosjektering," Statens vegvesen Vegdirektoratet, 2015.

[3] SBJ-33-C5-OON-22-RE-017-A-K12, Design of bridge girder.

[4] SBJ-32-C4-SVV-90-BA-001, "Design Basis Bjørnafjorden floating bridges," Statens Vegvesen, 2018.

[5] NS-EN 1993-1-1:2005+A1:2014+NA:2015, "Eurocode 3: Design of steel structures - Part 1-1: General rules and rules for buildings," Standard Norge, 2005.